# Modeling of bending-torsion couplings in active-bending structures. Application to the design of elastic gridshell.

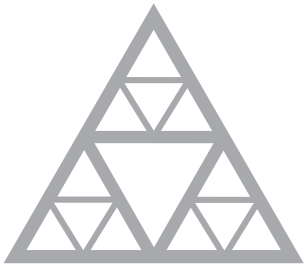

École des Ponts

ParisTech

Thèse n. xxxxx
présenté le 01 décembre 2017
à l'Ecole des Ponts ParisTech
laboratoire Navier
Université Paris-Est

pour l'obtention du grade de Docteur ès Sciences
par

Lionel du Peloux

acceptée sur proposition du jury:

Prof Name Surname, président du jury
Prof Name Surname, directeur de thèse
Prof Name Surname, rapporteur
Prof Name Surname, rapporteur
Prof Name Surname, rapporteur

Paris, Ecole des Ponts ParisTech, 2016

# Contents

# Elastic gridshells Part I

# 1 A neat way to build free-form architecture

# 2 Experimenting elastic gridshells

# Rich Kirchhoff beam model Part II

# 3 Geometry of smooth and discret space curves

## 3.1 Introduction

idée : Rapprocher l'étude des courbes continues et des discrétisées avec le concept de modèle de la «courbe polygone» de Leibniz et de ses successeurs, une infinité de côtés infiniment petits. [Del11, p.235]

Voir aussi que la geometry des space curves semble intimement liée à celle des surface. [Coo13, Del11]

> Car les courbes n'étant que des polygones d'une infinité de côtés, et ne différent entre elles que par la différence des angles que ces côtés infiniment petits font entre eux; il n'appartient qu'à l'Analyse des infiniment petits de déterminer la position de ces cotés pour avoir la courbure qu'ils forment [...] [, Liebniz].

Attention à la terminologie smooth vs. continious :

> A smooth curve is a curve which is a smooth function, where the word "curve" is interpreted in the analytic geometry context. In particular, a smooth curve is a continuous map f from a one-dimensional space to an n-dimensional space which on its domain has continuous derivatives up to a desired order. [1]

### 3.1.1 Goals and contributions

Dans ce chapitre, après un bref rappel sur le cadre mathématique d'étude des courbes paramétrique de l'espace, on présente les notions de courbures et de torsion géométrique associées au repère de Frenet. On montre ensuite le cas plus général d'un repère mobile

[1] Definition of a smooth curve from mathworld : http://mathworld.wolfram.com/SmoothCurve.html

quelconque attaché à une courbe gamma. On définit enfin la particularité d'un repère mobile adapté à un courbe, et on présente, en sus du repère de Frenet, une approche différente pour accrocher des repères le long d'une courbe (Bishop / RMF / Zéro-twisting frame)

Contributions : présentation et comparaison de différentes façons d'estimer la courbure discrete

### 3.1.2 Related work

**(author?)** [Bis75] [Bis75] **(author?) (year?)**

[Bis75] [BWR+08] [Hof08] [BELT14] [Fre52] [Del07] [FGSS14] [Gug89] [Klo86]

### 3.1.3 Overview

## 3.2 Parametric curves

### 3.2.1 Definition

Let $I$ be an interval of $\mathbb{R}$ and $F: t \mapsto F(t)$ be a map of $\mathcal{C}(I, \mathbb{R}^3)$. Then $\gamma = (I, F)$ is called a *parametric curve* and :

- The 2-uplet $(I, F)$ is called a *parametrization* of $\gamma$
- $\gamma = F(I) = \{F(t), t \in I\}$ is called the *graph* or *trace* of $\gamma$
- $\gamma$ is said to be $\mathcal{C}^k$ if $F \in \mathcal{C}^k(I, \mathbb{R}^3)$

Note that for a given graph in $\mathbb{R}^3$ they may be different possible parameterizations. Thereafter $\gamma$ will simply refers to its graph $F(I)$.

### 3.2.2 Regularity

Let $\gamma = (I, F)$ be a parametric curve, and $t_0 \in I$ be a parameter.

- A point of parameter $t_0$ is called *regular* if $F'(t_0) \neq 0$.
  The curve $\gamma$ is called *regular* if $\gamma$ is $\mathcal{C}^1$ and $F'(t) \neq 0, \forall t \in I$
- A point of parameter $t_0$ is called *biregular* if $F'(t_0)$ and $F''(t_0)$ are not collinear
  The curve $\gamma$ is called *biregular* if $\gamma$ is $\mathcal{C}^2$ and $F'(t) \cdot F''(t) \neq 0, \forall t \in I$

### 3.2.3 Reparametrization

Let $\gamma = (I, F)$ be a parametric curve of class $\mathcal{C}^k$, $J \in \mathbb{R}^3$ an interval, and $\varphi : I \mapsto J$ be a $\mathcal{C}^k$ diffeomorphisme. Lets define $G = F \circ \varphi$. Then :

- $G \in \mathcal{C}^k(J, \mathbb{R}^3)$
- $G(J) = F(I)$
- $\varphi$ is said to be an admissible *change of parameter* for $\gamma$
- $(J, G)$ is said to be another *admissible parametrization* for $\gamma$

### 3.2.4 Natural parametrization

Let $\gamma$ be a space curve of class $\mathcal{C}^1$. A parametrization $(I, F)$ of $\gamma$ is called *natural* if $\|F'(t)\| = 1, \forall t \in I$. Thus :

- The curve is necessarily regular
- F is strictly monotonic

### 3.2.5 Curve length

Let $\gamma = (I, F)$ be a parametric curve of class $\mathcal{C}^1$. The length of $\gamma$ is define as :

$$L = \int_I \|F'(t)\| dt \tag{3.1}$$

Note that the length of $\gamma$ is invariant under reparametrization.

### 3.2.6 Arc-length parametrization

Let $\gamma = (I, F)$ be a regular parametric curve. Let $t_0 \in I$ be a given parameter. The following map is said to be the *arc-length of origin* $t_0$ of $\gamma$ :

$$s : t \mapsto \int_{t_0}^{t} \|F'(u)\| du \quad , \quad s \in I \times \mathbb{R} \tag{3.2}$$

The arc-length $s : I \mapsto s(I)$ is an admissible change of parameter for $\gamma$. Indeed, $s$ is a $\mathcal{C}^1$ diffeomorphisme because it is bijective ($s' > 0$).

Lets define $G = F \circ s^{-1}$ and $J = s(I)$. Thus $(J, G)$ is a natural reparametrization of $\gamma$ and $\|G'(s)\| = 1, \forall s \in J$. This parametrization is preferred because the natural parameter s traverses the image of $\gamma$ at unit speed[2] ($\|G'\| = 1$).

[2] Regular curves are also known as *unit-speed* curves.

Thereafter, for a regular curve $\gamma$ : $\gamma(t)$ will denote the point $F(t)$ of parameter $t \in I$ ; while $\gamma(s)$ will denote the point $G(s)$ of arc-length $s \in J = [0, L]$.

## 3.3 Frenet trihedron

The Frenet trihedron is a fundamental mathematical tool from the field of differential geometry to study local characterization of planar and non-planar space curves. It is a direct orthonormal basis attached to any point $P$, of parameter $t \in I$, on a parametric curve $\gamma$. This basis is composed of three unit vectors $\{\boldsymbol{t}(t), \boldsymbol{n}(t), \boldsymbol{b}(t)\}$ called respectively the *tangent*, the *normal*, and the *binormal* unit vectors[3].

Introduced by Frenet in 1847 in his thesis "Courbes à Double Courbure" [Fre52], it brings out intrinsic local properties of space curves : the curvature ($\kappa$) which evaluates the deviance of $\gamma$ from being a straight line (see §3.4.1) ; and the torsion ($\tau_f$) which evaluates the deviance of $\gamma$ from being a planar curve (see §3.4.2).

These quantities, also known as "generalized curvatures" in modern differential geometry, are essential to understand the geometry of space curves. As stated by the *Fundamental Theorem of Space Curves*[4], a curve is fully determined by its curvature and torsion up to a solid movement in space (see §3.4.3).

### 3.3.1 Tangent vector

The first component of the Frenet trihedron is called the *unit tangent vector*. Let $\gamma = (I, F)$ be a regular parametric curve. Let $t \in I$ be a parameter. The *unit tangent vector* is defined as :

$$\boldsymbol{t}(t) = \frac{\gamma'(t)}{\|\gamma'(t)\|} \quad , \quad \|\boldsymbol{t}(t)\| = 1 \tag{3.3}$$

For an arc-length parametrized curve, this expression simply becomes :

$$\boldsymbol{t}(s) = \gamma'(s) \quad , \quad s \in [0, L] \tag{3.4}$$

In differential geometry, the unit tangente to the curve $\gamma$ at point $P_0$ is obtained as the limit of the (normalized) vector $\overrightarrow{P_0P}$, as $P$ approches $P_0$ on the path $\gamma$ (fig. 3.1). For a regular curve, the left-sided and right-sided limits coïncide as $P^-$ and $P^+$ approche $P_0$ respectively from its left and right sides :

$$\boldsymbol{t}(P_0) = \lim_{P \to P_0} \frac{\overrightarrow{P_0P}}{\left\|\overrightarrow{P_0P}\right\|} = \lim_{P^- \to P_0} \frac{\overrightarrow{P_0P^-}}{\left\|\overrightarrow{P_0P^-}\right\|} = \lim_{P^+ \to P_0} \frac{\overrightarrow{P_0P^+}}{\|\overrightarrow{P_0P^+}\|} \tag{3.5}$$

[3] Strictly speaking, the map $\boldsymbol{t} : t \longmapsto \boldsymbol{t}(t)$ is a *vector field* while $\boldsymbol{t}(t)$ is a *vector* of $\mathbb{R}^3$. For the sake of simplicity, and if there is no ambiguity, these two notions will not be explicitly distinguished hereinafter.

[4] The full demonstration of this theorem is attributed to Darboux in [Del07, p.11].

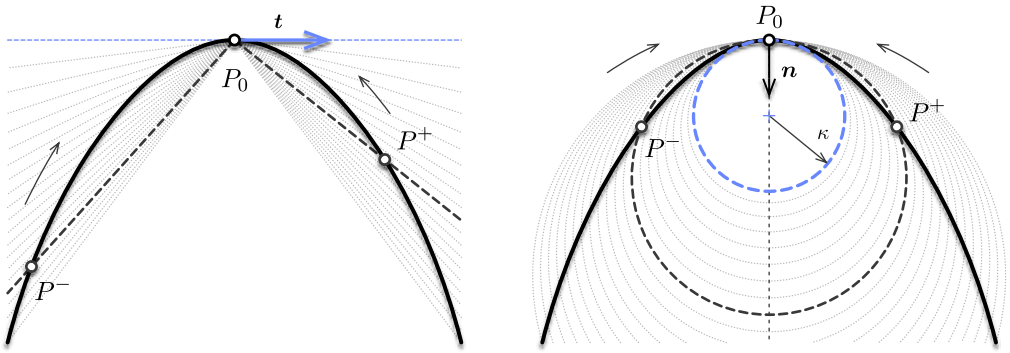


(a) Curve's tangent.

(b) Curve's normal and osculating circle.

Figure 3.1 – Differential definition of Frenet's trihedron at given point $P_0$.

### 3.3.2 Normal vector

The second component of the Frenet trihedron is called the *unit normal vector*. It is constructed from $\boldsymbol{t}'$ which is necessarily orthogonal to $\boldsymbol{t}$. Indeed :

$$\|\boldsymbol{t}\| = 1 \Rightarrow \boldsymbol{t}' \cdot \boldsymbol{t} = 0 \Leftrightarrow \boldsymbol{t}' \perp \boldsymbol{t} \tag{3.6}$$

Let $\gamma = (I, F)$ be a biregular[5] parametric curve. Let $t \in I$ be a parameter. The *unit normal vector* is defined as :

$$\boldsymbol{n}(t) = \frac{\boldsymbol{t}'(t)}{\|\boldsymbol{t}'(t)\|} = \frac{\gamma'(t) \times (\gamma''(t) \times \gamma'(t))}{\|\gamma'(t)\|^3} \quad , \quad \|\boldsymbol{n}(t)\| = 1 \tag{3.7}$$

For an arc-length parametrized curve, this expression simply becomes :

$$\boldsymbol{n}(s) = \frac{\boldsymbol{t}'(s)}{\|\boldsymbol{t}'(s)\|} = \gamma'(s) \times (\gamma''(s) \times \gamma'(s)) \quad , \quad s \in [0, L] \tag{3.8}$$

In differential geometry, the unit normal to the curve $\gamma$ at point $P_0$ is obtained as the limit of the (normalized) vector $\overrightarrow{P_0P^+} - \overrightarrow{P_0P^-}$, as $P^-$ and $P^+$ approche $P_0$ respectively from its left and right sides (fig. 3.1) :

$$\boldsymbol{n}(P_0) = \lim \frac{\overrightarrow{P_0P^+} - \overrightarrow{P_0P^-}}{\left\| \overrightarrow{P_0P^+} - \overrightarrow{P_0P^-} \right\|} \tag{3.9}$$

Remark that the notion of *normal vector* is ambiguous for non-planar curves as there is an infinite number of possible normal vectors lying in the plane orthogonal to the curve's tangent. In practice, the tangent derivative is a convenient choice as it allows to extend the notion of curvature from planar to non-planar space curves. However, we will see (§3.5.6) that other kind of trihedron can be constructed regarding this choice and that one of them is especially suitable for the study of slender beams.

[5] Note that $\boldsymbol{n}$ exists if only $\gamma$ is biregular, that is $\boldsymbol{t}'$ never vanishes or, equivalently, $\gamma$ is never locally a straight line.

### 3.3.3 Binormal vector

The third vector of Frenet's trihedron is called the *unit binormal vector*. It is constructed from $\boldsymbol{t}$ and $\boldsymbol{n}$ to form an orthonormal direct basis of $\mathbb{R}^3$. Let $\gamma = (I, F)$ be a biregular parametric curve. Let $t \in I$ be a parameter. The *unit binormal vector* is defined as :

$$\boldsymbol{b}(t) = \boldsymbol{t}(t) \times \boldsymbol{n}(t) = \frac{\gamma'(t) \times \gamma''(t)}{\|\gamma'(t) \times \gamma''(t)\|} \quad , \quad \|\boldsymbol{b}(t)\| = 1 \tag{3.10}$$

For an arc-length parametrized curve, this expression simply becomes :

$$\boldsymbol{b}(s) = \boldsymbol{t}(s) \times \boldsymbol{n}(s) = \gamma'(s) \times \gamma''(s) \quad , \quad s \in [0, L] \tag{3.11}$$

### 3.3.4 Osculating plane

The tangent and normal unit vectors $\{\boldsymbol{t}, \boldsymbol{n}\}$ form an orthonormal basis of the so-called *osculating plane*, whereas the binormal vector $(\boldsymbol{b})$ is orthogonal to it. This plane is of prime importance because it is the plane in which the curve takes its curvature (see §3.4.1).

As reported in [Del07, p.45], the osculating plane seems to have been first introduced by Bernoulli as the plane passing through three infinitely near points on a curve[6]. Likewise, in modern differential geometry, the osculating plane is defined as the limit of the plane passing through the points $P^-$, $P_0$ and $P^+$ while $P^-$ and $P^+$ approche $P_0$ respectively from its left and right side (fig. 3.1).

Note that the normal unit vector and the binormal unit vector $\{\boldsymbol{n}, \boldsymbol{b}\}$ define the so-called *normal plane*, while the normal tangent vector and the binormal unit vector $\{\boldsymbol{t}, \boldsymbol{b}\}$ define the so-called *rectifying plane*. This planes are secondary for the present study.

## 3.4 Curves of double curvature

The study of space curves belongs to the field of differential geometry. According to [Del07, p.28], the terminology *curve of double curvature* is attributed to Pitot around 1724[7]. However, as stated in [Coo13, p.321], curvature and torsion where probably first thought by Monge around 1771[8]. It is also interesting to note that, at that time, "curvature" was

[6] "Voco autem planum osculans, quod transit per tria curvae quaesitae puncta infinite sibi invicem propinqua" [Ber28, p.113].

[7] " Les Anciens ont nommé cette courbe Spirale ou Hélice ; parce que la formation sur le cylindre suit la même analogie que la formation d'une spirale ordinaire sur un plan; mais elle est bien différente de la spirale ordinaire, étant une des courbes à double courbure, ou une des lignes qu'on conçoit tracée sur la surface des Solides. Peut-être que ces sortes de courbes à double courbure, ou prises sur la surface des Solides, feront un jour l'objet des recherches des géomètres. Celle que nous venons d'examiner est, je crois, la plus simple de toutes. " [Pit26, p.28]

[8] "On appelle point d'inflexion, dans une courbe plane, le point où cette ligne, après avoir été concave dans un sens, cesse de l'être pour devenir concave dans l'autre sens. Il est évident que dans ce point, la courbe perd sa courbure, et que les deux élémens consécutifs sont en ligne droite. Mais une courbe à double courbure peut perdre chacune de ses courbures en particulier, ou les perdre toutes deux dans le même point ; c'est-à-dire, qu'il peut arriver ou que trois élémens consécutifs d'une même courbe à double courbure se trouvent dans un même plan, ou que deux de ces élémens soient en ligne droite. Il suit de là que les

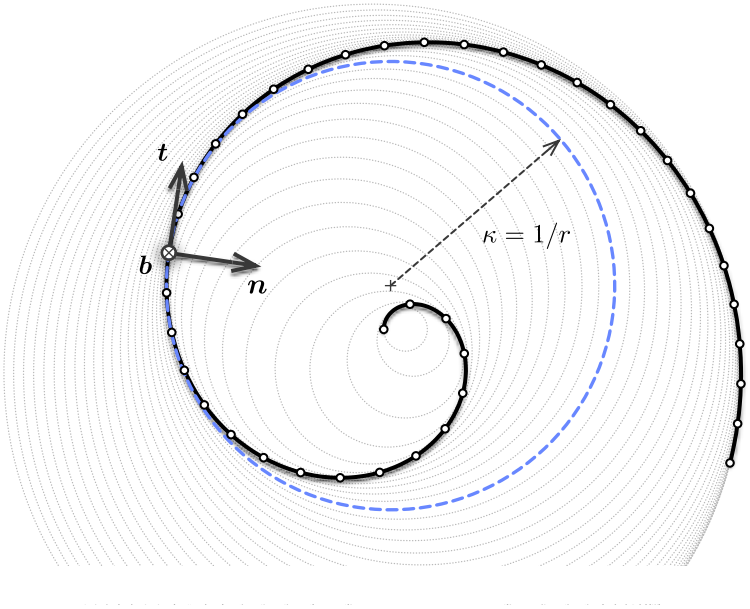


Figure 3.2 – Osculating circles for a spiral curve at different parameters.

also referred to as "flexure", reflecting that the study of physical problems (e.g. *elastica*) and the study of curves of double curvature were intimately related to each other.

Space curves were historically understood as *curves of double curvature* by extension to the case of planar curves, where the curvature measures the deviance of a curve from being a straight line. The second curvature, nowadays known as the "torsion" or "second generalized curvature", measures the deviance of a curve from being plane.

### 3.4.1 First invariant : the curvature

In differential geometry, the *osculating circle* is defined as the limit of the circle passing through the points $P^-$, $P_0$ and $P^+$ while $P^-$ and $P^+$ approche $P_0$ (fig. 3.1). This circle lies on the osculating plane and its radius is nothing but the inverse of the local curvature of a curve[9]. While the tangent gives the best local approximation of the curve as a straight line, the osculating circle gives the best local approximation of that curve as an arc.

courbes à double courbure peuvent avoir deux espèces d'inflexions; la première a lieu lorsque la courbe devient plane, et nous l'appellerons simple inflexion; la seconde, que nous appellerons double inflexion, a lieu lorsque la courbe devient droite dans un de ses points. " [Mon09, p.363]

[9] As explained by Euler itself, at a given arc-length parameter ($s$), the osculating plane is the plane in which a curve takes its curvature : "in quo bina fili elementa proxima in curvantur" [Eul75, p.364].

### Curvature

Let $\gamma$ be a regular arc-length parametrized curve. Let $s \in [0, L]$ be an arc-length parameter. The *curvature* is a positive scalar quantity defined as :

$$\kappa(s) = \|\boldsymbol{t}'(s)\| \geq 0 \quad , \quad \boldsymbol{t}'(s) = \kappa(s)\boldsymbol{n}(s) \tag{3.12}$$

The curvature is *independent* regarding the choice of parametrization. This makes the curvature an *intrinsic property* of a given curve and that is why it is also referred to as a *geometric invariant*. Following [GAS06, pp.203-204] it can be computed for any parametrization $(I, F)$ of $\gamma$ as :

$$\kappa(t) = \frac{\|\gamma'(t) \times \gamma''(t)\|}{\|\gamma'(t)\|^3} \quad , \quad \boldsymbol{t}'(t) = \|\gamma'(t)\|\kappa(t)\boldsymbol{n}(t) \tag{3.13}$$

Note that in eq. (3.12) the prime denotes the derivative regarding the natural parameter $(s)$ while it denotes the derivative regarding any parameter $(t)$ in eq. (3.13). Consequently, the *speed* of the curve's parametrization appears in the latter equation :

$$v(t) = \frac{ds}{dt} = \|\gamma'(t)\| = s'(t) \tag{3.14}$$

The curvature measures how much a curve *bends instantaneously* in its osculating plane, that is how fast the tangent vector is rotating in the osculating plane around the binormal vector. In differential geometry this is expressed as :

$$\kappa(s) = \lim_{ds \to 0} \frac{\measuredangle(\boldsymbol{t}(s), \boldsymbol{t}(s+ds))}{ds} = \lim_{ds \to 0} \frac{(\boldsymbol{t}(s+ds) - \boldsymbol{t}(s)) \cdot \boldsymbol{n}(s)}{ds} \tag{3.15}$$

This is equivalent as measuring how fast the osculating plane itself is rotating around the binormal vector. Consequently a curve is locally a *straight line* when its curvature vanishes $(\kappa(s) = 0)$.

### Radius of curvature

The *radius of curvature* is defined as the inverse of the curvature $(r = 1/\kappa)$. From a geometric point of view, one can demonstrate that it is the radius of the osculating circle (fig. 3.2). Remark that where the curvature vanishes the radius of curvature goes to infinity ; that is the osculating circle becomes a line, a circle of infinite radius.

### Center of curvature

The *center of curvature* is defined as the center of the osculating circle (fig. 3.2). The locus of all the centers of curvature of a curve is called the *evolute*.

### Curvature binormal vector

Finally, following [BWR+08] we define the *curvature binormal vector*. Let $\gamma$ be a biregular arc-length parametrized curve. Let $s \in [0, L]$ be an arc-length parameter. The *curvature binormal vector* is defined as :

$$\boldsymbol{\kappa b}(s) = \boldsymbol{t}(s) \times \boldsymbol{t}'(s) = \kappa(s) \cdot \boldsymbol{b}(s) \quad , \quad \|\boldsymbol{\kappa b}(s)\| = \kappa(s) \tag{3.16}$$

This vector will be useful as it embed all the necessary information on the curve's curvature. We will see (§3.5.6) that this vector is associated to the angular velocity of a specific adapted moving frame attached to the curve and called the *Bishop frame*.

## 3.4.2 Second invariant : the torsion

Let $\gamma$ be a biregular arc-length parametrized curve. Let $s \in [0, L]$ be an arc-length parameter. The *torsion* is a scalar quantity defined as :

$$\tau_f(s) = \boldsymbol{n}'(s) \cdot \boldsymbol{b}(s) = -\boldsymbol{b}'(s) \cdot \boldsymbol{n}(s) \tag{3.17}$$

The torsion is *independent* regarding the choice of parametrization. This makes the torsion an *intrinsic property* of a given curve and that is why it is also referred to as a *geometric invariant*. Following [GAS06, p.204] it can be computed for any parametrization $(I, F)$ of $\gamma$ as :

$$\tau_f(s) = \frac{(\gamma'(s) \times \gamma'(s)) \cdot \gamma''(s)}{\|\gamma'(s) \times \gamma''(s)\|^2} \quad when \quad \kappa(s) > 0 \tag{3.18}$$

The torsion measures how much a curve goes *instantaneously out of its plane*, that is to say how fast the normal or binormal vectors are rotating in the normal plane around the tangent vector. In differential geometry this is expressed as :

$$\tau_f(s) = \lim_{ds \to 0} \frac{\measuredangle(\boldsymbol{n}(s), \boldsymbol{n}(s+ds))}{ds} = \lim_{ds \to 0} \frac{(\boldsymbol{n}(s+ds) - \boldsymbol{n}(s)) \cdot \boldsymbol{b}(s)}{ds} \tag{3.19}$$

This is equivalent as measuring how fast the osculating plane is rotating around the tangent vector. Consequently a curve is locally *plane* when its torsion vanishes ($\tau_f(s) = 0$).

Remark that the *torsion* is denoted "$\tau_f$" and not simply "$\tau$" as the latter will be reserved to denote any angular velocity of a moving adapted frame around its tangent vector. Thus, $\tau_f$ refers to the particular angular velocity of the Frenet trihedron around it's tangent vector. This torsion, which is a geometric property of the curve, will be indifferently referred to as the *Frenet torsion* or the *geometric torsion*.

## 3.4.3 Fundamental theorem of space curves

This two *generalized curvatures*, respectively the curvature ($\kappa$) and the torsion ($\tau_f$), are *invariant* regarding the choice of parametrization and under *euclidean motions*. The

*Fundamental theorem of space curves* states that a curve is fully described, up to a Euclidean motion of $\mathbb{R}^3$, by its positive curvature ($\kappa > 0$) and torsion ($\tau$) [GAS06, p.229].

### 3.4.4 Serret-Frenet formulas

The *Fundamental theorem of space curves* is somehow a consequence of the *Serret-Frenet formulas*, which is the first-order system of differential equations satisfied by the Frenet trihedron. Let $\gamma$ be a biregular arc-length parametrized curve. Let $s \in [0, L]$ be an arc-length parameter. Then, the Frenet trihedron satisfies the following formulas :

$$\begin{cases} \boldsymbol{t}'(s) = \kappa(s)\boldsymbol{n}(s) \\ \boldsymbol{n}'(s) = -\kappa(s)\boldsymbol{t}(s) + \tau_f(s)\boldsymbol{b}(s) \\ \boldsymbol{b}'(s) = -\tau_f(s)\boldsymbol{n}(s) \end{cases} \tag{3.20}$$

This system can be seen as the *equations of motion* of the Frenet trihedron moving along the curve $\gamma$ at unit speed ($\|\gamma'\| = 1$). Indeed, introducing its *angular velocity vector* also known as the *Darboux vector* ($\boldsymbol{\Omega_f}$), the previous system is expressed as :

$$\begin{bmatrix} \boldsymbol{t}'(s) \\ \boldsymbol{n}'(s) \\ \boldsymbol{b}'(s) \end{bmatrix} = \boldsymbol{\Omega_f}(s) \times \begin{bmatrix} \boldsymbol{t}(s) \\ \boldsymbol{n}(s) \\ \boldsymbol{b}(s) \end{bmatrix} \quad \textit{where} \quad \boldsymbol{\Omega_f}(s) = \begin{bmatrix} \tau_f(s) \\ 0 \\ \kappa(s) \end{bmatrix} \tag{3.21}$$

Because the Frenet trihedron satisfies a first-order system of differential equations of parameters $\kappa$ and $\tau_f$ it is possible, by integration, to reconstruct the trace of the moving frame and thus the curve, up to a constant of integration (a trihedron in this case).

Finally, those formulas can be generalized to any non unit-speed parametrization of a curve[10]. Let $\gamma = (I, F)$ be a biregular parametric curve. Let $t \in I$ be a parameter. Then the following *generalized Serret-Frenet formulas* hold :

$$\begin{cases} \boldsymbol{t}'(t) = v(t)\kappa(t)\boldsymbol{n}(t) \\ \boldsymbol{n}'(t) = -v(t)\kappa(t)\boldsymbol{t}(t) + v(t)\tau_f(s)\boldsymbol{b}(t) \\ \boldsymbol{b}'(t) = -v(t)\tau_f(t)\boldsymbol{n}(t) \end{cases} \tag{3.22}$$

Again, this system can be seen as the *equations of motion* of the Frenet trihedron moving along the curve $\gamma$ at non unit-speed ($v(t) = \|\gamma'(t)\|$). This time the *angular velocity vector* ($\boldsymbol{\Omega}$) is distinct from the *Darboux vector* ($\boldsymbol{\Omega_f}$) and the previous system is expressed as :

$$\begin{bmatrix} \boldsymbol{t}'(t) \\ \boldsymbol{n}'(t) \\ \boldsymbol{b}'(t) \end{bmatrix} = \boldsymbol{\Omega}(t) \times \begin{bmatrix} \boldsymbol{t}(t) \\ \boldsymbol{n}(t) \\ \boldsymbol{b}(t) \end{bmatrix} \quad \textit{where} \quad \boldsymbol{\Omega}(t) = v(t) \begin{bmatrix} \tau_f(t) \\ 0 \\ \kappa(t) \end{bmatrix} \tag{3.23}$$

[10] See [GAS06, p.203] for a complete proof.

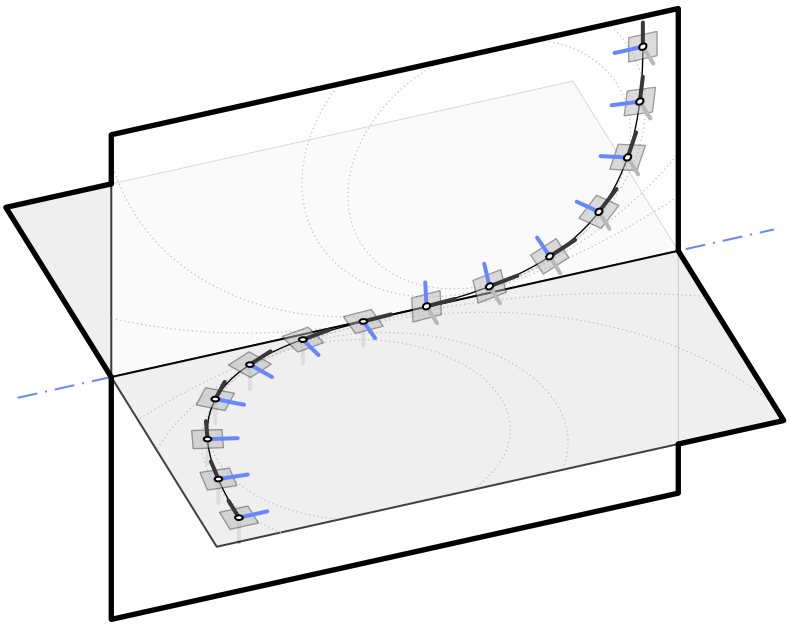

Figure 3.3 – Geometric torsion and rotation of the osculating plane. Note the existence of an inflexion point with a vanishing curvature and a discontinuity of both $\tau_f$ and the osculating plane.

## 3.5 Curve framing

While the Frenet trihedron "has long been the standard vehicle for analysing properties of the curve invariant[11] under euclidean motions" [Bis75, p.1], a curve can be potentially framed with any arbitrary *moving frame*, understood as an *orthonormal basis field*. Thus, the Frenet frame is not the only way to frame a curve[12] and other frames may or may not exhibit some interesting properties.

In his paper [Bis75] Bishop establishes the differential equation that a moving frame must satisfy and remarks that, because of the orthnormality condition, the first derivatives of the frame components can be expressed in terms of themselves through a skew-symmetric coefficient matrix. For such a frame, the understanding of its motion along the curve is thus reduced to the knowledge of only three scalar coefficient functions. He remarks that most of the interesting properties that the Frenet frame exhibits are due to the fact that one of this coefficient function is vanishing everywhere on the curve (that is the frame is *rotation-minimizing* regarding one of its components) ; and that the Frenet frame is *adapted* to the curve (that is one of its components is nothing but the unit tangent vector).

In this section we introduce the *moving frame* notion and two properties of interest such a frame can exhibit in addition, that is : to be *adapted* to the curve ; and to be *rotation-minimizing* regrading a given direction. We then reconsider the case of the Frenet frame

[11] Namely the curvature ($\kappa$) and the Frenet torsion ($\tau_f$).
[12] Recall the title of Bishop's paper : "There is more than one way to frame a curve" [Bis75].

regrading this mathematical framework. Finally, we introduce the *zero-twisting* frame also known as the *bishop* frame[13]. This tool will be fundamental for our futur study of slender beams.

### 3.5.1 Moving frame

Let $\gamma$ be an arc-length parametrized curve. A map $F$ which associates to each point of arc-length parameter $s$ a direct orthonormal trihedron is said toi be a *moving frame* :

$$\begin{array}{rccl} F: & [0,L] & \longrightarrow & \mathcal{SO}_3(\mathbb{R}) \\ & s & \longmapsto & F(s) = \{\boldsymbol{e}_3(s), \boldsymbol{e}_1(s), \boldsymbol{e}_2(s)\} \end{array} \tag{3.24}$$

Consequently, a moving frame $F$ attached to $\gamma$ satisfies for all $s \in [0,L]$ :

$$\begin{cases} \|\boldsymbol{e}_i(s)\| = 1 \\ \boldsymbol{e}_i(s) \cdot \boldsymbol{e}_j(s) = 0 \quad , \quad i \neq j \end{cases} \tag{3.25}$$

The term "moving frame" will refer indifferently to the map itself (denoted $F = \{\boldsymbol{e}_3, \boldsymbol{e}_1, \boldsymbol{e}_2\}$), or to a specific evaluation of the map (denoted $F(s) = \{\boldsymbol{e}_3(s), \boldsymbol{e}_1(s), \boldsymbol{e}_2(s)\}$).

#### Governing equations

Computing the derivatives of the previous relationships leads to the following system of differential equations that the frame must satisfy for all $s \in [0,L]$ :

$$\begin{cases} \boldsymbol{e}_i'(s) \cdot \boldsymbol{e}_i(s) = 0 \\ \boldsymbol{e}_i'(s) \cdot \boldsymbol{e}_j(s) = -\boldsymbol{e}_i(s) \cdot \boldsymbol{e}_j'(s) \quad , \quad i \neq j \end{cases} \tag{3.26}$$

Thus, there exists 3 scalar functions ($\tau$, $k_1$, $k_2$) such that $\{\boldsymbol{e}_3', \boldsymbol{e}_1', \boldsymbol{e}_2'\}$ can be expressed in the basis $\{\boldsymbol{e}_3, \boldsymbol{e}_1, \boldsymbol{e}_2\}$ :

$$\begin{cases} \boldsymbol{e}_3'(s) = k_2(s)\boldsymbol{e}_1(s) - k_1(s)\boldsymbol{e}_2(s) \\ \boldsymbol{e}_1'(s) = -k_2(s)\boldsymbol{e}_3(s) + \tau(s)\boldsymbol{e}_2(s) \\ \boldsymbol{e}_2'(s) = k_1(s)\boldsymbol{e}_3(s) - \tau(s)\boldsymbol{e}_1(s) \end{cases} \tag{3.27}$$

It is common to rewrite this first-order linear system of differential equations[14,15] as a matrix equation :

$$\begin{bmatrix} \boldsymbol{e}_3'(s) \\ \boldsymbol{e}_1'(s) \\ \boldsymbol{e}_2'(s) \end{bmatrix} = \begin{bmatrix} 0 & k_2(s) & -k_1(s) \\ -k_2(s) & 0 & \tau(s) \\ k_1(s) & -\tau(s) & 0 \end{bmatrix} \begin{bmatrix} \boldsymbol{e}_3(s) \\ \boldsymbol{e}_1(s) \\ \boldsymbol{e}_2(s) \end{bmatrix} \tag{3.28}$$

[13] Named after Bishop who introduced it.

[14] In the case of a space curve, where $\boldsymbol{e}_3$ is chosen to be the curve tangent unit vector and $\boldsymbol{e}_1$ is chosen to be the curve normal unit vector, this set of equations is known as the *Serret-Frenet formulas*.

[15] In the case of a space curve drawn on a surface, where $\boldsymbol{e}_3$ is chosen to be the curve tangent unit vector and $\boldsymbol{e}_1$ is chosen to be the surface normal unit vector, this set of equations is known as the *Darboux-Ribaucour formulas*.

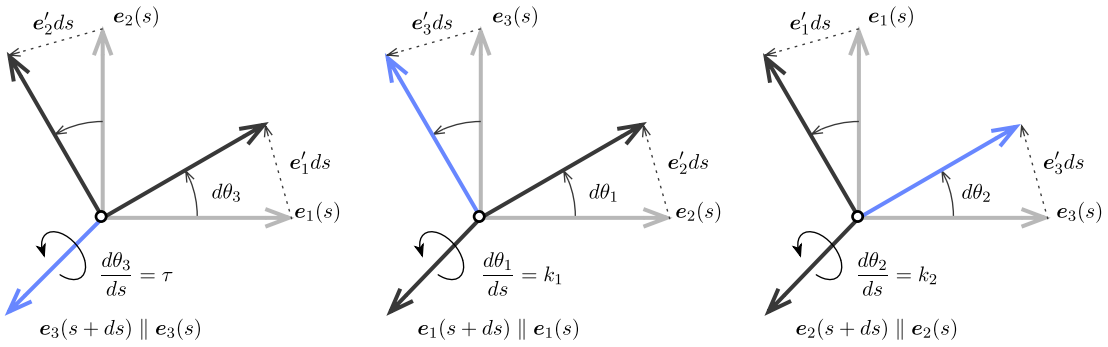


Figure 3.4 – Geometric interpretation of the angular velocity vector of a moving frame.

Since the progression of any moving frame along $\gamma$ is ruled by a first-order system of differential equations, a unique triplet $\{\tau, k_1, k_2\}$ leads to a set of moving frames equal to each other within a constant of integration[16]. Basically, with a given triplet $\{\tau, k_1, k_2\}$, one can propagate a given initial direct orthonormal trihedron (at $s = 0$ for instance) through the whole curve by integrating the system of differential equations. In general, a moving frame will be fully determined by $\tau$, $\kappa_1$ and $\kappa_2$ together with the initial condition $\{\boldsymbol{e}_3(s=0), \boldsymbol{e}_1(s=0), \boldsymbol{e}_2(s=0)\}$.

### Angular velocity

This system can be seen as the *equations of motion* of the frame moving along the curve $\gamma$ at unit speed ($\|\gamma'\| = 1$). Indeed, introducing its *angular velocity vector* ($\boldsymbol{\Omega}$), the previous system is expressed as :

$$\boldsymbol{e}_i'(s) = \boldsymbol{\Omega}(s) \times \boldsymbol{e}_i(s) \quad avec \quad \boldsymbol{\Omega}(s) = \begin{bmatrix} \tau(s) \\ k_1(s) \\ k_2(s) \end{bmatrix} \tag{3.29}$$

This result is straightforward deduced from eq. (3.28). Note that the cross product reveals the skew-symmetric nature of the system, which could already be seen in eq. (3.28). Geometrically, decomposing the infinitesimal rotation of the moving frame around its directors between arc-length $s$ and $s+ds$ (fig. 3.4) shows that the scalar functions $\tau$, $k_1$ and $k_2$ effectively correspond to the angular speed of the frame moving along $\gamma$, respectively around $\boldsymbol{e}_3$, $\boldsymbol{e}_1$ and $\boldsymbol{e}_2$ :

$$\frac{d\theta_3}{ds}(s) = \tau(s) \quad , \quad \frac{d\theta_1}{ds}(s) = k_1(s) \quad , \quad \frac{d\theta_2}{ds}(s) = k_2(s) \tag{3.30}$$

[16] This assumption reminds the *Fundamental theorem of space curves* (§3.4.3).

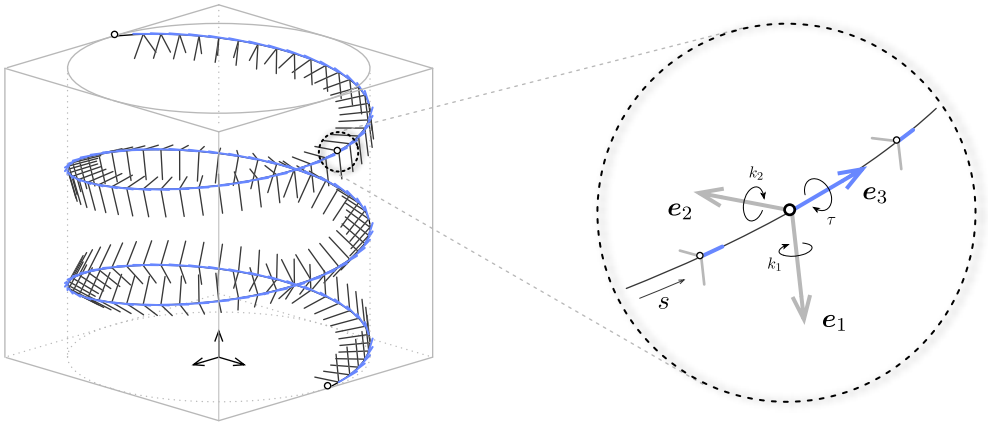


Figure 3.5 – Adapted moving frame $F(s) = \{\boldsymbol{e}_3(s), \boldsymbol{e}_1(s), \boldsymbol{e}_2(s)\}$ where $\boldsymbol{e}_3(s) = \boldsymbol{t}(s)$.

### 3.5.2 Adapted moving frame

Let $F$ be a moving frame as defined in the previous section. $F$ is said to be *adapted* to $\gamma$ if at each point $\gamma(s)$, $\boldsymbol{e}_3(s)$ is the unit tangent vector of $\gamma$ (fig. 3.5) :

$$\boldsymbol{e_3}(s) = \boldsymbol{t}(s) = \frac{\gamma'(s)}{\|\gamma(s)\|} \tag{3.31}$$

For an adapted frame, the components $k_1$ and $k_2$ of the angular velocity vector are related to the curvature of $\gamma$[17] :

$$\kappa(s) = \|\boldsymbol{e}_3'(s)\| = \|k_2(s)\boldsymbol{e}_1(s) + k_1(s)\boldsymbol{e}_2(s)\| = \sqrt{k_1(s)^2 + k_2(s)^2} \tag{3.32}$$

Moreover, recalling the definition of the curvature binormal vector ($\boldsymbol{\kappa b}$) from eq. (3.16), it is easy to see that for an adapted moving frame the following relation holds :

$$\boldsymbol{\kappa b}(s) = k_1(s)\boldsymbol{e}_1(s) + k_2(s)\boldsymbol{e}_2(s) \tag{3.33}$$

Consequently, the angular velocity vector of an adapted moving frame can be written as :

$$\boldsymbol{\Omega}(s) = \boldsymbol{\kappa b}(s) + \tau(s)\boldsymbol{t}(s) \tag{3.34}$$

This last result is very interesting as it shows that any adapted moving frame will differ from each other only by their twisting speed as $\boldsymbol{\Omega}_\perp = \boldsymbol{\kappa b}$ only depends on the curve.

[17] Faire le lien avec l'énergie de flexion, qui ne dépend donc que de la géométrie de la courbe dans le cas d'une isotropic rod $\mathcal{E}_b = EI\kappa^2$.

### 3.5.3 Rotation-minimizing frame

Following [FGSS14, WJZL08] we introduce the *rotation-miniminzing frame* notion. A frame $\{\boldsymbol{e}_3, \boldsymbol{e}_1, \boldsymbol{e}_2\}$ is said to be *rotation-miniminzing* regrading a given direction $\boldsymbol{d}$ if :

$$\boldsymbol{\Omega}(s) \cdot \boldsymbol{d}(s) = 0 \tag{3.35}$$

### 3.5.4 Parallel transport

The notion of *parallel transport* is somehow a generalization of the classical notion of collinearity in flat euclidean spaces (e.g. $\mathbb{R}^2$ or $\mathbb{R}^3$), to spaces that exhibit some non vanishing curvature (e.g. spheric or hyperbolic spaces)[18].

#### Relatively parallel fields

Following [Bis75], we define what is a *(relatively) parallel field*. Let $\gamma$ be a regular arc-length parametrized curve. Let $\boldsymbol{p}$ be a vector field along $\gamma$. The vector field $\boldsymbol{p}$ is said to be *parallel* if its derivative is purely tangential, that is :

$$\boldsymbol{p}'(s) \times \boldsymbol{t}(s) = 0 \tag{3.36}$$

Consequently, for an adapted moving frame, the *normal fields*[19] $\boldsymbol{e}_1$ and $\boldsymbol{e}_2$ are both *relatively parallels* if and only if the frame angular velocity is itself a normal field, that is :

$$\boldsymbol{\Omega}(s) = \boldsymbol{\Omega}_{\perp}(s) = \kappa \boldsymbol{b}(s) \Leftrightarrow \boldsymbol{\Omega}(s) \cdot \boldsymbol{t}(s) = 0 \Leftrightarrow \tau(s) = 0 \tag{3.37}$$

In other words, a *relatively parallel normal field* : "turns, only whatever amount is necessary for it to remain normal, so it is as close to being parallel as possible without losing normality" [Bis75].

#### Parallel transport of vectors along a curve

Reciprocally, it is possible to define the *parallel transport* of a vector along a curve $\gamma$ as its propagation along $\gamma$ at angular speed $\kappa \boldsymbol{b}$. An initial vector $\boldsymbol{p}_0 = \boldsymbol{p}(s_0)$ is parallel transported at arc-length parameter $s$ into the vector $\boldsymbol{p}(s)$ by integrating the following first-order differential equation along $\gamma$ :

$$\boldsymbol{p}'(s) = \kappa \boldsymbol{b}(s) \times \boldsymbol{p}(s) \tag{3.38}$$

Consequently, the resulting vector field $\boldsymbol{p}$ is a parallel field. Note that a parallel field is not necessarily a normal field.

From the point of view of differential geometry, this means that the next vector $\boldsymbol{p}(s + ds)$ is obtained by rotating the previous one $\boldsymbol{p}(s)$ around the curve binormal $\boldsymbol{b}(s)$ by an

[18] https://www.youtube.com/watch?v=p1tfZD2Bm0w

[19] A vector field $\boldsymbol{p}$ is said to be *normal* along a curve $\gamma$ if : $\forall s \in [0, L]$, $\boldsymbol{p} \cdot \boldsymbol{t} = 0$.

infinitesimal angle $d\theta(s) = \kappa(s)ds$. Note that $\boldsymbol{b}(s)$ has the same direction as $\boldsymbol{t}(s) \times \boldsymbol{t}(s+ds)$.

#### Parallel transport of frames along a curve

Identically, the *parallel transport* of an adapted frame is defined as the parallel transport of its components along $\gamma$.

### 3.5.5 Frenet frame

The Frenet frame is a well-known particular adapted moving frame. It is defined as the map that attach to any given point of $\gamma$ the corresponding Frenet trihedron $\{\boldsymbol{t}(s), \boldsymbol{n}(s), \boldsymbol{b}(s)\}$ where :

$$\boldsymbol{t}(s) = \frac{\gamma'(s)}{\|\gamma'(s)\|} \quad , \quad \boldsymbol{n}(s) = \frac{\boldsymbol{t}'(s)}{\boldsymbol{\kappa}(s)} \quad , \quad \boldsymbol{b}(s) = \boldsymbol{t}(s) \times \boldsymbol{n}(s) \tag{3.39}$$

#### Governing equations

The Frenet frame satisfies the *Frenet-Serret formulas* (see §3.4.4), which govern the evolution of the frame along the curve $\gamma$ :

$$\begin{bmatrix} \boldsymbol{t}'(s) \\ \boldsymbol{n}'(s) \\ \boldsymbol{b}'(s) \end{bmatrix} = \begin{bmatrix} 0 & \kappa(s) & 0 \\ -\kappa(s) & 0 & \tau_f(s) \\ 0 & -\tau_f(s) & 0 \end{bmatrix} \begin{bmatrix} \boldsymbol{t}(s) \\ \boldsymbol{n}(s) \\ \boldsymbol{b}(s) \end{bmatrix} \tag{3.40}$$

Remember the generic system of differential equations of an adapted moving frame attached to a curve, established in eq. (3.28), where :

$$\boldsymbol{e_3}(s) = \boldsymbol{t}(s) \quad , \quad k_1(s) = 0 \quad , \quad k_2(s) = \kappa(s) \quad , \quad \tau(s) = \tau_f(s) \tag{3.41}$$

#### Angular velocity

Consequently, the angular velocity vector ($\boldsymbol{\Omega_f}$) of the Frenet frame, also known as the *Darboux vector* in this particular case, is given by :

$$\boldsymbol{\Omega_f}(s) = \begin{bmatrix} \tau_f(s) \\ 0 \\ \kappa(s) \end{bmatrix} = \boldsymbol{\kappa b}(s) + \tau_f(s)\boldsymbol{t}(s) \tag{3.42}$$

Remark that the Frenet frame satisfies $\boldsymbol{\Omega_f}(s) \cdot \boldsymbol{n}(s) = 0$ and is thus a *rotation-miniminzing* frame regarding the normal vector ($\boldsymbol{n}$). The motion of this frame through the curve is known as "pitch-free".

Note also that $\boldsymbol{t}'(s)$ and $\boldsymbol{b}'(s)$ are colinear to $\boldsymbol{n}(s)$. This means that the projection of $\boldsymbol{t}(s)$ and $\boldsymbol{b}(s)$ is conserved from one normal plane to another, that is $\boldsymbol{t}$ and $\boldsymbol{b}$ are parallel

transported along the vector field $\boldsymbol{n}$.

### Drawbacks and benefits

20 , 21 , 22

The Frenet frame is not continuously defined if $\gamma$ is not $\mathcal{C}^2$. This is problematic for the study of slender beams as the centerline of a beam subject to punctual external forces and moments or to material discontinuities will not be $\mathcal{C}^2$ but only picewise $\mathcal{C}^2$. In that case, the centerline tangent will be continuously defined everywhere but the curvature will be subject to discontinuities, that is $\boldsymbol{t}'$ will not be continuously defined.

Moreover, even if $\gamma$ is $\mathcal{C}^2$, the Frenet frame is not defined where the curvature vanishes, which obviously is an admissible configuration for a beam centerline. This issue can be partially addressed by parallel transporting the normal vector along the straight regions of the curve. Thus, the extended frame will still satisfy the governing equations exposed in eq. (3.40). However, if the osculating planes are not parallels on both sides of a region of null curvature, torsion will be subject to a discontinuity and so the Frenet frame[23] (fig. 3.3). Again, if the region of null curvature is not a point, that is the region is not an inflexion point but a locus where the curve is locally a straight line, the change in torsion on both sides of the region can be accommodated by a continuous rotation from one end to the other.

One benefit of the Frenet frame is that, when transported along a *closed curve*, the frame at the end of the curve will align back with the frame at the beginning of the curve, that is the frame will returns to its initial value after a complete turn. During its trip, the frame will make a total twist of $\int_0^L \tau_f(s)ds = 0[2\pi]$ around the tangent vector.

A second benefit is that any adapted frame can be obtained by a rotation of the Frenet frame around the unit tangent vector [Gug89, p.2].

## 3.5.6 Bishop frame

A *Bishop frame*[24] denoted $\{\boldsymbol{t}, \boldsymbol{u}, \boldsymbol{v}\}$, also known as *zero-twisting* or *parallel-transported* frame, is an adapted moving frame that has no tangential angular velocity :

$$\boldsymbol{\Omega} \cdot \boldsymbol{t} = \tau = \boldsymbol{u}' \cdot \boldsymbol{v} = -\boldsymbol{u} \cdot \boldsymbol{v}' = 0 \tag{3.43}$$

Because a Bishop frame is an adapted frame, it can be defined relatively to the Frenet frame by a rotation around the unit tangent vector. A Bishop frame is a frame that cancels

[20] une perturbation de la courbe dans le sens de la courbure engendre une variation de longueur de la courbe proportionnelle à l'inverse de la courbure (au premier ordre) + schéma.

[21] une perturbation de la courbe dans le sens de la binormale (en tout point) préserve la longueur de la courbe au 1er ordre : c'est un déplacement qui conserve l'hypothèse d'inextensibilité au premier ordre.

[22] Examiner la question de la fermeture sur une boucle fermée. Schéma.

[23] This is also highlighted in [Blo90, WJZL08].

[24] Introduce as *relatively parallel adapted frame* in [**?** ].

out the rotational movement of the Frenet frame around the tangent vector. At arc-length parameter $s$, the Frenet frame has continuously rotated around its tangent vector of a cumulative angle : $\int_0^s \tau_f(t)dt$. Thus, any Bishop frame will be obtained, within a constant rotation angle $\theta_0$, through a rotation of the Frenet frame around the tangent vector by an angle :

$$\theta(s) = -\int_0^s \tau_f(t)dt + \theta_0(s) \tag{3.44}$$

Consequently, a Bishop frame can be expressed relatively to the Frenet frame as :

$$\begin{cases} \boldsymbol{u} = \cos\theta\boldsymbol{n} + \sin\theta\boldsymbol{b} \\ \boldsymbol{v} = -\sin\theta\boldsymbol{n} + \cos\theta\boldsymbol{b} \end{cases} \tag{3.45}$$

### Governing equations

The Bishop frame satisfies the following system of differential equations, which govern the evolution of the frame along the curve $\gamma$ :

$$\begin{bmatrix} \boldsymbol{t}'(s) \\ \boldsymbol{u}'(s) \\ \boldsymbol{v}'(s) \end{bmatrix} = \begin{bmatrix} 0 & \kappa(s)\sin\theta(s) & -\kappa(s)\cos\theta(s) \\ -\kappa(s)\sin\theta(s) & 0 & 0 \\ \kappa(s)\cos\theta(s) & 0 & 0 \end{bmatrix} \begin{bmatrix} \boldsymbol{t}(s) \\ \boldsymbol{u}(s) \\ \boldsymbol{v}(s) \end{bmatrix} \tag{3.46}$$

One can remember the generic differential equations of an adapted moving frame attached to a curve, where[25] :

$$k_1(s) = \kappa(s)\sin\theta(s) \quad , \quad k_2(s) = \kappa(s)\cos\theta(s) \quad , \quad \tau(s) = 0 \tag{3.48}$$

### Angular velocity

Consequently, the angular velocity vector ($\boldsymbol{\Omega_b}$) of the Bishop frame is given by :

$$\boldsymbol{\Omega_b}(s) = \begin{bmatrix} 0 \\ \kappa(s)\sin\theta(s) \\ \kappa(s)\cos\theta(s) \end{bmatrix} = \boldsymbol{\kappa b}(s) \tag{3.49}$$

Remark that the Bishop frame satisfies $\boldsymbol{\Omega_b}(s)\cdot\boldsymbol{t}(s) = 0$ and is thus *rotation-miniminzing* regarding the tangent vector. The motion of this frame through the curve is known as "roll-free".

Because the motion of this frame is described by an angular velocity vector that is nothing

[25]

$$\begin{aligned} \tau &= \boldsymbol{u}'\cdot\boldsymbol{v} = (\boldsymbol{\Omega_f}\times\boldsymbol{u} + \theta'\boldsymbol{v})\cdot\boldsymbol{v} = \tau_f - \tau_f = 0 \\ k_1 &= -\boldsymbol{t}'\cdot\boldsymbol{v} = -\kappa\boldsymbol{n}\cdot\boldsymbol{v} = \kappa\sin\theta \\ k_2 &= \boldsymbol{t}'\cdot\boldsymbol{u} = \kappa\boldsymbol{n}\cdot\boldsymbol{u} = \kappa\cos\theta \end{aligned} \tag{3.47}$$

but the curvature binormal vector ($\boldsymbol{\Omega_b} = \kappa \boldsymbol{b}$), it can be interpreted in terms of *parallel transport* as defined in §3.5.4. Thus, given an initial frame at arc-length parameter $s = 0$, the Bishop frame at any arc-length parameter ($s$) is obtained by parallel transporting the initial frame $\{\boldsymbol{t}(0), \boldsymbol{u}(0), \boldsymbol{v}(0)\}$ along the curve from 0 to $s$.

#### Drawbacks and benefits

[26] [27]

One of the main benefits of the Bishop frame is that its generative method : "is immune to degeneracies in the curvature vector" [Blo90]. Although we first expressed the construction of the Bishop frame relatively to the Frenet frame (which exists wherever $\gamma$ is biregular), the existence of the Bishop frame, understood in terms of parallel transport, is guaranteed wherever the curvature binormal ($\kappa \boldsymbol{b} = \boldsymbol{t} \times \boldsymbol{t}'$) is defined. To be continuously defined over $[0, L]$, a Bishop frame only needs the curvature binormal vector to be picewise continuously defined over $[0, L]$, which only requires that $\gamma'$ is $\mathcal{C}^0$ and that $\gamma''$ is picewise $\mathcal{C}^0$. Obviously, those weaker existence conditions are profitables to bypass the drawbacks of the Frenet frame regarding the modeling of slender beams listed in §3.5.5.

Strictly speaking, a Bishop frame is not a reference frame as it is defined within an initial condition. However, we will see later that strains in a beam are modeled as a rate of change in the Bishop frame, and consequently the initial condition will disappear in the equations.

Unlike the Frenet frame, when transported along a *closed curve*, the Bishop frame at the end of the curve will not necessarily align back with the frame at the beginning of the curve[28]. Even if the frame returns to its initial value after a complete turn, it may returns in its position after several complete turns ($2k\pi$) around the curve tangent. During its trip, the frame will make a total twist of $\int_0^L \tau_f(s)ds = \alpha[2\pi]$ around the tangent vector. This difference of angle is related to the concept of *holonomy*.

Remark also that Frenet and Bishop frames coincide for planar curves ($\tau_f = 0$), within a constant rotation around the unit tangent vector.

### 3.5.7 Comparison between Frenet and Bishop frames

#### Application A : circular helix

Let $\gamma$ be a *circular helix* of parameter $a$ and $k$. In a cartesian coordinate system, it is defined as :

$$\boldsymbol{r}(\theta) = \left[a\cos\theta, a\sin\theta, k\theta\right] = a\cos\theta\boldsymbol{e}_x + a\sin\theta\boldsymbol{e}_y + k\theta\boldsymbol{e}_z \tag{3.50}$$

[26] [Gug89, Klo86, Blo90, WJZL08, PFL95, Men13]

[27] "Regarder la méthode de la bi-reflexion pour le calcul du repère de bishop" [WJZL08, p.6]

[28] "it is possible for closed curves to have parallel transport frames that do not match up after one full circuit of the curve" [HM95]

The speed of this parametrization, the curvature and the geometric torsion are uniform and given by :

$$v(\theta) = \sqrt{a^2 + k^2} \quad , \quad \kappa(\theta) = \frac{a}{a^2 + k^2} \quad , \quad \tau_f(\theta) = \frac{k}{a^2 + k^2} \tag{3.51}$$

The Frenet frame components are given by (with $\alpha = v\kappa$ and $\beta = v\tau_f$) :

$$\begin{aligned} \boldsymbol{t}(\theta) &= \left[-\alpha\cos\theta, \alpha\sin\theta, \beta\theta\right] \\ \boldsymbol{n}(\theta) &= \left[-\cos\theta, -\sin\theta, 0\right] \\ \boldsymbol{b}(\theta) &= \left[\beta\sin\theta, -\beta\cos\theta, \alpha\right] \end{aligned} \tag{3.52}$$

And the Bishop frame components are given by :

$$\begin{aligned} \boldsymbol{u}(\theta) &= \left[-\cos\theta\cos\beta\theta - \beta\sin\theta\sin\beta\theta, -\sin\theta\cos\beta\theta + \beta\cos\theta\sin\beta\theta, -\alpha\sin\beta\theta\right] \\ \boldsymbol{v}(\theta) &= \left[-\cos\theta\sin\beta\theta + \beta\sin\theta\cos\beta\theta, -\sin\theta\sin\beta\theta - \beta\cos\theta\cos\beta\theta, \alpha\cos\beta\theta\right] \end{aligned} \tag{3.53}$$

**Application B : conical helix (spiral)**

$$\begin{cases} \rho = ae^{k\theta} \\ z = \rho\cot\alpha \end{cases} \tag{3.54}$$

soit pour une spirale dont on connait

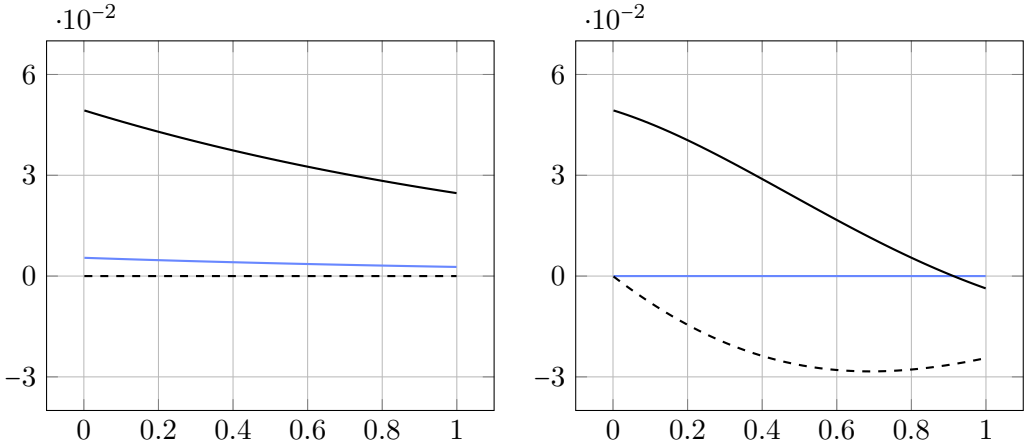


(a) Frenet frame (b) Bishop frame

Figure 3.6 – Comparison between Frenet and Bishop frame velocity for a spirale curve.

## 3.6 Discret curves

### 3.6.1 Definition and arc-length parametrization

### 3.6.2 Discret curvature : an equivocal concept

Curvature is defined from the osculating circle, which is the best approcximation of a curve by a circle. We can define such a circle and it's radius will be the curvature at that point. Problem : there are several ways to define such a circle.

#### Definition

Très intéressant de constater que cette vision 3 verticies vs. 2 edges est déjà présente dès le début dans l'histoire de la compréhension de la courbure.

Pour Euler, le rayon de courbure est le rapport de l'élément d'arc sur l'angle de contingence entre deux tangentes infiniment proches. Par ailleurs, la définition du plan osculateur n'est pas tout à fait lamêmeque chez Bernoulli, plan passant par trois points consécutifs, puis- qu'Euler dit que ce plan contient deux éléments successifs. Il le définit aussi en disant que c'est le plan où la courbe s'incurve. Pour le dire de façon un peu différente : la tangente contient un élément, c'est le lieu où la courbe est droite, la plan osculateur représente l'étape suivante, c'est le lieu où la courbe est arc de cercle. Nous ne pensons pas trahir Euler en faisant cette présen- tation : cela justifie que, pour lui, il est naturel de se placer sur le plan osculateur pour calculer le rayon de courbure. [Del07]

[Hof08]

The edge osculating circle. The vertex osculating circle. La localité est meilleur dans le cas du vertex-based discret osculating circle. Pour des anlges élevés, le edge-based discret osculating circle est plus pertinent. La courbure tend vers l'infini quand les 2 edges deviennent colineaires.

La définition du plan osculateur est univoque dans le cas discret : c'est localement le plan défini par 2 edges consécutifs.

Ce n'est pas le cas de la courbure qui perd son côté intrinsèque.

courbure discrete dans le cas général

#### Vertex-based osculating circle

$$\kappa_1 = \frac{2\,sin(\varphi_i)}{\|\boldsymbol{e}_{i-1} + \boldsymbol{e}_i\|}, \tag{3.55}$$

Problème de convergence lorsque l'angle tend vers pi et que les segments ont même longueur. En pratique peut probable.

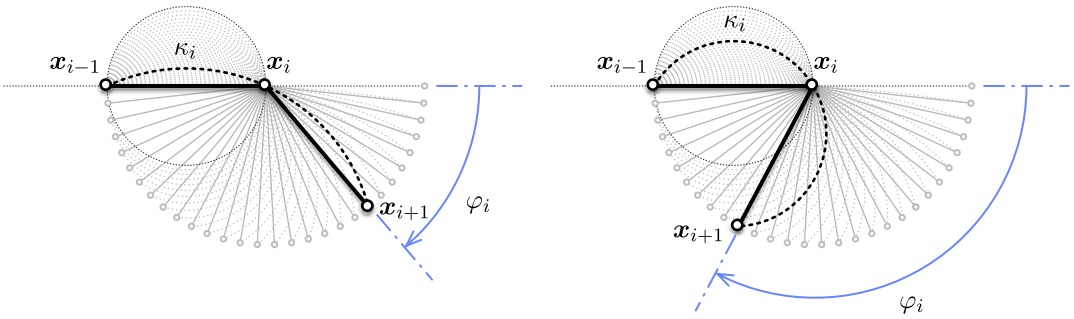


Figure 3.7 – Variation of the vertex-based discrete curvature.

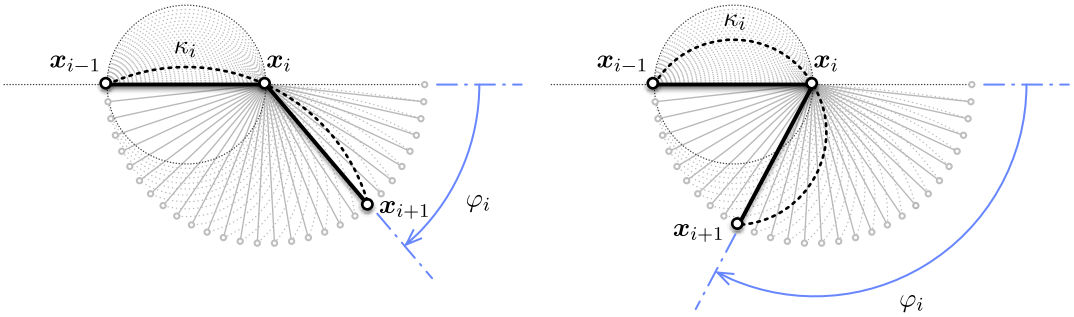


(a) vertex-based osculating circle

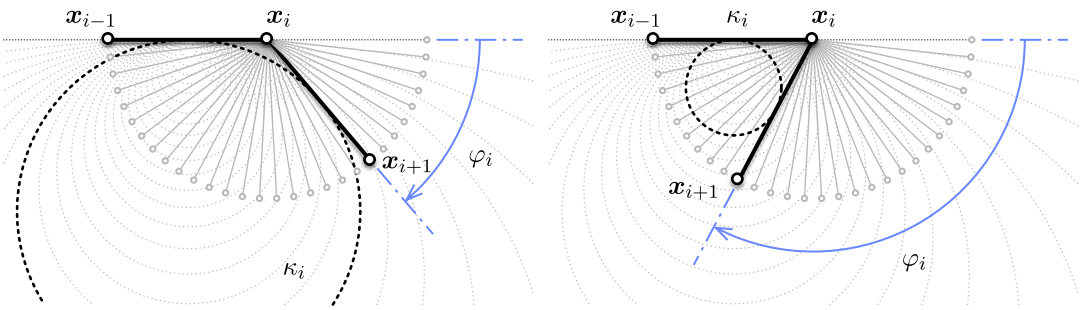


(b) edge-based osculating circle

Figure 3.8 – Definition of the osculating circle for discrete curves.

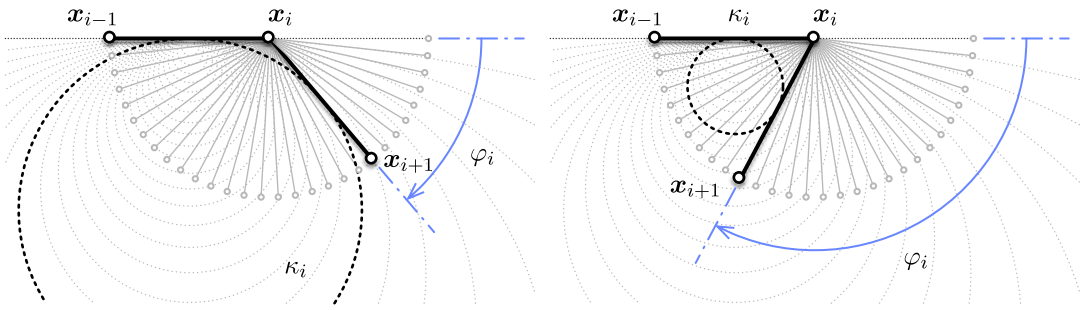


Figure 3.9 – Variation of the edge-based discrete curvature.

### Edge-based osculating circle

$$\kappa_2 = \frac{tan(\varphi_i/2) + tan(\varphi_{i+1}/2)}{\|\boldsymbol{e}_i\|} \tag{3.56}$$

Bon comportement lorsque l'angle tend vers pi. Demande que les 3 segments soient coplanaires.

### Osculating circle for an arc-length parametrized curve

$$\kappa_3 = \frac{2\,tan(\varphi_i/2)}{l} \quad , \quad l = \|\boldsymbol{e}_i\| = cst \tag{3.57}$$

Qu'on peut réécrire pour des segments de longueur variable, avec la moyenne

$$\kappa_3 = \frac{2\,tan(\varphi_i/2)}{l_i} \quad , \quad l_i = \frac{\|\boldsymbol{e}_{i-1}\|\|\boldsymbol{e}_i\|}{\|\boldsymbol{e}_{i-1}\| + \|\boldsymbol{e}_i\|} \tag{3.58}$$

Unlike the smooth case we can not reparameterize a curve. A discrete curve is parameterized by arc-length or it is not [Hof08, p. 10].

Cette condition est extrêmement exigente $\|\boldsymbol{e}_i\| = cst$. Elle est tenable pour des modèles de poutre non connectées (où le pas de disctrétisation peut-être choisi uniform) mais pour en cas de connexion. Ce point n'est pas éclairci dans les articles de Audoly.

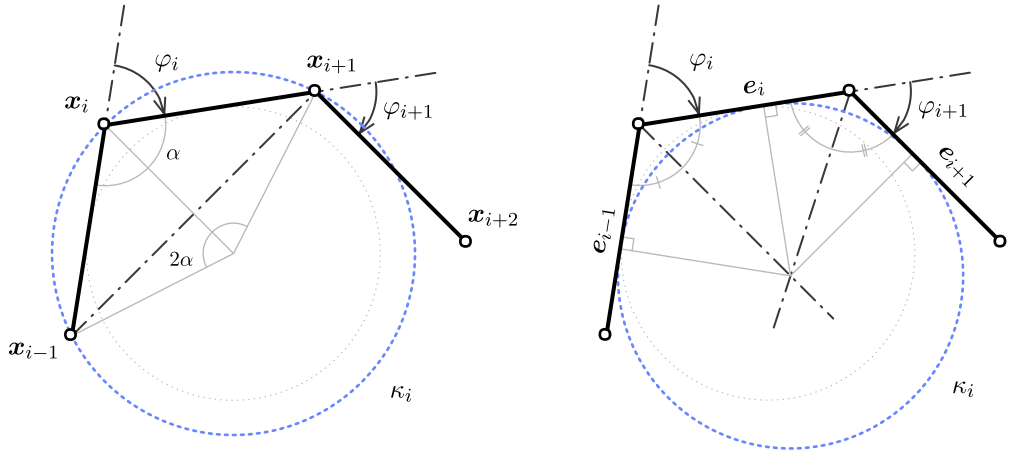


(a) vertex-based osculating circle (b) edge-based osculating circle

Figure 3.10 – Definition of the osculating circle for discrete curves.

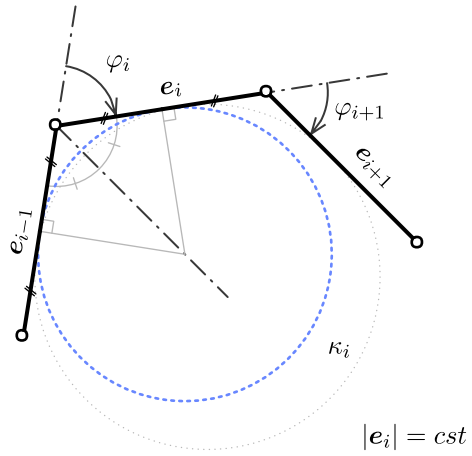


Figure 3.11 – Another definition of the osculating circle for arc-length parametrized curves.

### 3.6.3 Variability of discrete curvature regarding $\alpha$

Qu'on réécrit en posant $\|\boldsymbol{e}_{i-1}\| = \alpha\|\boldsymbol{e}_i\|$, $\alpha \geq 0$ :

$$\kappa_1 = \frac{2\,sin(\varphi_i)}{\|\boldsymbol{e}_i\|(1+\alpha^2+2\alpha\,cos(\varphi_i))^{1/2}}, \quad \kappa_2 = \frac{4\,tan(\varphi_i/2)}{\|\boldsymbol{e}_i\|(1+\alpha)} \tag{3.59}$$

$$\frac{\kappa_1}{\kappa_2}(\alpha) = \frac{\kappa_1}{\kappa_2}(1/\alpha) = \frac{1+\alpha}{(1+\alpha^2+2\alpha\,cos(\varphi_i))^{1/2}}\,cos^2(\varphi_i/2) \tag{3.60}$$

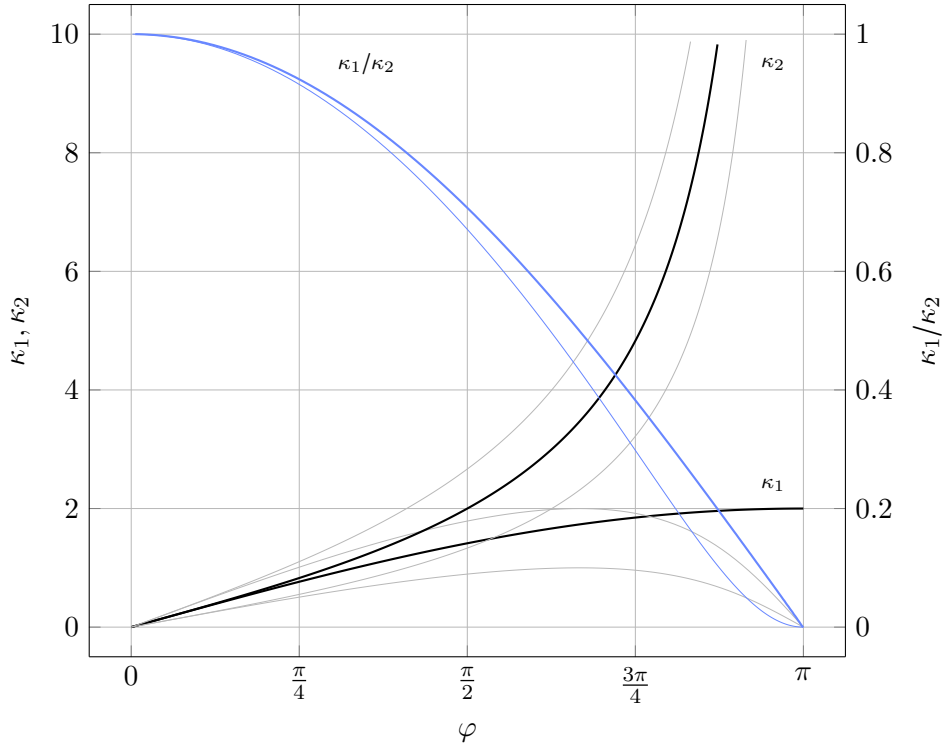


Figure 3.12 – Discrete curvature comparison for $\alpha \in [0.5, 2]$

### 3.6.4 Convergence benchmark $\kappa_1$ vs. $\kappa_2$

**Straight line**

**Circle**

Smooth curve settings:

$$\mathcal{E} = \int_0^l \kappa^2 ds = \kappa\pi, \quad l = \pi r, \quad \kappa = \frac{1}{r} \tag{3.61}$$

Discrete curve :

$$\varphi_N = \tfrac{\pi}{N}, \quad |\boldsymbol{e}| = 2r \sin\tfrac{\varphi}{2}, \quad l_N = N|\boldsymbol{e}| = 2Nr \sin\tfrac{\varphi}{2} = l\frac{\sin\frac{\varphi}{2}}{\frac{\varphi}{2}} \tag{3.62}$$

Discrete bending energies :

$$\mathcal{E}_1 = \mathcal{E}\frac{\sin\frac{\varphi}{2}}{\frac{\varphi}{2}}, \quad \mathcal{E}_2 = \mathcal{E}\frac{\sin\frac{\varphi}{2}}{\frac{\varphi}{2}\cos^2\frac{\varphi}{2}}, \tag{3.63}$$

Remarque that ratios are independent of scale change (independent of R)

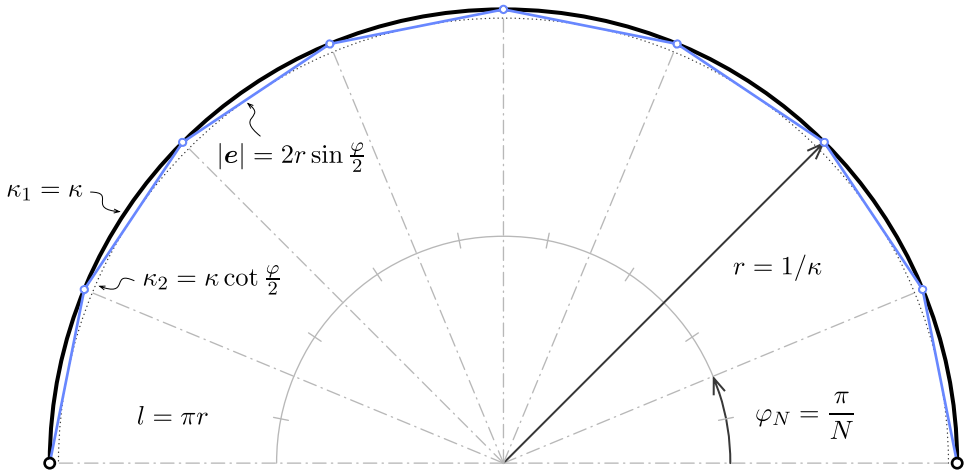


Figure 3.13 – Another definition of the osculating circle for arc-length parametrized curves.

qsmldkqsmldk s qsd qsd sqd qs dqs=dlk qs=ldk sq

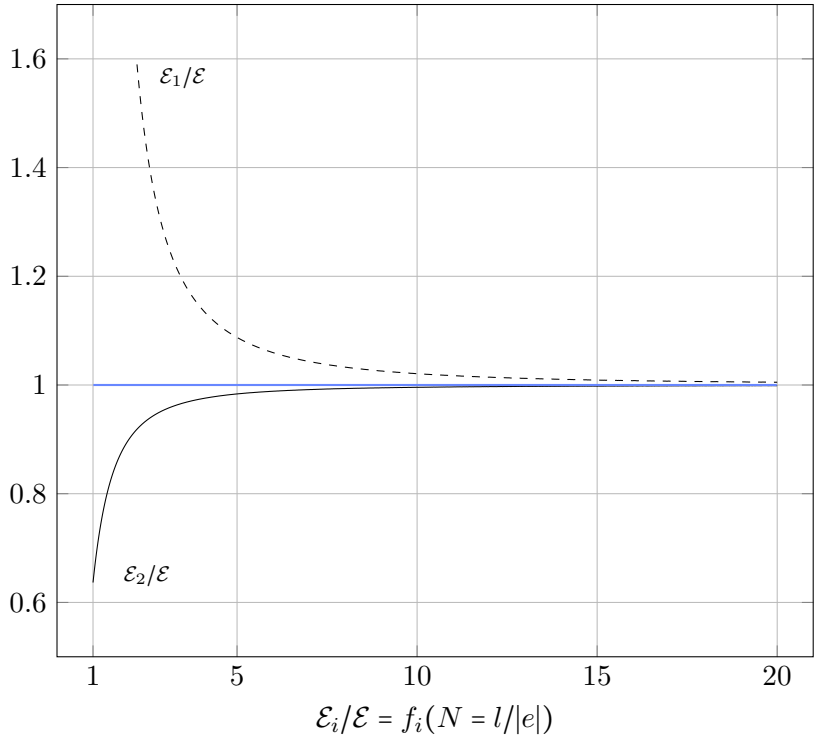


Figure 3.14 – Discrete curvature comparison for $\alpha \in [0.5, 2]$

**Elastica**

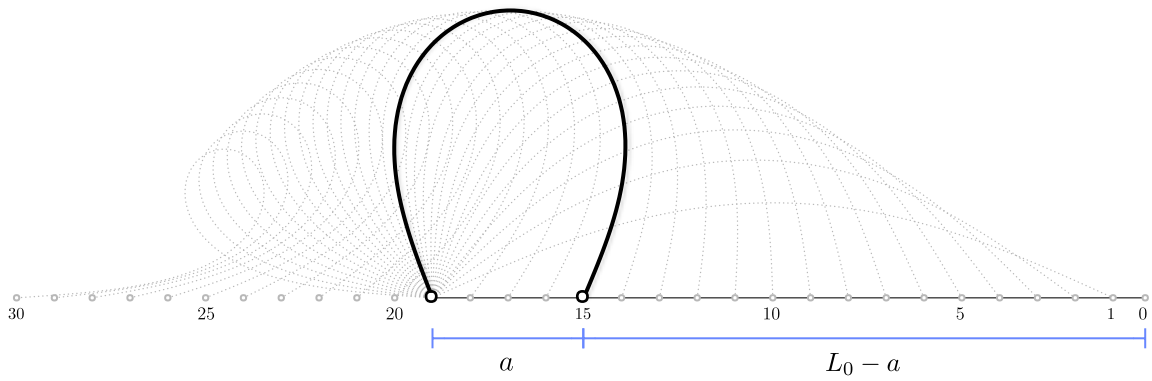


Figure 3.15 – Another definition of the osculating circle for arc-length parametrized curves.

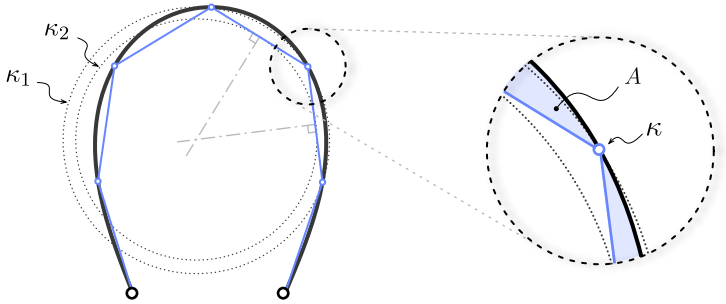


Figure 3.16 – Another definition of the osculating circle for arc-length parametrized curves.

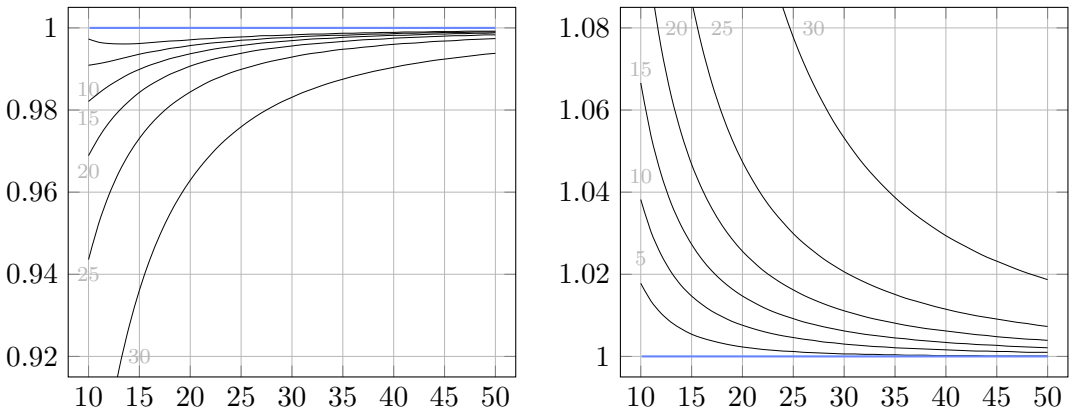


(a) $\mathcal{E}_1/\mathcal{E} = f(N = l/|e|)$ (b) $\mathcal{E}_2/\mathcal{E} = f(N = l/|e|)$

Figure 3.17 – Bending energy representativity

### 3.6.5 Edge versus vertex based tangent vector

Problème de définition. Facile de définir une tangente sur un edge. Mais une infinité de tangentes possibles à chaque vertex.

So in case of an arc-length parameterized curve the vertex tangent vector points in the same direction as the averaged edge tangent vectors [Hof08, p. 12].

Nous verrons que le cercle 3 points, en plus de mieux représenter l'énergie d'une courbe discrete dans les cas typiques, offre un choix de tangente non ambïgu.

## Bibliography

[BELT14] J. Bluth, Alain Ehrlacher, Baptiste Lefevre, and Frédéric Tayeb. Modélisation de poutres en torsion. Technical report, Na, Paris, 2014.

[Ber28] Johannis Bernoulli. *Johannis Bernoulli... Opera omnia, tam antea sparsim*

*edita, quam hactenus inedita*. Number IV. sumptibus Marci-Michaelis Bousquet, 1728.

[Bis75] Richard Bishop. There is more than one way to frame a curve. *Mathematical Association of America*, 1975.

[Blo90] Jules Bloomenthal. Calculation of reference frames along a space curve. In Andrew S Glassner, editor, *Graphics Gems*, volume 1, pages 567–571. Academic Press Professional, Inc., San Diego, CA, USA, 1990.

[BWR+08] Miklós Bergou, Max Wardetzky, Stephen Robinson, Basile Audoly, and Eitan Grinspun. Discrete elastic rods. *ACM SIGGRAPH*, pages 1–12, 2008.

[Coo13] Julian Lowell Coolidge. *A history of geometrical methods*. Dover Books on Mathematics. Dover Publications, 2013.

[Del07] Jean Delcourt. *Analyse et géométrie : les courbes gauches de Clairaut à Serret*. PhD thesis, Université de Paris VI, 2007.

[Del11] Jean Delcourt. Analyse et géométrie, histoire des courbes gauches de Clairaut à Darboux. *Archive for History of Exact Sciences*, 65(3):229–293, 2011.

[Eul75] Leonhard Euler. Continens analysin, pro incuruatione fili in fingulis punctis inueniendia. *Novi Commentarii academiae scientiarum Petropolitanae*, 19:340–370, 1775.

[FGSS14] Rida T. Farouki, Carlotta Giannelli, Maria Lucia Sampoli, and Alessandra Sestini. Rotation-minimizing osculating frames. *Computer Aided Geometric Design*, 31(1):27–42, 2014.

[Fre52] Frédéric Frenet. Sur les courbes à double courbure. *Journal de Mathématiques Pures et Appliquées*, 17:437–447, 1852.

[GAS06] Alfred Gray, Elsa Abbena, and Simon Salamon. *Modern differential geometry of curves and surfaces with Mathematica*. CRC Press, third edition, 2006.

[Gug89] H. Guggenheimer. Computing frames along a trajectory. *Computer Aided Geometric Design*, 6(1):77–78, 1989.

[HM95] Andrew J Hanson and Hui Ma. Parallel Transport Approach to Curve Framing. Technical report, 1995.

[Hof08] Tim Hoffmann. Discrete Differential Geometry of Curves and Surfaces, 2008.

[Klo86] Fopke Klok. Two moving coordinate frames for sweeping along a 3D trajectory. *Computer Aided Geometric Design*, 3(3):217–229, 1986.

[Men13] Toni Menninger. Frenet curves and successor curves : generic parametrizations of the helix and slant helix. Technical report, 2013.

[Mon09] Gaspard Monge. *Application de l'analyse à la géométrie*. 1809.

[PFL95] Tim Poston, Shiaofen Fang, and Wayne Lawton. Computing and approximating sweeping surfaces based on rotation minimizing frames. In *Proceedings of the 4th International Conference on CAD/CG*, pages 1–8, 1995.

[Pit26] Henri Pitot. Quadrature de la moitié d'une courbe des arcs appelée la compagne de la cycloïde. *Mémoires de l'Académie Royale des Sciences (1724)*, pages 107–113, 1726.

[WJZL08] Wenping Wang, Bert Jüttler, Dayue Zheng, and Yang Liu. Computation of rotation minimizing frames. *ACM Transactions on Graphics*, 27(1):1–18, 2008.

# 4 Elastic rod : variational approch

## 4.1 Introduction

### 4.1.1 Goals and contribution

In this section a novel element with 4 degrees of freedom accounting for torsion and bending behaviours is presented. The beam is considered in Kirchhoff's theory framework, so that it is supposed to be inextensible and its sections are supposed to remain orthogonal to the centreline during deformation. The reduction from the classic 6-DoF model to this 4-DoF model is achieved by an appropriate curve-angle representation based on a relevant curve framing. Energies are then formulated and leads to internal forces and moments acting on the beam. The static equilibrium is deduced from a damped fictitious dynamic with an adapted dynamic relaxation algorithm.

### 4.1.2 Related work

Basile [BAV+10] Basile [BWR+08] Basile [**?** ] Sina [**?** ] [Ful78], [dV05], [Vau00], [Ber09]

Dynamic relaxation : [Lew03] En particulier,voir pour un comparatif avec une méthode implicite.

### 4.1.3 Overview

1. quaternion pour piloter les input / ouput ?
2. calcul de la hessienne au moins pour les $\theta$ comme Audoly. Ne serait-ce pas possible pour les $x$ ? Avec ma technique du transport parallèle il me semble pourvoir avoir accès au DL à l'ordre 2 ...
3. Formulation pour les efforts ponctuels / moments extérieurs en vue d'une résolution

par minimisation. Voir F. Bertails

4. prise en compte des contraintes => méméthide des multiplicateurs de lagrange

## 4.2 Kirchhoff rod

The geometric configuration of the rod is described by its centerline $\boldsymbol{x}(s)$ and its cross sections. The centerline is parameterized by its arc-length. Cross sections orientations are followed along the centerline by their material frame $\{\boldsymbol{d}_3(s), \boldsymbol{d}_1(s), \boldsymbol{d}_2(s)\}$ which is an adapted orthonormal moving frame aligned to section's principal axes of inertia. Here, "adapted" means $\boldsymbol{d}_3(s) = \boldsymbol{x}'(s) = \boldsymbol{t}(s)$ is aligned to the centerline's tangent. In the literature, this description is also known as a *Cosserat Curve* [ST07].

### 4.2.1 Inextensibility

Note the previous description is only valid for inextensible rods in order to follow material points by their arc-length indifferently in their rest or deformed configuration. As explained in [AAP10], this hypothesis is usually relevant for slender beams. Indeed, in practice, if a slender member faces substantial axial strain the bending behaviour would become negligible due to the important difference between axial and bending stiffness. The length of the rod will be denoted $L$ and the arc-length $s$ will vary (with no loss of generality) in $[0, L]$.

### 4.2.2 Euler-Bernouilli

Strains are supposed to remain small so that material frame remains orthogonal to the centerline in the deformed configuration. Thus, differentiating the conditions of orthonormality leads to the following differential equations governing the evolution of $\{\boldsymbol{d}_3(s), \boldsymbol{d}_1(s), \boldsymbol{d}_2(s)\}$ along the centerline :

$$\begin{bmatrix} \mathbf{d_3}'(s) \\ \mathbf{d_1}'(s) \\ \mathbf{d_2}'(s) \end{bmatrix} = \begin{bmatrix} 0 & \kappa_2(s) & -\kappa_1(s) \\ -\kappa_2(s) & 0 & \tau(s) \\ \kappa_1(s) & -\tau(s) & 0 \end{bmatrix} \begin{bmatrix} \mathbf{d_3}(s) \\ \mathbf{d_1}(s) \\ \mathbf{d_2}(s) \end{bmatrix} \tag{4.1}$$

La théorie des poutres est une application de la théorie de l'élasticité isotrope. Pour mener les calculs de résistance des matériaux, on considère les hypothèses suivantes :

(1) hypothèse de Bernoulli : au cours de la déformation, les sections droites restent perpendiculaires à la courbe moyenne ;

(2) les sections droites restent planes selon Navier-Bernoulli (pas de gauchissement).

L'hypothèse de Bernoulli permet de négliger le cisaillement dans le cas de la flexion : le risque de rupture est alors due à l'extension des fibres situées à l'extérieur de la flexion, et

la flèche est due au moment fléchissant. Cette hypothèse n'est pas valable pour les poutres courtes car ces dernières sont hors des limites de validité du modèle de poutre, à savoir que la dimension des sections doit être petite devant la longueur de la courbe moyenne. Le cisaillement est pris en compte dans le modèle de Timoshenko et Mindlin.

### 4.2.3 Darboux vector

Those equations can be formulated with the *Darboux vector* of the chosen material frame, which represents the rotational velocity of the frame along $\boldsymbol{x}(s)$ :

$$\boldsymbol{d}_i'(s) = \boldsymbol{\Omega}_m(s) \times \boldsymbol{d}_i(s) \quad , \quad \boldsymbol{\Omega}_m(s) = \begin{bmatrix} \tau(s) \\ \kappa_1(s) \\ \kappa_2(s) \end{bmatrix} \tag{4.2}$$

Where $\kappa_1(s)$, $\kappa_2(s)$ and $\tau(s)$ represent respectively the rate of rotation of the material frame around the axis $\boldsymbol{d}_1(s)$, $\boldsymbol{d}_2(s)$ and $\boldsymbol{d}_3(s)$.

### 4.2.4 Curvatures and twist

The material curvatures are denoted $\kappa_1(s)$ and $\kappa_2(s)$ and represent the rod's flexion in the principal planes respectively normal to $\boldsymbol{d}_1(s)$ and $\boldsymbol{d}_2(s)$ .The material twist is denoted $\tau(s)$ and represents the section's rate of rotation around $\boldsymbol{d}_3(s)$. Those scalar functions measure directly the strain as defined in Kirchhoff's theory (Figure 4). Recall that the Frenet frame $\{\boldsymbol{t}(s), \boldsymbol{n}(s), \boldsymbol{b}(s)\}$ defines the osculating plane and the total curvature ($\kappa$) of a spatial curve :

$$\boldsymbol{t}'(s) = \kappa(s)\boldsymbol{n}(s) \quad , \quad \kappa(s) = \left\|\boldsymbol{t}'(s)\right\| \quad , \quad \boldsymbol{b}(s) = \boldsymbol{t}(s) \times \boldsymbol{n}(s) = \frac{\boldsymbol{t}(s) \times \boldsymbol{t}'(s)}{\kappa(s)} \tag{4.3}$$

To describe the osculating plane in which lies the bending part of the deformation, let's introduce the *curvature binormal* $\kappa\boldsymbol{b}(s) = \boldsymbol{t}(s) \times \boldsymbol{t}'(s)$, the vector of direction $\boldsymbol{b}(s)$ and norm $\kappa(s)$. At each point of arc-length $s$ the osculating plane is normal to $\kappa\boldsymbol{b}(s)$.

### 4.2.5 Elastic energy

Kirrchhoff's theory assigns an elastic energy to beams according to their strain [AAP10]. In this theory, a beam is supposed to be inextensible. Thus the elastic energy ($\mathcal{E}_p$) only accounts for torsion and bending behaviors and is given by :

$$\mathcal{E}_p = \tfrac{1}{2}\int_0^L EI_1(\kappa_1 - \overline{\kappa_1})^2 + EI_2(\kappa_2 - \overline{\kappa_2})^2 ds + \tfrac{1}{2}\int_0^L \beta(\tau - \bar{\tau})^2 ds \tag{4.4}$$

Here, $\overline{\kappa_1}$, $\overline{\kappa_2}$ and $\bar{\tau}$ denote the natural curvature and twist of the rod in the rest position (no stress).

## 4.3 Curve-angle representation

The previous paragraph has shown how the elastic potential energy of a rod can be computed following both its centerline and its cross sections orientations, which represents a model with 6-DoF : 3 for centerline positions and 3 for cross section orientations.

Following [BWR+08], let's introduce a reduced coordinate formulation of the rod that account for only 4-DoF. This reduction of DoF relies on the concept of zero-twisting frame which gives a reference frame with zero twist along a given centerline. Thus, cross section orientations $\{\boldsymbol{d}_3(s), \boldsymbol{d}_1(s), \boldsymbol{d}_2(s)\}$ can be tracked only by the measure of an angle $\theta$ from this reference frame denoted $\{\boldsymbol{d}_3(s), \boldsymbol{u}(s), \boldsymbol{v}(s)\}$ (Figure 5).

Note that an alternative solution could be to parameterize the global rotations of local material frame and to compute the rotation needed to align two successive frames along the curve's tangent.

Ici, expliquer la succession des dépendances : les vecteurs matériaux dépendent du repère de bishop par la seule variable theta. Le repère de bishop quand à lui est entièrement déterminé (au choix d'une constante de départ près) par la donnée de la centerline x.

Faire un schéma explicatif.

quid du transport parallèle en temps et non en espace ?

### 4.3.1 Zero-twisting frame

Zero-twisting frame, also known as Bishop frame, was introduced by Bishop in 1964. Bishop remarked that there was more than one way to frame a curve [Bis75]. Indeed, for a given curve, any orthonormal moving frame would satisfy the following differential equations, where $k_1(s)$, $k_2(s)$ and $\tau(s)$ are scalar functions that define completely the moving frame :

$$\begin{bmatrix} \mathbf{e_3}'(s) \\ \mathbf{e_1}'(s) \\ \mathbf{e_2}'(s) \end{bmatrix} = \begin{bmatrix} 0 & k_2(s) & -k_1(s) \\ -k_2(s) & 0 & \tau(s) \\ k_1(s) & -\tau(s) & 0 \end{bmatrix} \begin{bmatrix} \mathbf{e_3}(s) \\ \mathbf{e_1}(s) \\ \mathbf{e_2}(s) \end{bmatrix} \tag{4.5}$$

For instance, a Frenet frame $\{\boldsymbol{t}(s), \boldsymbol{n}(s), \boldsymbol{b}(s)\}$ is a frame which satisfies $k_1(s) = 0$. Note that this frame suffers from major disadvantages : it is undefined where the curvature vanishes and it flips at inflexion points. A Bishop frame $\{\boldsymbol{t}(s), \boldsymbol{u}(s), \boldsymbol{v}(s)\}$ is a frame which satisfies $\tau(s) = 0$. By construction, this frame has no angular velocity (i.e. no twist) around the curve's tangent ($\boldsymbol{u} \cdot \boldsymbol{v}' = \boldsymbol{u}' \cdot \boldsymbol{v} = 0$). Its evolution along the curve is described by the corresponding Darboux vector : $\boldsymbol{\Omega}_b(s) = \kappa \boldsymbol{b} = \boldsymbol{t} \times \boldsymbol{t}'$. Remark that $\boldsymbol{\Omega}_b(s)$ only depends on the centerline and is well defined even when the curvature vanishes.

Thus, by the help of $\boldsymbol{\Omega}_b(s)$, it's possible to transport a given vector $\boldsymbol{e}$ along the centerline with no twist : $\boldsymbol{e}' = \kappa \boldsymbol{b} \times \boldsymbol{e}$. This is called *parallel transport*.

## 4.4 Strains

### 4.4.1 Axial strain

There is no axial strain to be considered as far as the rod is supposed to be unstretchable.

Remark that the inextensibility hypothesis implies that any admissible perturbation ($\lambda \boldsymbol{h}_x$) of the rod's centerline ($\boldsymbol{x}$) is locally orthogonal to the centerline itself. Indeed, at each arc-length $s$ an inextensible rod must satisfies :

$$\|\boldsymbol{x}'\| = \|(\boldsymbol{x} + \lambda \boldsymbol{h}_x)'\| = 1 \Rightarrow \boldsymbol{d}_3 \cdot \boldsymbol{h}'_x = -\frac{\lambda^2}{2}\|\boldsymbol{h}'_x\|^2 = o(\lambda) \simeq 0 \tag{4.6}$$

In other words, this means that the same arc-length parametrization can be used to locate beam sections along the centerline along the deformation path. This would not be the case if the centerline would shorten or stretch out during its deformation. It is worth to mention here that this property ($\boldsymbol{d}_3 \cdot \boldsymbol{h}'_x = 0$) will be used several times in the following sections.

### 4.4.2 Bending strain

Let's compute the bending strains $\kappa_1$ and $\kappa_2$ regarding the geometric configuration of the rod. Remark that :

$$\kappa \boldsymbol{b} \cdot \boldsymbol{d}_1 = (\boldsymbol{d}_3 \times \boldsymbol{d}'_3) \cdot \boldsymbol{d}_1 = (\boldsymbol{d}_1 \times \boldsymbol{d}_3) \cdot \boldsymbol{d}'_3 = -\boldsymbol{d}_2 \cdot \boldsymbol{d}'_3 = \kappa_1 \tag{4.7a}$$

$$\kappa \boldsymbol{b} \cdot \boldsymbol{d}_2 = (\boldsymbol{d}_3 \times \boldsymbol{d}'_3) \cdot \boldsymbol{d}_2 = (\boldsymbol{d}_2 \times \boldsymbol{d}_3) \cdot \boldsymbol{d}'_3 = \boldsymbol{d}_1 \cdot \boldsymbol{d}'_3 = \kappa_2 \tag{4.7b}$$

That is to say $\kappa \boldsymbol{b}$ is orthogonal to $\boldsymbol{d}_3$ :

$$\kappa \boldsymbol{b} = \kappa_1 \boldsymbol{d}_1 + \kappa_2 \boldsymbol{d}_2 \tag{4.8}$$

Thus, the vector of material curvatures ($\boldsymbol{\omega}$) expressed on material frame axes $\{\boldsymbol{d}_1(s), \boldsymbol{d}_2(s)\}$ is defined as :

$$\boldsymbol{\omega} = \begin{bmatrix} \kappa_1 \\ \kappa_2 \end{bmatrix} = \begin{bmatrix} \kappa \boldsymbol{b} \cdot \boldsymbol{d}_1 \\ \kappa \boldsymbol{b} \cdot \boldsymbol{d}_2 \end{bmatrix} = \begin{bmatrix} -\boldsymbol{x}'' \cdot \boldsymbol{d}_2 \\ \boldsymbol{x}'' \cdot \boldsymbol{d}_1 \end{bmatrix} \tag{4.9}$$

### 4.4.3 Torsional strain

Let's compute the twist or torsional strain $\tau$ regarding the geometric configuration of the rod. Decomposing the material frame on the bishop frame gives :

$$\begin{bmatrix} \boldsymbol{d}_1 \\ \boldsymbol{d}_2 \end{bmatrix} = \begin{bmatrix} \cos\theta & \sin\theta \\ -\sin\theta & \cos\theta \end{bmatrix} \begin{bmatrix} \boldsymbol{u} \\ \boldsymbol{v} \end{bmatrix} \tag{4.10}$$

Thus, the twist can be identified directly as the variation of $\theta$ along the curve :

$$\tau = \boldsymbol{d}'_1 \cdot \boldsymbol{d}_2 = (\theta' \boldsymbol{d}_2 + \kappa \boldsymbol{b} \times \boldsymbol{d}_1) \cdot \boldsymbol{d}_2 = \theta' + \boldsymbol{d}_3 \cdot \kappa \boldsymbol{b} = \theta' \tag{4.11}$$

Note that the Frenet frame does not lead to a correct evaluation of the twist.

## 4.5 Elastic energy

Introducing $\boldsymbol{\omega}$ and $\theta$, the elastic energy can be rewritten as follow :

$$\mathcal{E}_p = \mathcal{E}_b + \mathcal{E}_t = \frac{1}{2}\int_0^L (\boldsymbol{\omega} - \overline{\boldsymbol{\omega}})^T B(\boldsymbol{\omega} - \overline{\boldsymbol{\omega}})ds + \frac{1}{2}\int_0^L \beta(\theta' - \overline{\theta'})^2 ds \tag{4.12}$$

Where $B$ is the bending stiffness matrix along the principal axes of inertia and $\beta$ is the torsional stiffness :

$$B = \begin{bmatrix} EI_1 & 0 \\ 0 & EI_2 \end{bmatrix} \quad , \quad \beta = GJ \tag{4.13}$$

Recall that the rod is supposed to be inextensible in Kirchhoff's theory. Thus, there is no stretching energy associated with an axial strain. However, this constraint may be enforced via a penalty energy, which in practice is somehow very similar as considering an axial stiffness into the beam's

Remark that the twisting energy ($\mathcal{E}_t$) only depends on $\theta$ and is independent regarding $\boldsymbol{x}$ while the bending energy ($\mathcal{E}_b$) depends on both $\theta$ and $\boldsymbol{x}$ variables (remind that $\kappa_1$ and $\kappa_2$ are the projections of $\kappa\boldsymbol{b}$ over $\boldsymbol{d}_1$ over $\boldsymbol{d}_2$). Thus, a coupling between bending and twisting appears as the minimum of the whole elastic energy is not necessarily reached for concomitant minimums of bending and twisting energies.

From this energy formulation, an interesting an well-known result on elastic rods could be highlighted : "torsion is uniform in an isotropic rod that is straight in its rest configuration" [ABW99].

Indeed, let's take an isotropic rod ($EI_1 = EI_2 = EI$) that is straight in its rest configuration ($\overline{\kappa_1} = \overline{\kappa_2} = 0$). Then, the bending energy becomes : $\mathcal{E}_b = EI_1\kappa_1^2 + EI_2\kappa_2^2 = EI\kappa^2$, and consequently doesn't depends on $\theta$ anymore. The curvature of the rod only depends on the geometry of its centerline ($\kappa = ||\kappa\boldsymbol{b}|| = ||\boldsymbol{x}' \times \boldsymbol{x}''||$). Thus, there is no more coupling between bending and twisting and the global minimum of elastic energy is reached while minimizing separately bending an twisting energies. That is to say the geometry of the rod ($\boldsymbol{x}$) is the one that minimized $\mathcal{E}_b$. The minimum of $\mathcal{E}_t$ is zero and is achieved for a uniform twist along the centerline, only prescribed by the boundary conditions.

## 4.6 Quasistatic assumption

Following [BWR+08], it is relevant to assume that the propagation of twist waves is instantaneous compared to the one of bending waves. Thus, internal forces $\boldsymbol{f}^{int}$ and moment of torsion $\boldsymbol{m}^{int}$ acts on two different timescales in the rod dynamic. Thus on the timescale of action of the force $\boldsymbol{f}^{int}$ on the center line, driving the bending waves, the twist

waves propagate instantaneously, so that $\forall s \in [0, L]$, $\delta\mathcal{E}_p/\delta\theta = 0$ for the computation of $\boldsymbol{f}^{int}$. This assumption may not be enforced, as in [**?** ], but leads to simpler and faster computations.

## 4.7 Energy gradient with respect to $\theta$ : moment of torsion

Internal moment of torsion and forces acting on the rod are classically obtained by differentiating the potential energy of the system with respect to $\theta$ and $\boldsymbol{x}$. Here, the calculus is a bit tricky as far as the differentiation takes place in function spaces. After a brief reminder on functional derivative, the main results of the calculations of the energy derivatives are given.

### 4.7.1 Derivative of material directors with respect to $\theta$

Recalling that $\theta$ and $\boldsymbol{x}$ are independant variables and that Bishop frame $\{\boldsymbol{u}, \boldsymbol{v}\}$ only depends on $\boldsymbol{x}$, the decomposition of material frame directors $\{\boldsymbol{d}_1, \boldsymbol{d}_2\}$ on Bishop frame leads directly to the following expression for the derivative of the material directors :

$$\boldsymbol{D}_\theta \boldsymbol{d}_1(s) \cdot h_\theta = \frac{d}{d\lambda} \boldsymbol{d}_1[\theta + \lambda h_\theta]\Big|_{\lambda=0} = (-\sin\theta\, \boldsymbol{u} + \cos\theta\, \boldsymbol{v}) \cdot h_\theta = \boldsymbol{d}_2 \cdot h_\theta \tag{4.14a}$$

$$\boldsymbol{D}_\theta \boldsymbol{d}_2(s) \cdot h_\theta = \frac{d}{d\lambda} \boldsymbol{d}_2[\theta + \lambda h_\theta]\Big|_{\lambda=0} = (-\cos\theta\, \boldsymbol{u} - \sin\theta\, \boldsymbol{v}) \cdot h_\theta = -\boldsymbol{d}_1 \cdot h_\theta \tag{4.14b}$$

### 4.7.2 Derivative of the material curvatures vector with respect to $\theta$

Regarding the definition of the material curvatures vector and the derivative of material directors with respect to $\theta$, it follows immediately that :

$$\boldsymbol{D}_\theta \boldsymbol{\omega}(s) \cdot h_\theta = \frac{d}{d\lambda} \boldsymbol{\omega}[\theta + \lambda h_\theta]\Big|_{\lambda=0} = \begin{bmatrix} \kappa \boldsymbol{b} \cdot \boldsymbol{d}_2 \\ -\kappa \boldsymbol{b} \cdot \boldsymbol{d}_1 \end{bmatrix} \cdot h_\theta = -\boldsymbol{J}\boldsymbol{\omega} \cdot h_\theta \tag{4.15}$$

Where $\boldsymbol{J}$ is the matrix that acts on two dimensional vectors by counter-clockwise rotation of angle $\frac{\pi}{2}$ :

$$\boldsymbol{J} = \begin{bmatrix} 0 & -1 \\ 1 & 0 \end{bmatrix} \tag{4.16}$$

### 4.7.3 Computation of the moment of torsion

The moment of torsion is given by the functional derivative of the potential elastic energy with respect to $\theta$ which can be decomposed according to the chaine rule :

$$\begin{aligned} \langle -m(s)\,; h_\theta \rangle = \boldsymbol{D}_\theta \mathcal{E}_p(s) \cdot h_\theta &= \boldsymbol{D}_\theta \mathcal{E}_b(s) \cdot h_\theta + \boldsymbol{D}_\theta \mathcal{E}_t(s) \cdot h_\theta \\ &= \boldsymbol{D}_\theta \mathcal{E}_b[\boldsymbol{\omega}[\theta]](s) \cdot h_\theta + \boldsymbol{D}_\theta \mathcal{E}_t[\theta](s) \cdot h_\theta \end{aligned} \tag{4.17}$$

### Derivative of the torsion energy with respect to $\theta$

Decomposing the previous calculus gives:

$$\begin{aligned}
\boldsymbol{D}_\theta \mathcal{E}_t[\theta](s)\cdot h_\theta &= \frac{d}{d\lambda}\mathcal{E}_t[\theta+\lambda h_\theta]\Big|_{\lambda=0} \\
&= \frac{d}{d\lambda}\left(\tfrac{1}{2}\int_0^L \beta\left((\theta+\lambda h_\theta)'-\overline{\theta}'\right)^2\,dt\right)\Big|_{\lambda=0} \\
&= \int_0^L \beta(\theta'-\overline{\theta}')\cdot h_\theta'\,dt \\
&= \left[\beta(\theta'-\overline{\theta}')\cdot h_\theta\right]_0^L - \int_0^L \left(\beta(\theta'-\overline{\theta}')\right)'\cdot h_\theta\,dt \\
&= \int_0^L \left(\beta(\theta'-\overline{\theta}')(\delta_L-\delta_0) - \left(\beta(\theta'-\overline{\theta}')\right)'\right)\cdot h_\theta\,dt
\end{aligned} \tag{4.18}$$

### Derivative of the bending energy with respect to $\theta$

The derivative of $\mathcal{E}_b$ is obtained with the chaine rule :

$$\begin{aligned}
\boldsymbol{D}_\omega \mathcal{E}_b[\boldsymbol{\omega}](s)\cdot \boldsymbol{h}_\omega &= \frac{d}{d\lambda}\mathcal{E}_b[\boldsymbol{\omega}+\lambda\boldsymbol{h}_\omega]\Big|_{\lambda=0} \\
&= \frac{d}{d\lambda}\left(\tfrac{1}{2}\int_0^L \left((\boldsymbol{\omega}+\lambda\boldsymbol{h}_\omega)-\overline{\boldsymbol{\omega}}\right)^T \boldsymbol{B}\left((\boldsymbol{\omega}+\lambda\boldsymbol{h}_\omega)-\overline{\boldsymbol{\omega}}\right)\,dt\right)\Big|_{\lambda=0} \\
&= \int_0^L (\boldsymbol{\omega}-\overline{\boldsymbol{\omega}})^T\boldsymbol{B}\cdot\boldsymbol{h}_\omega\,dt
\end{aligned} \tag{4.19}$$

Finally, reminding eq 4.14 :

$$\begin{aligned}
\boldsymbol{D}_\theta \mathcal{E}_b[\boldsymbol{\omega}[\theta]](s)\cdot h_\theta &= \boldsymbol{D}_\omega \mathcal{E}_b[\boldsymbol{\omega}](s)\cdot(\boldsymbol{D}_\theta\boldsymbol{\omega}[\theta](s)\cdot h_\theta) \\
&= -\int_0^L (\boldsymbol{\omega}-\overline{\boldsymbol{\omega}})^T\boldsymbol{B}\boldsymbol{J}\boldsymbol{\omega}\cdot h_\theta\,dt
\end{aligned} \tag{4.20}$$

### Moment of torsion

Thus, the

$$\begin{aligned}
\langle -m(s)\,;h_\theta\rangle &= \boldsymbol{D}_\theta \mathcal{E}_b[\boldsymbol{\omega}[\theta]](s)\cdot h_\theta + \boldsymbol{D}_\theta \mathcal{E}_t[\theta](s)\cdot h_\theta \\
&= \int_0^L \left(\left(\beta(\theta'-\overline{\theta}')(\delta_L-\delta_0) - \left(\beta(\theta'-\overline{\theta}')\right)'\right) - (\boldsymbol{\omega}-\overline{\boldsymbol{\omega}})^T\boldsymbol{B}\boldsymbol{J}\boldsymbol{\omega}\right)\cdot h_\theta\,dt
\end{aligned} \tag{4.21}$$

Finally, we can conclude on the expression of the internal moment of torsion :

$$m(s) = -\left(\beta(\theta'-\overline{\theta}')(\delta_L-\delta_0) - \left(\beta(\theta'-\overline{\theta}')\right)'\right) + (\boldsymbol{\omega}-\overline{\boldsymbol{\omega}})^T\boldsymbol{B}\boldsymbol{J}\boldsymbol{\omega} \tag{4.22}$$

### Quasistatic hypothesis

$$\left(\beta(\theta'-\overline{\theta}')\right)' + (\boldsymbol{\omega}-\overline{\boldsymbol{\omega}})^T\boldsymbol{B}\boldsymbol{J}\boldsymbol{\omega} = 0 \tag{4.23}$$

## 4.8 Energy gradient with respect to $x$ : internal forces

Internal torsional moments and forces acting on the rod are classically obtained by differentiating the potential energy of the system with respect to $\theta$ and $\boldsymbol{x}$. Here, the calculus is a bit tricky as far as the differentiation takes place in function spaces. After a brief reminder on functional derivative, the main results of the calculations of the energy derivatives are given.

paragraphe entièrment à revoir. Expliquer le cheminement. x fixe bishop et theta fixe d1,d2 par rapport à bishop. x est indépendant de theta. Seul des CL peuvent créer des couplages entre x et theta

Donc les vrais degrés de liberté du problème sont en fait les vecteurs matériels et les positions x. Se reporter à une modélisation du pb dans SO3 comme Spillmann par exemple.

Le calcul des gradients se résume donc à calculer les gradients des vecteurs matériels par rapport à des perturbations infinitésimales en x et theta. Pour theta, c'est facile. Pour kb, c'est facile. Reste la variation par rapport à x, qui est en fait la variation de bishop qu'on explique avec le writhe (défaut de fermeture de bishop sur une boucle fermée) et le transport parallèle. Le calcul se fait aisément en écrivant la double rotation et en effectuant le DL au premier ordre.

Le reste est quasiment immédiat. Reste la question des CL et des termes aux bords.

Il faut aussi se positionner par rapport à l'article de Basile. Regarder la question applied displacement vs settlement pour imposer une CL.

### 4.8.1 Derivative of material directors with respect to $\boldsymbol{x}$

ici expliquer le fonctionnement de la figure

A variation of the centerline $\boldsymbol{x}$ by $\boldsymbol{\epsilon} = \lambda \boldsymbol{h}_x$ would cause a variation in the Bishop frame because parallel transport depends on the centerline itself. As far as $\boldsymbol{x}$ and $\theta$ are independent variables, this leads necessarily to a variation of the material frame. Let us denote :

- $F = \{\boldsymbol{t}, \boldsymbol{u}, \boldsymbol{v}\}$ : the Bishop frame in the reference configuration ;
- $F_\epsilon = \{\boldsymbol{t}_\epsilon, \boldsymbol{u}_\epsilon, \boldsymbol{v}_\epsilon\}$ : the Bishop frame in the deformed configuration ;
- $\tilde{F}_\epsilon = \{\boldsymbol{t}, \tilde{\boldsymbol{u}}_\epsilon, \tilde{\boldsymbol{v}}_\epsilon\}$ : the frame obtained by parallel transporting $F_\epsilon$ back on $F$.

What we want to achive is to write at arc-length $s$ the Bishop frame in the deformed configuration $\{\boldsymbol{t}_\epsilon, \boldsymbol{u}_\epsilon, \boldsymbol{v}_\epsilon\}$ on the Bishop frame in the reference configuration $\{\boldsymbol{t}, \boldsymbol{u}, \boldsymbol{v}\}$ for a small perturbation $\epsilon$ of the centerline. This transformation can be decomposed in two rotations :

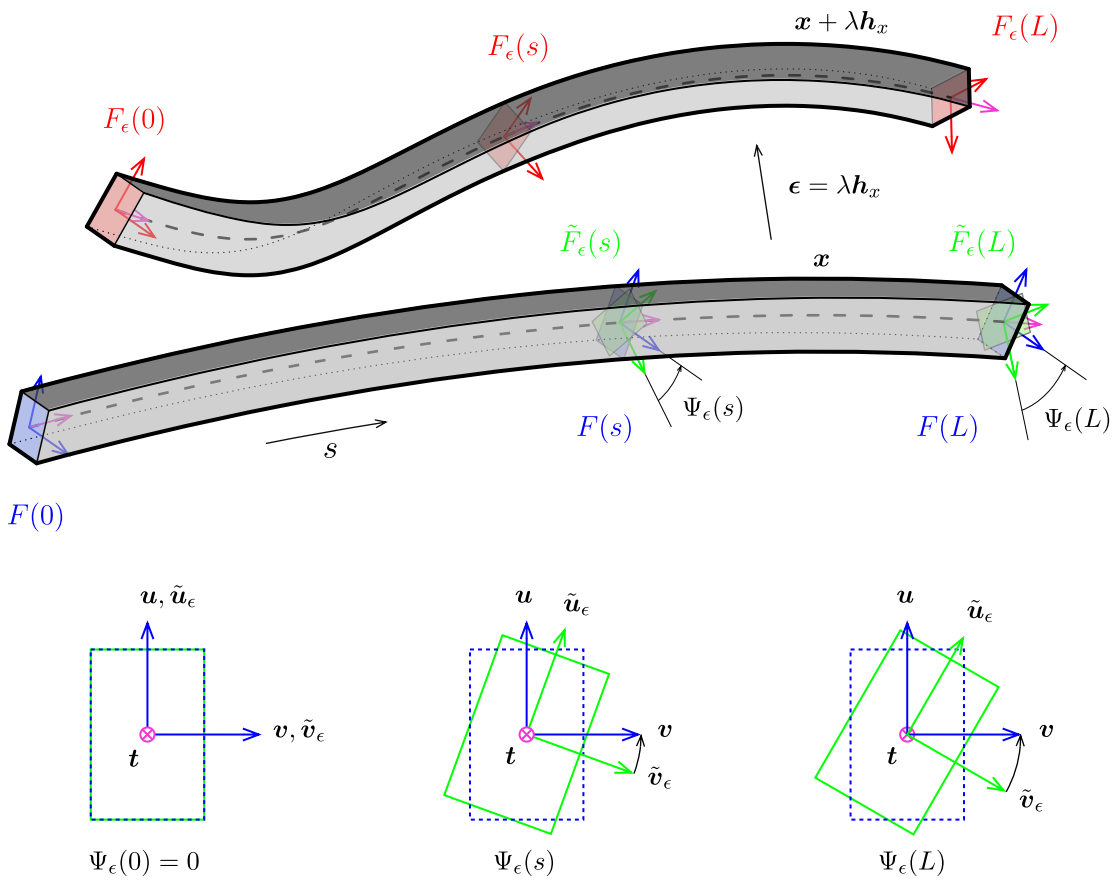


Figure 4.1 – Repères de Frenet attachés à $\gamma$.

- $F_\epsilon \to \tilde{F}_\epsilon$ : parallel transporting $F_\epsilon$ from $\boldsymbol{t}_\epsilon$ to $\boldsymbol{t}$. This is equivalent to a rotation around $\boldsymbol{t}_\epsilon \times \boldsymbol{t}$ by an angle $\alpha_\epsilon$.
- $\tilde{F}_\epsilon \to F$ : aligning $\tilde{F}_\epsilon$ over $F$. This is equivalent to a rotation around $\boldsymbol{t}$ of an angle $\Psi_\epsilon$.

Firstly, let's decompose $\{\boldsymbol{t}_\epsilon, \boldsymbol{u}_\epsilon, \boldsymbol{v}_\epsilon\}$ on the basis $\{\boldsymbol{t}, \tilde{\boldsymbol{u}}_\epsilon, \tilde{\boldsymbol{v}}_\epsilon\}$. Note that $\tilde{F}_\epsilon$ is expressed by rotating $\tilde{F}_\epsilon$ by an angle $\Psi_\epsilon[\boldsymbol{x}](s)$ around $\boldsymbol{t}$ because $\tilde{F}_\epsilon$ is obtained by parallel transporting $F_\epsilon$ from $\boldsymbol{t}_\epsilon$ to $\boldsymbol{t}$.

### Calculation of $\Psi_\epsilon$

This variation is closely related to the writhe of closed curves. As explained in [Ful78] when parallel transporting an adapted frame around a closed curve it might not realigned with itself after one complete loop. This "lack of alignement" is directly measured by the change of writhe which can be computed with Fuller's Formula [Ful78].

Note that the derivative of $\theta$ with respect to $\boldsymbol{x}$ can be evaluated by the change of writhe in the curve as suggested in [dV05]. This approach is completly equivalent.

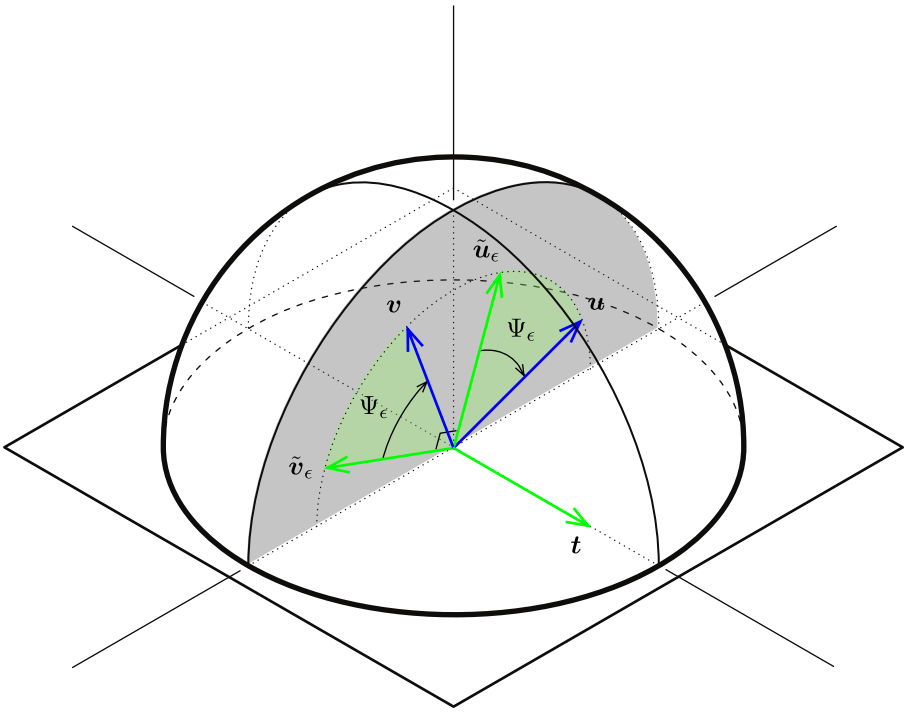


Figure 4.2 – $F$ is obtained by rotating $\tilde{F}_\epsilon$ around $\boldsymbol{t}$ of an angle $\Psi_\epsilon$.

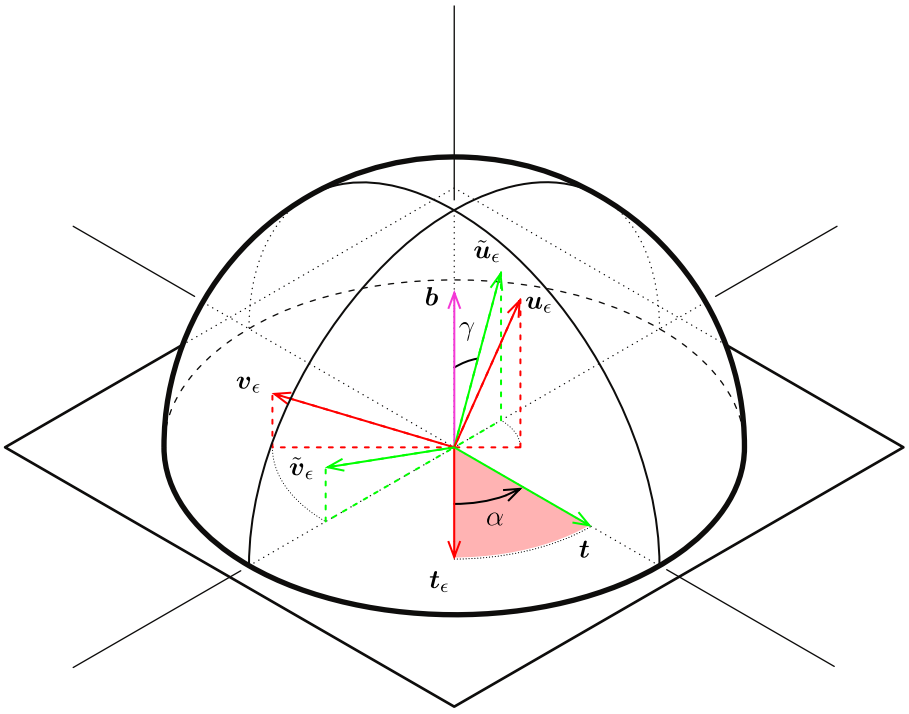


Figure 4.3 – $\tilde{F}_\epsilon$ is obtained by parallel tranpsporting $F_\epsilon$ from $\boldsymbol{t}_\epsilon$ to $\boldsymbol{t}$. This operation could be seen as a rotation around $\boldsymbol{t}_\epsilon \times \boldsymbol{t}$ of an angle $\alpha_\epsilon$.

One can also see this lack of alignement in terms of rotation. Parallel transport being a propagation of frame from $s = 0$, the cumulated rotation of Bishop frame from the deformed configuration around the initial configuration at arc-length $s$ is the cumulated angle of rotation of $\boldsymbol{u}[\boldsymbol{x} + \lambda \boldsymbol{h}_x]$ around $\boldsymbol{d}_3[\boldsymbol{x}]$. Recalling the rotation rate of $\boldsymbol{u}[\boldsymbol{x} + \lambda \boldsymbol{h}_x]$ is $\kappa \boldsymbol{b}[\boldsymbol{x} + \lambda \boldsymbol{h}_x]$ by definition of zero-twisting frame, one can write :

$$\Psi_\epsilon[\boldsymbol{x}](s) = -\int_0^s \kappa \boldsymbol{b}[\boldsymbol{x} + \lambda \boldsymbol{h}_x] \cdot \boldsymbol{d}_3[\boldsymbol{x}]\, dt \tag{4.24}$$

The calculation of $\kappa \boldsymbol{b}[\boldsymbol{x} + \lambda \boldsymbol{h}_x]$ is straight forward from the curvature binormal definition :

$$\begin{aligned} \kappa \boldsymbol{b}[\boldsymbol{x} + \lambda \boldsymbol{h}_x] &= (\boldsymbol{x} + \lambda \boldsymbol{h}_x)' \times (\boldsymbol{x} + \lambda \boldsymbol{h}_x)'' \\ &= \kappa \boldsymbol{b}[\boldsymbol{x}] + \lambda(\boldsymbol{x}' \times \boldsymbol{h}_x'' + \boldsymbol{h}_x' \times \boldsymbol{x}'') + \lambda^2(\boldsymbol{h}_x' \times \boldsymbol{h}_x'') \\ &= \kappa \boldsymbol{b}[\boldsymbol{x}] + \lambda(\boldsymbol{x}' \times \boldsymbol{h}_x'' + \boldsymbol{h}_x' \times \boldsymbol{x}'') + o(\lambda) \end{aligned} \tag{4.25}$$

Thus, reminding that $\boldsymbol{d}_3[\boldsymbol{x}] = \boldsymbol{x}'$ and $\kappa \boldsymbol{b}[\boldsymbol{x}] \cdot \boldsymbol{d}_3[\boldsymbol{x}] = 0$, and using the invariance of circular product by cyclic permutation, one can express :

$$\begin{aligned} \Psi_\epsilon[\boldsymbol{x}](s) &= -\int_0^s \kappa \boldsymbol{b}[\boldsymbol{x} + \lambda \boldsymbol{h}_x] \cdot \boldsymbol{d}_3[\boldsymbol{x}]\, dt \\ &= -\lambda \int_0^s (\boldsymbol{x}' \times \boldsymbol{h}_x'' + \boldsymbol{h}_x' \times \boldsymbol{x}'') \cdot \boldsymbol{x}'\, dt + o(\lambda) \\ &= -\lambda \int_0^s \kappa \boldsymbol{b}[\boldsymbol{x}] \cdot \boldsymbol{h}_x'\, dt + o(\lambda) \end{aligned} \tag{4.26}$$

By integration by parts, dropping the implicit reference to $\boldsymbol{x}$ in the notation, and denoting by $\delta_s$ and $H_s$ the Dirac function and the Heaviside step function centered at $s$, $\Psi_\epsilon(s)$ could be rewritten as :

$$\begin{aligned} \Psi_\epsilon(s) &= -\lambda \int_0^s \kappa \boldsymbol{b} \cdot \boldsymbol{h}_x'\, dt + o(\lambda) \\ &= -\lambda \left( \left[ \kappa \boldsymbol{b} \cdot \boldsymbol{h}_x \right]_0^s - \int_0^s \kappa \boldsymbol{b}' \cdot \boldsymbol{h}_x\, dt \right) + o(\lambda) \\ &= -\lambda \left( \int_0^s \left( (\delta_s - \delta_0)\, \kappa \boldsymbol{b} - \kappa \boldsymbol{b}' \right) \cdot \boldsymbol{h}_x\, dt \right) + o(\lambda) \\ &= -\lambda \left( \int_0^L \left( (\delta_s - \delta_0)\, \kappa \boldsymbol{b} - (1 - H_s) \kappa \boldsymbol{b}' \right) \cdot \boldsymbol{h}_x\, dt \right) + o(\lambda) \end{aligned} \tag{4.27}$$

Note that, as expected, $\Psi_\epsilon(s)$ is in first order of $\lambda$ and thus gets negligible when $\lambda$ tends to zero, that is to say when the perturbation of $\boldsymbol{x}$ is infinitesimal :

$$\lim_{\lambda \to 0} \Psi_\epsilon(s) = 0 \tag{4.28}$$

$H_s : t \mapsto \begin{cases} 0, & t < s \\ 1, & t \geqslant s \end{cases}$ est la fonction de Heaviside.

$\delta_s : t \mapsto \delta(t - s)$ est la distribution de dirac centrée en $s$.

### Calculation of $\alpha_\epsilon$

Recall that $\tilde{F_\epsilon}$ is obtained by parallel tranpsporting $F_\epsilon$ from $\boldsymbol{t_\epsilon}$ to $\boldsymbol{t}$. $\tilde{F_\epsilon}$ results from the rotation of $F_\epsilon$ around $\boldsymbol{b} = \boldsymbol{t_\epsilon} \times \boldsymbol{t}$ by an angle $\alpha_\epsilon$.

Recall from (4.6) that because the rod is supposed to be unstretchable, $\boldsymbol{t_\epsilon}$ stays collinear to $\boldsymbol{t}$ for an infinitesimal perturbation of the centerline :

$$\|\boldsymbol{t}\| = \|\boldsymbol{t_\epsilon}\| = 1 \Rightarrow (\boldsymbol{x} + \boldsymbol{\epsilon})' \cdot (\boldsymbol{x} + \boldsymbol{\epsilon})' = 1 \Leftrightarrow \boldsymbol{x}' \cdot \boldsymbol{\epsilon}' = -\tfrac{\lambda^2}{2} \|\boldsymbol{h}_x'\|^2 \tag{4.29}$$

Which leeds to :

$$\cos \alpha_\epsilon(s) = \boldsymbol{t} \cdot \boldsymbol{t_\epsilon} = \boldsymbol{x}' \cdot (\boldsymbol{x} + \boldsymbol{\epsilon})' = 1 + \boldsymbol{x}' \cdot \boldsymbol{\epsilon}' = 1 - \tfrac{\lambda^2}{2} \|\boldsymbol{h}_x'\|^2 \tag{4.30}$$

Thus, at second order in $\lambda$ :

$$\cos \alpha_\epsilon = 1 - \tfrac{\lambda^2}{2} \|\boldsymbol{h}_x'\|^2 \tag{4.31a}$$

$$\sin \alpha_\epsilon = \sqrt{1 - \cos^2 \alpha_\epsilon} = \lambda \|\boldsymbol{h}_x'\| + o(\lambda^2) \tag{4.31b}$$

$$\sin^2 \alpha_\epsilon / 2 = \tfrac{\lambda^2}{4} \|\boldsymbol{h}_x'\|^2 \tag{4.31c}$$

Finally, it's possible to conclude that $\alpha_\epsilon(s)$ is in first order of $\lambda$ and thus gets negligible when $\lambda$ tends to zero :

$$\lim_{\lambda \to 0} \alpha_\epsilon(s) = 0 \tag{4.32}$$

### Aligning $\tilde{F_\epsilon}$ towards $F_\epsilon$

Recall that aligning $\tilde{F_\epsilon}$ over $F$ is nothing but a rotation around $\boldsymbol{t}$ by an angle $\Psi_\epsilon$. This leads to :

$$\tilde{\boldsymbol{u}}_\epsilon = \cos \Psi_\epsilon \, \boldsymbol{u} + \sin \Psi_\epsilon \, \boldsymbol{v} \tag{4.33a}$$

$$\tilde{\boldsymbol{v}}_\epsilon = -\sin \Psi_\epsilon \, \boldsymbol{u} + \cos \Psi_\epsilon \, \boldsymbol{v} \tag{4.33b}$$

### Aligning $F_\epsilon$ towards $\boldsymbol{t}$

Recall that $\tilde{F_\epsilon}$ is obtained by parallel tranpsporting $F_\epsilon$ from $\boldsymbol{t_\epsilon}$ to $\boldsymbol{t}$. This operation could be seen as a rotation around $\boldsymbol{t_\epsilon} \times \boldsymbol{t}$ of an angle $\alpha_\epsilon$. Where :

$$\boldsymbol{b} = \boldsymbol{t_\epsilon} \times \boldsymbol{t} = \cos \gamma \, \tilde{\boldsymbol{u}}_\epsilon + \sin \gamma \, \tilde{\boldsymbol{v}}_\epsilon = \cos \gamma \, \boldsymbol{u}_\epsilon + \sin \gamma \, \boldsymbol{v}_\epsilon \tag{4.34}$$

Expressing $F_\epsilon$ on the basis $\tilde{F}_\epsilon$ gives for $\boldsymbol{u}_\epsilon$ and $\boldsymbol{v}_\epsilon$ :

$$\boldsymbol{u}_\epsilon = \sin\gamma\, \boldsymbol{b} + \cos\gamma \left( \sin\alpha_\epsilon\, \tilde{\boldsymbol{t}} + \cos\alpha_\epsilon \left( \cos\gamma\, \tilde{\boldsymbol{u}}_{\boldsymbol{\epsilon}} - \sin\gamma\, \tilde{\boldsymbol{v}}_{\boldsymbol{\epsilon}} \right) \right) \tag{4.35a}$$

$$\boldsymbol{v}_\epsilon = \cos\gamma\, \boldsymbol{b} + \sin\gamma \left( -\sin\alpha_\epsilon\, \tilde{\boldsymbol{t}} + \cos\alpha_\epsilon \left( \sin\gamma\, \tilde{\boldsymbol{u}}_{\boldsymbol{\epsilon}} - \cos\gamma\, \tilde{\boldsymbol{v}}_{\boldsymbol{\epsilon}} \right) \right) \tag{4.35b}$$

Which can be rearranged in :

$$\boldsymbol{u}_\epsilon = \cos\gamma \sin\alpha_\epsilon\, \boldsymbol{t} + (\cos\alpha_\epsilon \cos^2\gamma + \cos^2\gamma)\tilde{\boldsymbol{u}}_{\boldsymbol{\epsilon}} + \sin\gamma\cos\gamma\,(1-\cos\alpha_\epsilon)\tilde{\boldsymbol{v}}_{\boldsymbol{\epsilon}} \tag{4.36a}$$

$$\boldsymbol{v}_\epsilon = -\sin\gamma \sin\alpha_\epsilon\, \boldsymbol{t} + \cos\gamma\sin\gamma\,(1-\cos\alpha_\epsilon)\tilde{\boldsymbol{u}}_{\boldsymbol{\epsilon}} + (\cos^2\gamma + \cos\alpha_\epsilon \sin^2\gamma)\tilde{\boldsymbol{v}}_{\boldsymbol{\epsilon}} \tag{4.36b}$$

### Variation of Bishop frame with respect to $\boldsymbol{x}$

Finally, one can express $F_\epsilon$ on the basis $F$ as the composition of two rotations :

$$\boldsymbol{u}_\epsilon = \begin{bmatrix} 1 & 0 & 0 \\ 0 & \cos\Psi_\epsilon & -\sin\Psi_\epsilon \\ 0 & \sin\Psi_\epsilon & \cos\Psi_\epsilon \end{bmatrix} \begin{bmatrix} \cos\gamma\sin\alpha_\epsilon \\ 1 - 2\cos^2\gamma\sin^2\alpha_\epsilon/2 \\ 2\sin\gamma\cos\gamma\sin^2\alpha_\epsilon/2 \end{bmatrix} = \begin{bmatrix} \alpha_\epsilon\cos\gamma \\ 1 \\ \Psi_\epsilon \end{bmatrix} + o(\lambda) \tag{4.37a}$$

$$\boldsymbol{v}_\epsilon = \begin{bmatrix} 1 & 0 & 0 \\ 0 & \cos\Psi_\epsilon & -\sin\Psi_\epsilon \\ 0 & \sin\Psi_\epsilon & \cos\Psi_\epsilon \end{bmatrix} \begin{bmatrix} -\sin\gamma\sin\alpha_\epsilon \\ 2\sin\gamma\cos\gamma\sin^2\alpha_\epsilon/2 \\ 1 - 2\sin\gamma^2\sin^2\alpha_\epsilon/2 \end{bmatrix} = \begin{bmatrix} -\alpha_\epsilon\sin\gamma \\ -\Psi_\epsilon \\ 1 \end{bmatrix} + o(\lambda) \tag{4.37b}$$

Here, the expressions have been developed in first order of $\lambda$ as far as $\alpha_\epsilon$ and $\Psi_\epsilon$ it's been proofed in eq [] that those quantities tends two zero when the perturbation of the centerline is infinitesimal.

Finally, one can express the variation of material directors with respect to an infinitesimal variation of rod's centerline :

$$\boldsymbol{u}_\epsilon = \alpha_\epsilon\cos\gamma\, \boldsymbol{t} + \boldsymbol{u} + \Psi_\epsilon \boldsymbol{v} + o(\lambda) \tag{4.38a}$$

$$\boldsymbol{v}_\epsilon = -\alpha_\epsilon\sin\gamma\, \boldsymbol{t} + \boldsymbol{v} - \Psi_\epsilon \boldsymbol{u} + o(\lambda) \tag{4.38b}$$

### Variation of material frame with respect to $\boldsymbol{x}$

Recalling the expression of the material frame expressed in the reference Bishop frame, it's now easy to deduce the variation of material frame with respect to a variation of the rod's centerline :

$$\boldsymbol{d}_1[\boldsymbol{x} + \lambda\boldsymbol{h}_x] = \cos\theta\, \boldsymbol{u}_\epsilon + \sin\theta\, \boldsymbol{v}_\epsilon \tag{4.39a}$$

$$\boldsymbol{d}_2[\boldsymbol{x} + \lambda\boldsymbol{h}_x] = -\sin\theta\, \boldsymbol{u}_\epsilon + \cos\theta\, \boldsymbol{v}_\epsilon \tag{4.39b}$$

Which leads according to the previous equation to :

$$\boldsymbol{d}_1[\boldsymbol{x} + \lambda\boldsymbol{h}_x] = \boldsymbol{d}_1[\boldsymbol{x}] + \Psi_\epsilon \boldsymbol{d}_2[\boldsymbol{x}] + \alpha_\epsilon\cos(\theta-\gamma)\, \boldsymbol{t}[\boldsymbol{x}] + o(\lambda) \tag{4.40a}$$

$$\boldsymbol{d}_2[\boldsymbol{x} + \lambda\boldsymbol{h}_x] = \boldsymbol{d}_2[\boldsymbol{x}] - \Psi_\epsilon \boldsymbol{d}_1[\boldsymbol{x}] - \alpha_\epsilon\sin(\theta+\gamma)\, \boldsymbol{t}[\boldsymbol{x}] + o(\lambda) \tag{4.40b}$$

### 4.8.2 Derivative of the material curvatures vector with respect to $\boldsymbol{x}$

It's know straightforward from the previous section to express the variation of the material curvatures with respect to a variation $\boldsymbol{\epsilon} = \lambda \boldsymbol{h}_x$ of $\boldsymbol{x}$ while $\theta$ remains unchanged.

$$(\boldsymbol{x} + \lambda \boldsymbol{h}_x)'' \cdot \boldsymbol{d}_1[\boldsymbol{x} + \lambda \boldsymbol{h}_x] = (\boldsymbol{x}'' + \lambda \boldsymbol{h}_x'') \cdot \Big(\boldsymbol{d}_1 + \Psi_\epsilon \boldsymbol{d}_2 + \alpha_\epsilon \cos(\theta - \gamma)\, \boldsymbol{t} + o(\lambda)\Big) \tag{4.41a}$$

$$(\boldsymbol{x} + \lambda \boldsymbol{h}_x)'' \cdot \boldsymbol{d}_2[\boldsymbol{x} + \lambda \boldsymbol{h}_x] = (\boldsymbol{x}'' + \lambda \boldsymbol{h}_x'') \cdot \Big(\boldsymbol{d}_2 - \Psi_\epsilon \boldsymbol{d}_1 - \alpha_\epsilon \sin(\theta + \gamma)\, \boldsymbol{t} + o(\lambda)\Big) \tag{4.41b}$$

Thus, recalling that $\boldsymbol{x}'' \cdot \boldsymbol{d}_3 = 0$ and that $\alpha_\epsilon$ and $\Psi_\epsilon$ are first order quantities in $\lambda$ :

$$(\boldsymbol{x} + \lambda \boldsymbol{h}_x)'' \cdot \boldsymbol{d}_1[\boldsymbol{x} + \lambda \boldsymbol{h}_x] = \boldsymbol{x}'' \cdot \boldsymbol{d}_1 + \Psi_\epsilon \boldsymbol{x}'' \cdot \boldsymbol{d}_2 + \lambda \boldsymbol{h}_x'' \cdot \boldsymbol{d}_1 + o(\lambda) \tag{4.42a}$$

$$(\boldsymbol{x} + \lambda \boldsymbol{h}_x)'' \cdot \boldsymbol{d}_2[\boldsymbol{x} + \lambda \boldsymbol{h}_x] = \boldsymbol{x}'' \cdot \boldsymbol{d}_2 - \Psi_\epsilon \boldsymbol{x}'' \cdot \boldsymbol{d}_1 + \lambda \boldsymbol{h}_x'' \cdot \boldsymbol{d}_2 + o(\lambda) \tag{4.42b}$$

Which finally leads to :

$$\boldsymbol{\omega}[\boldsymbol{x} + \lambda \boldsymbol{h}_x] = \boldsymbol{\omega}[\boldsymbol{x}] - \Psi_\epsilon \boldsymbol{J}\boldsymbol{\omega}[\boldsymbol{x}] + \lambda \begin{bmatrix} -\boldsymbol{h}_x'' \cdot \boldsymbol{d}_2 \\ \boldsymbol{h}_x'' \cdot \boldsymbol{d}_1 \end{bmatrix} + o(\lambda) \tag{4.43}$$

Reminding the expression of $\Psi_\epsilon$ computed in paragraphe[], one can express the derivative of the material curvatures vector with respect to $\boldsymbol{x}$ :

$$\boldsymbol{D}_x\boldsymbol{\omega}(s) \cdot \boldsymbol{h}_x = \left( \int_0^L \Big( (\delta_s - \delta_0)\, \kappa \boldsymbol{b} - (1 - H_s) \kappa \boldsymbol{b}' \Big) \cdot \boldsymbol{h}_x \, dt \right) \boldsymbol{J}\boldsymbol{\omega} + \begin{bmatrix} -\boldsymbol{d}_2{}^T \\ \boldsymbol{d}_1{}^T \end{bmatrix} \cdot \boldsymbol{h}_x'' \tag{4.44}$$

### 4.8.3 Computation of the forces acting on the centerline

The forces acting on the centerline are given by the functional derivative of the potential elastic energy with respect to $x$ which can be decomposed according to the chaine rule :

$$\begin{aligned} \langle -f(s)\,; \boldsymbol{h}_x \rangle = \boldsymbol{D}_x \mathcal{E}_p(s) \cdot \boldsymbol{h}_x &= \boldsymbol{D}_x \mathcal{E}_b(s) \cdot \boldsymbol{h}_x + \boldsymbol{D}_x \mathcal{E}_t(s) \cdot \boldsymbol{h}_x \\ &= \boldsymbol{D}_x \mathcal{E}_b[\boldsymbol{\omega}[\boldsymbol{x}]](s) \cdot \boldsymbol{h}_x + \boldsymbol{D}_x \mathcal{E}_t[\boldsymbol{x}](s) \cdot \boldsymbol{h}_x \end{aligned} \tag{4.45}$$

#### Derivative of the torsion energy with respect to $x$

Recall that the torsion energy only depends on $\theta$ which is independent of $x$. Thus, $\mathcal{E}_t$ is independent of $x$ :

$$\boldsymbol{D}_x \mathcal{E}_t[\boldsymbol{x}](s) \cdot \boldsymbol{h}_x = \frac{d}{d\lambda} \mathcal{E}_t[\boldsymbol{x} + \lambda \boldsymbol{h}_x] \Big|_{\lambda=0} = 0 \tag{4.46}$$

#### Derivative of the bending energy with respect to $x$

The derivative of $\mathcal{E}_b$ is obtained with the chaine rule :

$$\boldsymbol{D}_\omega \mathcal{E}_b[\boldsymbol{\omega}](s) \cdot \boldsymbol{h}_\omega = \frac{d}{d\lambda} \mathcal{E}_b[\boldsymbol{\omega} + \lambda \boldsymbol{h}_\omega] \Big|_{\lambda=0} = \int_0^L (\boldsymbol{\omega} - \overline{\boldsymbol{\omega}})^T \boldsymbol{B} \cdot \boldsymbol{h}_\omega \, dt \tag{4.47}$$

Finally, reminding eq 4.14 :

$$\boldsymbol{D}_x\mathcal{E}_b[\boldsymbol{\omega}[\boldsymbol{x}]](s)\cdot\boldsymbol{h}_x = \boldsymbol{D}_\omega\mathcal{E}_b[\boldsymbol{\omega}](s)\cdot(\boldsymbol{D}_x\boldsymbol{\omega}[\boldsymbol{x}](s)\cdot\boldsymbol{h}_x) = \mathcal{A}+\mathcal{B}+\mathcal{C} \tag{4.48}$$

Where :

$$\mathcal{A} = \int_0^L (\boldsymbol{\omega}-\overline{\boldsymbol{\omega}})^T\boldsymbol{B}\begin{bmatrix}-\boldsymbol{d}_2{}^T\\ \boldsymbol{d}_1{}^T\end{bmatrix}\cdot\boldsymbol{h}_x''\,dt \tag{4.49a}$$

$$\mathcal{B} = \int_{t=0}^L (\boldsymbol{\omega}-\overline{\boldsymbol{\omega}})^T\boldsymbol{B}\boldsymbol{J}\boldsymbol{\omega}\left(\int_{u=0}^L(\delta_t-\delta_0)\,\kappa\boldsymbol{b}\cdot\boldsymbol{h}_x\,du\right)dt \tag{4.49b}$$

$$\mathcal{C} = \int_{t=0}^L -(\boldsymbol{\omega}-\overline{\boldsymbol{\omega}})^T\boldsymbol{B}\boldsymbol{J}\boldsymbol{\omega}\left(\int_{u=0}^L(1-H_t)\,\kappa\boldsymbol{b}'\cdot\boldsymbol{h}_x\,du\right)dt \tag{4.49c}$$

Calculus of $\mathcal{A}$ :

$$\mathcal{A} = \int_0^L (\boldsymbol{\omega}-\overline{\boldsymbol{\omega}})^T\boldsymbol{B}\begin{bmatrix}-\boldsymbol{d}_2{}^T\\ \boldsymbol{d}_1{}^T\end{bmatrix}\cdot\boldsymbol{h}_x''\,dt \tag{4.50}$$

Recalling the bending moment is given by :

$$\boldsymbol{M} = (\kappa_1-\overline{\kappa_1})EI_1\boldsymbol{d}_1+(\kappa_2-\overline{\kappa_2})EI_2\boldsymbol{d}_2 = M_1\boldsymbol{d}_1+M_2\boldsymbol{d}_2 \tag{4.51}$$

One can remark that :

$$(\boldsymbol{\omega}-\overline{\boldsymbol{\omega}})^T\,\boldsymbol{B}\begin{bmatrix}-\boldsymbol{d}_2{}^T\\ \boldsymbol{d}_1{}^T\end{bmatrix} = M_2\boldsymbol{d}_1{}^T - M_1\boldsymbol{d}_2{}^T = -(\boldsymbol{d}_3\times\boldsymbol{M})^T \tag{4.52}$$

Rq : on mixe abusivement 2 formes d'écritures, matricielle et vectorielle, à cause du produit scalaire que l'on écrit tantôt sous sa forme vectorielle et parfois matricielle (à l'aide de la transposée).

Thus, $\mathcal{A}$ could be rewritten in it's vectoriel form :

$$\begin{aligned}\mathcal{A} &= -\int_0^L(\boldsymbol{d}_3\times\boldsymbol{M})\cdot\boldsymbol{h}_x''\,dt\\ &= -\left[(\boldsymbol{d}_3\times\boldsymbol{M})\cdot\boldsymbol{h}_x'\right]_0^L+\int_0^L(\boldsymbol{d}_3\times\boldsymbol{M})'\cdot\boldsymbol{h}_x'\,dt\\ &= -\left[(\boldsymbol{d}_3\times\boldsymbol{M})\cdot\boldsymbol{h}_x'\right]_0^L+\int_0^L\left(\left(\boldsymbol{d}_3\times\boldsymbol{M}'\right)\cdot\boldsymbol{h}_x'+\left(\boldsymbol{h}_x'\times\boldsymbol{d}_3'\right)\cdot\boldsymbol{M}\right)dt\end{aligned} \tag{4.53}$$

Recall that from (4.6) that $\boldsymbol{h}_x'\cdot\boldsymbol{d}_3 = 0$ and from (4.1) that $\boldsymbol{d}_3'\cdot\boldsymbol{d}_3 = 0$. Hence, $\boldsymbol{h}_x'\times\boldsymbol{d}_3'$ is colinear to $\boldsymbol{d}_3$. Or by definition $\boldsymbol{M}$ is orthogonal to $\boldsymbol{d}_3$. Thus, $\left(\boldsymbol{h}_x'\times\boldsymbol{d}_3'\right)\cdot\boldsymbol{M} = 0$. Finally, after a second integration by parts :

$$\begin{aligned}\mathcal{A} &= -\left[(\boldsymbol{d}_3\times\boldsymbol{M})\cdot\boldsymbol{h}_x'\right]_0^L+\int_0^L\left(\boldsymbol{d}_3\times\boldsymbol{M}'\right)\cdot\boldsymbol{h}_x'\,dt\\ &= \left[(\boldsymbol{d}_3\times\boldsymbol{M}')\cdot\boldsymbol{h}_x''\;-(\boldsymbol{d}_3\times\boldsymbol{M})\cdot\boldsymbol{h}_x'\right]_0^L-\int_0^L\left(\boldsymbol{d}_3\times\boldsymbol{M}'\right)'\cdot\boldsymbol{h}_x\,dt\end{aligned} \tag{4.54}$$

Calculus of $\mathcal{B}$ :

$$\begin{aligned}\mathcal{B} &= \int_{t=0}^{L}(\boldsymbol{\omega}-\overline{\boldsymbol{\omega}})^T\boldsymbol{J}\boldsymbol{\omega}\left(\int_{u=0}^{L}(\delta_t-\delta_0)\,\kappa\boldsymbol{b}\cdot\boldsymbol{h}_x\,du\right)\,dt \\ &= -\left(\kappa\boldsymbol{b}\cdot\boldsymbol{h}_x\right)(0)\int_{t=0}^{L}(\boldsymbol{\omega}-\overline{\boldsymbol{\omega}})^T\boldsymbol{J}\boldsymbol{\omega}\,dt+\int_{t=0}^{L}(\boldsymbol{\omega}-\overline{\boldsymbol{\omega}})^T\boldsymbol{J}\boldsymbol{\omega}\kappa\boldsymbol{b}\cdot\boldsymbol{h}_x\,dt\end{aligned} \tag{4.55}$$

Calculus of $\mathcal{C}$ :

$$\begin{aligned}\mathcal{C} &= \int_{t=0}^{L}-(\boldsymbol{\omega}-\overline{\boldsymbol{\omega}})^T\boldsymbol{J}\boldsymbol{\omega}\left(\int_{u=0}^{L}(1-H_t)\,\kappa\boldsymbol{b}'\cdot\boldsymbol{h}_x\,du\right)\,dt \\ &= \int_{u=0}^{L}\int_{t=u}^{L}-\left((\boldsymbol{\omega}-\overline{\boldsymbol{\omega}})^T\boldsymbol{J}\boldsymbol{\omega}\right)(t)\left(\kappa\boldsymbol{b}'\cdot\boldsymbol{h}_x\right)(u)\,dt\,du \\ &= \int_{u=0}^{L}-\left(\int_{t=u}^{L}(\boldsymbol{\omega}-\overline{\boldsymbol{\omega}})^T\boldsymbol{J}\boldsymbol{\omega}\,dt\right)\left(\kappa\boldsymbol{b}'\cdot\boldsymbol{h}_x\right)\,du\end{aligned} \tag{4.56}$$

By several integration by parts, using Fubini's theorem once and supposing that the terms vanishes at $s=0$ and $s=L$ :

$$\begin{aligned}\mathcal{B}+\mathcal{C} &= \int_{t=0}^{L}\left((\boldsymbol{\omega}-\overline{\boldsymbol{\omega}})^T\boldsymbol{J}\boldsymbol{\omega}\kappa\boldsymbol{b}-\left(\int_{u=t}^{L}(\boldsymbol{\omega}-\overline{\boldsymbol{\omega}})^T\boldsymbol{J}\boldsymbol{\omega}\,du\right)\kappa\boldsymbol{b}'\right)\cdot\boldsymbol{h}_x\,dt \\ &= \int_{t=0}^{L}\left(-\left(\int_{u=t}^{L}(\boldsymbol{\omega}-\overline{\boldsymbol{\omega}})^T\boldsymbol{J}\boldsymbol{\omega}\,du\right)'\kappa\boldsymbol{b}-\left(\int_{u=t}^{L}(\boldsymbol{\omega}-\overline{\boldsymbol{\omega}})^T\boldsymbol{J}\boldsymbol{\omega}\,du\right)\kappa\boldsymbol{b}'\right)\cdot\boldsymbol{h}_x\,dt \\ &= \int_{t=0}^{L}\left(-\left(\int_{u=t}^{L}(\boldsymbol{\omega}-\overline{\boldsymbol{\omega}})^T\boldsymbol{J}\boldsymbol{\omega}\,du\right)\kappa\boldsymbol{b}\right)'\cdot\boldsymbol{h}_x\,dt\end{aligned} \tag{4.57}$$

Which can be rewritted using the quasi-static hypothesis :

$$\begin{aligned}\mathcal{B}+\mathcal{C} &= \int_{t=0}^{L}\left(-\left(\int_{u=t}^{L}(\boldsymbol{\omega}-\overline{\boldsymbol{\omega}})^T\boldsymbol{J}\boldsymbol{\omega}\,du\right)\kappa\boldsymbol{b}\right)'\cdot\boldsymbol{h}_x\,dt \\ &= \int_{t=0}^{L}\left(-\left(\int_{u=t}^{L}\beta(\theta'-\overline{\theta}')(\delta_L-\delta_0)-\left(\beta(\theta'-\overline{\theta}')\right)'\,du\right)\kappa\boldsymbol{b}\right)'\cdot\boldsymbol{h}_x\,dt \\ &= \int_{t=0}^{L}\left(-\left(\beta(\theta'-\overline{\theta}')(L)-\left[\beta(\theta'-\overline{\theta}')\right]_t^L\right)\kappa\boldsymbol{b}\right)'\cdot\boldsymbol{h}_x\,dt \\ &= \int_{t=0}^{L}-\left(\beta(\theta'-\overline{\theta}')\kappa\boldsymbol{b}\right)'\cdot\boldsymbol{h}_x\,dt\end{aligned} \tag{4.58}$$

Finally :

$$\boldsymbol{D}_x\mathcal{E}_b[\boldsymbol{\omega}[\boldsymbol{x}]](s)\cdot\boldsymbol{h}_x=\int_0^L\left(-\left(\boldsymbol{d}_3\times\boldsymbol{M}'\right)'-\left(\beta(\theta'-\overline{\theta}')\kappa\boldsymbol{b}\right)'\right)\cdot\boldsymbol{h}_x\,dt \tag{4.59}$$

**Internal forces**

Thus, the internal forces are related to the variation of internal elastic energy as :

$$\langle-\boldsymbol{f}(s)\,;\boldsymbol{h}_x\rangle=\boldsymbol{D}_x\mathcal{E}_p(s)\cdot\boldsymbol{h}_x=-\int_0^L\left(\left(\boldsymbol{d}_3\times\boldsymbol{M}'\right)'+\left(\beta(\theta'-\overline{\theta}')\kappa\boldsymbol{b}\right)'\right)\cdot\boldsymbol{h}_x\,dt \tag{4.60}$$

Finally, we can conclude on the expression of the internal forces :

$$\boldsymbol{f}(s) = \left(\boldsymbol{d}_3 \times \boldsymbol{M}'\right)' + \left(\beta(\theta' - \overline{\theta}')\kappa\boldsymbol{b}\right)' \tag{4.61}$$

Remarquer ici que l'expression est purement locale. Elle ne dépend pas du sens de parcours de la poutre, contrairement au raisonnement suivi. Cette différence est notable avec la démarche de B. Audoly. Faire le bilan des bénéfices de l'hypothèse quasi-statique : - expressions rigoureusement vraies à l'équilibre statique - simplification ds le calcul des efforts - rapidité dans le calcul avec des expressions plus simples - il n'est pas forcément intéressant en terme d'algorithmie d'imposer l'hypothèse quasistatique au cours du calcul. Il faudrait faire un bench pour savoir.

On retombe sur les équations de Kirchhoff à un terme manquant pret. Qui exprime la contribution de la variation moment de flexion à cause de la torsion $\tau\boldsymbol{M}$'. Peut-être que ce terme est finalement d'un ordre supérieur, si l'on suppose une variation lente de la torsion ? Comment comprendre la disparition de ce terme qui semble nécessaire à l'équilibre statique d'un élément de poutre si l'on en croit les équations de Kirchhoff ?

## 4.9 Conclusion

On retrouve les équations de kirchhoff dynamique où l'on a négligé les forces inertielles de rotation d'un élément de poutre autour de $\boldsymbol{d}_1$ et $\boldsymbol{d}_2$ pour ne garder que la dynamique de rotation de la section autour de la fibre neutre $\boldsymbol{d}_3$.

The shear force acting on the right side of a section is nothing but $\boldsymbol{T} = \int \boldsymbol{f}$ :

$$\boldsymbol{T}(s) = \boldsymbol{d}_3 \times \boldsymbol{M}' + Q\kappa\boldsymbol{b} \tag{4.62}$$

The linear momentum acting on the centerline is given by :

$$m(s) = Q' - \kappa\boldsymbol{b} \cdot (\boldsymbol{d}_3 \times \boldsymbol{M}) \tag{4.63}$$

The main hypothesis are :

- Bernoulli : $\boldsymbol{d}_i \cdot \boldsymbol{d}_j = \delta_{ij}$
- Inextensibility : $\|\boldsymbol{d}_3'\| = 1$
- Quasistatic : at each timestep regarding bending motion $m(s) = 0$

# Bibliography

[AAP10] Basile Audoly, M Amar, and Yves Pomeau. *Elasticity and geometry.* 2010.

[ABW99] Sigrid Adriaenssens, Michael Barnes, and Christopher Williams. A new analytic and numerical basis for the form-finding and analysis of spline and gridshell

structures. In B Kumar and B H V Topping, editors, *Computing Developments in Civil and Structural Engineering*, pages 83–91. Civil-Comp Press, Edinburgh, 1999.

[BAV+10] Miklós Bergou, Basile Audoly, Etienne Vouga, Max Wardetzky, and Eitan Grinspun. Discrete viscous threads. *ACM Transactions on ...*, pages 1–10, 2010.

[Ber09] Mitchell Berger. Topological Quantities: Calculating Winding, Writhing, Linking, and Higher order Invariants. *Lecture Notes in Mathematics*, 1973:75–97, 2009.

[Bis75] Richard Bishop. There is more than one way to frame a curve. *Mathematical Association of America*, 1975.

[BWR+08] Miklós Bergou, Max Wardetzky, Stephen Robinson, Basile Audoly, and Eitan Grinspun. Discrete elastic rods. *ACM SIGGRAPH*, pages 1–12, 2008.

[dV05] Renko de Vries. Evaluating changes of writhe in computer simulations of supercoiled DNA. *The Journal of Chemical Physics*, 122(6), 2005.

[Ful78] F Brock Fuller. Decomposition of the linking number of a closed ribbon : A problem from molecular biology. 75(8):3557–3561, 1978.

[Lew03] Wanda Lewis. *Tension structures: form and behaviour*. Telford, Thomas, 2003.

[ST07] Jonas Spillmann and Matthias Teschner. CORDE : Cosserat Rod Elements for the Dynamic Simulation of One-Dimensional Elastic Objects. *Eurographics/ ACM SIGGRAPH Symposium on Computer Animation*, pages 1–10, 2007.

[Vau00] Rue Vauquelin. Writhing Geometry at Finite Temperature : Random Walks and Geometric phases for Stiff Polymers. (1), 2000.

# 5 Elastic rod : equilibrium approach

## 5.1 Introduction

Ici on explique que l'approche par les équations d'équilibre est beaucoup plus directe que l'approche énergétique.

### 5.1.1 Goals and contribution

Dans ce chapitre, après un bref rappel sur le cadre mathématique d'étude des courbes paramétrique de l'espace, on présente les notions de courbures et de torsion géométrique associées au repère de fraient. On montre ensuite le cas plus général d'un repère mobile quelconque attaché à une courbe gamma. On définit enfin la particularité d'un repère mobile adapté à un courbe, et on présente, en sus du repère de Frenet, une approche différente pour accrocher des repères le long d'une courbe (Bishop / RMF / Zéro-twisting frame)

Ici il faudrait préciser la terminologie des auteurs / équations / hypothèses : Euler-Bernoulli, Navier-Bernoulli, Kirchhoff, Love, Clebesh, Cosserat, Vlassov

### 5.1.2 Related work

On peu s'instruire dans la publi de Dill [Dil92]. Regarder en particulier le premier chapitre de l'HDR de Neukirch [Neu09]. Regarder également la chronologie des modèles proposée dans la thèse de Theetten [The07]. Pourquoi pas proposer une frise chronologique + un tableau de synthèse des hyptohèses.

[Dil92] **(author?)** [Neu09] [ABW99] [Hoo06] [LL09] [Spi08] [Ant05]

[Neu09] : p69 - [Dil92] : p16

### 5.1.3 Overview

Résumé du chapitre

## 5.2 Dynamic Kirchhoff equations

### 5.2.1 Balance of the linear momentum

On fait un bilan sur une tranche d'épaisseur $ds$, de centre de gravité $G$ positionné en $\boldsymbol{x}_G$ :

$$\boldsymbol{F}(s+ds) - \boldsymbol{F}(s) + \boldsymbol{f}(s)ds = \left(\frac{\partial \boldsymbol{F}}{\partial s}(s) + \boldsymbol{f}(s)\right)ds = (\rho S ds)\ddot{\boldsymbol{x}}_G \tag{5.1}$$

Which leads to the first equation of Kirchhoff law :

$$\frac{\partial \boldsymbol{F}}{\partial s} + \boldsymbol{f} = \rho S \ddot{\boldsymbol{x}}_G \tag{5.2}$$

### 5.2.2 Balance of the angular momentum

On fait un bilan sur une tranche d'épaisseur $ds$, de centre de gravité $G$ positionné en $\boldsymbol{x}_G$. On applique le théorème du moment cinétique dans un référentiel inertiel :

$$\begin{aligned}\frac{d}{dt}(dI_G) &= \boldsymbol{M}(s+ds) - \boldsymbol{M}(s) + \boldsymbol{m}(s)ds + (\tfrac{1}{2}ds\boldsymbol{x}') \times \boldsymbol{F}(s+ds) + (-\tfrac{1}{2}ds\boldsymbol{x}') \times -\boldsymbol{F}(s) \\ &= \left(\frac{\partial \boldsymbol{M}}{\partial s}(s) + \boldsymbol{m}(s) + \boldsymbol{x}' \times \boldsymbol{F}(s)\right)ds\end{aligned} \tag{5.3}$$

L'évolution temporelle des vecteurs matériels est cette fois décrite par un vecteur de Darboux temporel noté $\boldsymbol{\Lambda}$ tel que :

$$\dot{\boldsymbol{d}}_i(s) = \boldsymbol{\Lambda}(t) \times \boldsymbol{d}_i(s) \quad , \quad \boldsymbol{\Lambda}(t) = \begin{bmatrix}\Lambda_3(t) \\ \Lambda_1(t) \\ \Lambda_2(t)\end{bmatrix} \tag{5.4}$$

Les lois de composition / dérivation de la mécanique nous permettent décrire :

$$\frac{d}{dt}(dI_G) = dI_G\dot{\boldsymbol{\Lambda}} + \boldsymbol{\Lambda} \times dI_G \tag{5.5}$$

Qu'est ce qu'on met dans $dI_G$ ? Et bien tout simplement l'opérateur d'inertie de la section, qui s'exprime à l'aide des moments quadratiques des directions principales de la façon suivante, dans la base des directions principales d'inertie au premier ordre en $ds$ :

$$dI_G = \begin{bmatrix}dI_{G3} & 0 & 0 \\ 0 & dI_{G1} & 0 \\ 0 & 0 & dI_{G2}\end{bmatrix} \simeq \rho ds \begin{bmatrix}I_1 + I_2 & 0 & 0 \\ 0 & I_1 & 0 \\ 0 & 0 & I_2\end{bmatrix} \tag{5.6}$$

Where :

$$dI_{G3} = \int_V \rho(x_1^2 + x_2^2)\, dV \simeq \rho ds \int_V (x_1^2 + x_2^2)\, dx_1 dx_2 \simeq \rho ds (I_1 + I_2) \tag{5.7a}$$

$$dI_{G1} = \int_V \rho(x_2^2 + x_3^2)\, dV \simeq \rho ds \int_V x_2^2\, dx_1 dx_2 \simeq \rho ds I_1 \tag{5.7b}$$

$$dI_{G2} = \int_V \rho(x_1^2 + x_3^2)\, dV \simeq \rho ds \int_V x_1^2\, dx_1 dx_2 \simeq \rho ds I_2 \tag{5.7c}$$

Et l'on peut alors écrire la seconde loi de Kirchhoff sous la forme suivante :

$$\frac{\partial \boldsymbol{M}}{\partial s}(s) + \boldsymbol{m}(s) + \boldsymbol{x}' \times \boldsymbol{F}(s) = \rho \begin{bmatrix} (I_1 + I_2)\dot{\Lambda}_3 + (I_2 - I_1)\Lambda_1\Lambda_2 \\ I_1(\dot{\Lambda}_1 + \Lambda_2\Lambda_3) \\ I_2(\dot{\Lambda}_2 - \Lambda_3\Lambda_1) \end{bmatrix} \tag{5.8}$$

On montre ensuite :

$$\begin{cases} \dot{\boldsymbol{d}}_3 = \boldsymbol{\Lambda} \times \boldsymbol{d}_3 \;\; = \Lambda_2 \boldsymbol{d_1} - \Lambda_1 \boldsymbol{d_2} \\ \dot{\boldsymbol{d}}_1 = \boldsymbol{\Lambda} \times \boldsymbol{d}_1 \;\; = -\Lambda_2 \boldsymbol{d_3} + \Lambda_3 \boldsymbol{d_2} \\ \dot{\boldsymbol{d}}_2 = \boldsymbol{\Lambda} \times \boldsymbol{d}_2 \;\; = \Lambda_1 \boldsymbol{d_3} - \Lambda_3 \boldsymbol{d_1} \end{cases} \Rightarrow \begin{cases} \ddot{\boldsymbol{d}}_3 = \dot{\Lambda}_2 \boldsymbol{d_1} - \dot{\Lambda}_1 \boldsymbol{d_2} + \boldsymbol{\Lambda} \times \dot{\boldsymbol{d}}_3 \\ \ddot{\boldsymbol{d}}_1 = -\dot{\Lambda}_2 \boldsymbol{d_3} + \dot{\Lambda}_3 \boldsymbol{d_2} + \boldsymbol{\Lambda} \times \dot{\boldsymbol{d}}_1 \\ \ddot{\boldsymbol{d}}_2 = \dot{\Lambda}_1 \boldsymbol{d_3} - \dot{\Lambda}_3 \boldsymbol{d_1} + \boldsymbol{\Lambda} \times \dot{\boldsymbol{d}}_2 \end{cases} \tag{5.9}$$

On en déduit en remarquant que $(\boldsymbol{\Lambda} \times \dot{\boldsymbol{d}}_i) \times \boldsymbol{d}_i = \Lambda_i(\boldsymbol{\Lambda} \times \dot{\boldsymbol{d}}_i)$ que :

$$\begin{cases} \ddot{\boldsymbol{d}}_3 \times \boldsymbol{d}_3 = (\dot{\Lambda}_2 \boldsymbol{d_1} - \dot{\Lambda}_1 \boldsymbol{d_2} + \boldsymbol{\Lambda} \times \dot{\boldsymbol{d}}_3) \times \boldsymbol{d}_3 = (-\dot{\Lambda}_1 + \Lambda_2\Lambda_3)\boldsymbol{d}_1 - (\dot{\Lambda}_2 + \Lambda_1\Lambda_3)\boldsymbol{d}_2 \\ \ddot{\boldsymbol{d}}_1 \times \boldsymbol{d}_1 = -\dot{\Lambda}_2 \boldsymbol{d_3} + \dot{\Lambda}_3 \boldsymbol{d_2} + \boldsymbol{\Lambda} \times \dot{\boldsymbol{d}}_1 \times \boldsymbol{d}_1 = -(\dot{\Lambda}_3 + \Lambda_1\Lambda_2)\boldsymbol{d}_3 + (-\dot{\Lambda}_2 + \Lambda_1\Lambda_3)\boldsymbol{d}_2 \\ \ddot{\boldsymbol{d}}_2 \times \boldsymbol{d}_2 = \dot{\Lambda}_1 \boldsymbol{d_3} - \dot{\Lambda}_3 \boldsymbol{d_1} + \boldsymbol{\Lambda} \times \dot{\boldsymbol{d}}_2 \times \boldsymbol{d}_2 = (-\dot{\Lambda}_3 + \Lambda_1\Lambda_2)\boldsymbol{d}_3 - (\dot{\Lambda}_1 + \Lambda_2\Lambda_3)\boldsymbol{d}_1 \end{cases} \tag{5.10}$$

On peut alors conclure sur l'expression de l'equation de kirchoff :

$$\frac{\partial \boldsymbol{M}}{\partial s}(s) + \boldsymbol{m}(s) + \boldsymbol{d}_3' \times \boldsymbol{F}(s) = I_1 \boldsymbol{d}_1 \times \ddot{\boldsymbol{d}}_1 + I_2 \boldsymbol{d}_2 \times \ddot{\boldsymbol{d}}_2 \tag{5.11}$$

## 5.3 Equations of motion

### 5.3.1 Constitutive equations

Attention, pas d'effort normal par loi constitutive en principe car on est dans un modèle inextensible. L'effort normal est calculé par la loi d'équilibre avec les moments et/ou efforts tranchants. Ici, on postulera tout de même une telle loi constitutive pour la résolution numérique. Ce qui nous amène à considérer une tige quasiment inextensible.

point à creuser. en gros je suis entrain de dire que dans le modèle classique à 3DOF type Douthe ou Barnes, il n'est pas nécessaire d'introduire la raideur axiale (mais alors où intervient la section ?). L'effort normal est déduit des équations d'équilibre.

En fait cela ne semble pas possible. Il faaut alors revenir à l'équation constitutive qui donne l'effort normal, mais alors quid de l'hypothèse quasistatique ?

Dans le fond, l'hyptohèse d'inextensibilité c'est dire que les déformations axiales sont négligeable devant les autres modes de déformation (flexion et/ou torsion). Mais pour caractériser l'effort normal lui même, il faut bien considérer une élongation.

Ou alors, peut-être qu'il faut comprendre que l'effort normal est déduit uniquement des conditions aux limites et/ou éventuellement des efforts extérieurs appliqués à la centerline.

Pour comprendre le traitement de l'inextensibilité, regarder [Ant05] p50. Qu'apporte l'hypothèse d'inextensibilité. Est-elle raisonnable. Tps de calcul par rapport au cas extensible.

$$\boldsymbol{N} = ES(\|\boldsymbol{d}_3'\| - \|\overline{\boldsymbol{d}_3}'\|)\boldsymbol{d}_3 \tag{5.12a}$$
$$\boldsymbol{M_1} = EI_1(\kappa_1 - \overline{\kappa_1})\boldsymbol{d}_1 \tag{5.12b}$$
$$\boldsymbol{M_2} = EI_2(\kappa_2 - \overline{\kappa_2})\boldsymbol{d}_2 \tag{5.12c}$$
$$\boldsymbol{Q} = [GJ(\theta' - \bar{\theta}') - EC_w(\theta''' - \bar{\theta}''')]\boldsymbol{d}_3 \tag{5.12d}$$

### 5.3.2 Internal forces and moments

Efforts internes de coupure :

$$\boldsymbol{F}_{int} = N\boldsymbol{d}_3 + T_1\boldsymbol{d}_1 + T_2\boldsymbol{d}_2 \tag{5.13a}$$
$$\boldsymbol{M}_{int} = Q\boldsymbol{d}_3 + M_1\boldsymbol{d}_1 + M_2\boldsymbol{d}_2 \tag{5.13b}$$

Efforts externes appliqués linéiques :

$$\boldsymbol{f}_{ext} = f_3\boldsymbol{d}_3 + f_1\boldsymbol{d}_1 + f_2\boldsymbol{d}_2 \tag{5.14a}$$
$$\boldsymbol{m}_{ext} = m_3\boldsymbol{d}_3 + m_1\boldsymbol{d}_1 + m_2\boldsymbol{d}_2 \tag{5.14b}$$

### 5.3.3 Rod dynamic

First Kirchhoff law projecting on the material frame basis :

$$N' + \kappa_1 T_2 - \kappa_2 T_1 + f_3 = \rho S\ddot{x}_3 \tag{5.15a}$$
$$T_1' + \kappa_2 N - \tau T_2 + f_1 = \rho S\ddot{x}_1 \tag{5.15b}$$
$$T_2' - \kappa_1 N + \tau T_1 + f_2 = \rho S\ddot{x}_2 \tag{5.15c}$$

Second Kirchhoff law projecting on the material frame basis :

$$Q' + \kappa_1 M_2 - \kappa_2 M_1 + m_3 = (I_1 + I_2)\dot{\Lambda}_3 + (I_2 - I_1)\Lambda_1\Lambda_2 \tag{5.16a}$$
$$M_1' + \kappa_2 Q - \tau M_2 - T_2 + m_1 = I_1(\dot{\Lambda}_1 + \Lambda_2\Lambda_3) \tag{5.16b}$$
$$M_2' - \kappa_1 Q + \tau M_1 + T_1 + m_2 = I_2(\dot{\Lambda}_2 - \Lambda_3\Lambda_1) \tag{5.16c}$$

## 5.4 Geometric interpretation

Ici, on peut mettre l'interprétation géométrique (cf pdf LDP notes). Cela consiste essentiellement à 2/3 schémas bien pensés à produire + à écrire les projections au 1er ordre.

## 5.5 Main hypothesis

On néglige les forces d'inertie liées à la rotation de l'élément (devant quoi ?? traitement quasi-statique par rapport à la rotation). Cette hypothèse est faite explicitement chez Florence Bertail :

[CBd13] "neglecting inertial momentum due to the vanishing cross- section lead to the following dynamic equations for a Kirchhoff rod"

Cette hypothèse est faite mais passée sous silence chez Douthe, Adriaenssen, D'Amico lorsqu'ils déduisent l'effort tranchant du moment de flexion.

Principe :

- les équations constitutives permettent le calcul de $M_1$, $M_2$, $Q$ à partir de la géométrie $\{\boldsymbol{x}, \theta\}$.

- La seconde loi de kirchhoff projetée sur les axes matériels 1 et 2 de la section me donnent accès aux efforts tranchants $T_1$ et $T_2$.

- La seconde loi de kirchhoff projetée sur les axes matériel 3 (tangente à la centerline) de la section me donnent l"hypothèse quasi-statique de Audoly.

## 5.6 Conclusion

Remind that the beam is subject to a distributed external force $\boldsymbol{f}_{ext}$ and a distributed external moment $\boldsymbol{m}_{ext}$.

We neglect rotational inertial effects on $\boldsymbol{d}_1$ et $\boldsymbol{d}_2$ in (5.16b) and (5.16c) which leads to the following shear force :

$$\boldsymbol{T}(s) = \boldsymbol{d}_3 \times (\boldsymbol{M}' + \boldsymbol{m}_{ext}) + Q\kappa\boldsymbol{b} - \tau\boldsymbol{M} \tag{5.17}$$

We may neglect as well the last term ($\tau\boldsymbol{M}$) and get back to the shear force obtained by the variational approach.The total internal force acting on the beam is hence given by :

$$\boldsymbol{F}(s) = \boldsymbol{N}(s) + \boldsymbol{T}(s) \tag{5.18}$$

Sections are subject to the following rotational moment around the centerline :

$$\boldsymbol{\Gamma}(s) = Q' + \boldsymbol{d}_3 \cdot (\kappa \boldsymbol{b} \times \boldsymbol{M} + \boldsymbol{m}_{ext}) \tag{5.19}$$

# Bibliography


[ABW99] Sigrid Adriaenssens, Michael Barnes, and Christopher Williams. A new analytic and numerical basis for the form-finding and analysis of spline and gridshell structures. In B Kumar and B H V Topping, editors, *Computing Developments in Civil and Structural Engineering*, pages 83–91. Civil-Comp Press, Edinburgh, 1999.

[Ant05] Stuart Antman. *Nonlinear problems of elasticity.* Applied mathematical sciences. Springer, New York, 2005.

[CBd13] Romain Casati and Florence Bertails-descoubes. Super space clothoids. In *SIGGRAPH*, 2013.

[Dil92] Ellis Harold Dill. Kirchhoff's theory of rods. *Archive for History of Exact Sciences*, 1992.

[Hoo06] P C J Hoogenboom. 7 Vlasov torsion theory. (October):1–12, 2006.

[LL09] Holger Lang and Joachim Linn. Lagrangian field theory in space-time for geometrically exact Cosserat rods. 150:21, 2009.

[Neu09] S. Neukirch. *Enroulement, contact et vibrations de tiges élastiques.* PhD thesis, 2009.

[Spi08] Jonas Spillmann. *CORDE : Cosserat rod elements for the animation of interacting elastic rods.* PhD thesis, 2008.

[The07] Adrien Theetten. *Splines dynamiques géométriquement exactes : simulation haute performance et interaction.* PhD thesis, Université des Sciences et Technologies de Lille, 2007.

# 6 Numerical model

## 6.1 Introduction

Introduction du chapitre

### 6.1.1 Goals and contribution

Ici on rappelle les objectifs du chapitre ; on identifie clairement mes contributions. Dans ce chapitre on s'attache à la résolution de l'équilibre statique par relaxation dynamique. Peut-être qu'il faudra faire un chapitre "Marsupilami" plus détaillé qui regroupe les différents éléments formulés et les connexions / liaisons On formule l'élément en torsion à partir des équations de Kirchhoff et non du modèle énergétique (un terme est manquant). On effectue une validation numérique. Penser à tracer la contribution de chaque terme pour vérifier les approximations effectuées.

### 6.1.2 Related work

Ici on fait l'analyse bibliographique pour le chapitre concerné. [Day65] [Ott65] [Pap81] [MAIK14] [Ala12] [RPKAZ11]

Idée pour l'article avec sigrid [Ala12]

### 6.1.3 Overview

## 6.2 Dynamic relaxation

### 6.2.1 Overview

Ici, repartir de l'explication donnée par Alister Days en 65. Proposer une illustration avec un pendule. Pourquoi pas le système masse-ressort proposé par Days, à savoir une masse au bout d'une poutre encastrée.

### 6.2.2 Finite difference integration

### 6.2.3 Kinetic damping

## 6.3 Discret curve-angle representation

### 6.3.1 Discrete centerline

On discrétise la centerline de la façon suivante :

$$s_i = \sum_{0}^{i} |\boldsymbol{e}_{i-1}| \quad , \quad i = 0..n \tag{6.1a}$$

$$\boldsymbol{x}_i \quad , \quad i = 0..n \tag{6.1b}$$

$$\boldsymbol{e}_i = \boldsymbol{x}_{i+1} - \boldsymbol{x}_i \quad , \quad i = 0..n-1 \tag{6.1c}$$

### 6.3.2 Discrete bishop frame

#### Discrete parallel transport at edges

#### Discrete parallel at vertices

On définit ici le transport parrallele discret entre edges et entre vertices. A chaque vertex, on associe un repère de bishop et un repère matériel

$$\theta_i \quad , \quad i = 0..n \tag{6.2a}$$

$$\{\boldsymbol{u}_i, \boldsymbol{v}_i\} \quad , \quad i = 0..n \tag{6.2b}$$

$$\{\boldsymbol{d}_i^1, \boldsymbol{d}_i^2\} \quad , \quad i = 0..n \tag{6.2c}$$

### 6.3.3 Discrete material frame

## 6.4 Interpolation rules

On fait des hypothèses sur la forme des efforts pour pouvoir effectuer une interpolation entre les noeuds. Thus, we define edge quantities and vertex quantities.

### 6.4.1 Geometric and material properties

We suppose that the sections are defined at verticies and that section properties remain uniform over $]s_{i-1/2}, s_{i+1/2}[$. Thus, the material and geometric properties $(P)$ of the beam $(E_i, G_i, S_i, I_i^1, I_i^2, J_i, m_i)$ are supposed to be piecewise constant functions of $s$ on [0,L] :

$$P(s) = P_i \quad , \quad s \in [s_{i-1/2}, s_{i+1/2}] \tag{6.3}$$

Note that this functions may be discontinous at edges midspan $(s_{i+1/2})$.

### 6.4.2 Axial force and strain

#### Axial force

$\boldsymbol{N}$ is supposed to be piecewise constant between verticies on $[0, L]$ :

$$\boldsymbol{N}(s) = N_i \boldsymbol{t}_i \quad , \quad s \in ]s_i, s_{i+1}[ \tag{6.4}$$

Note that this functions may be discontinous at edges midspan $(s_{i+1/2})$.

#### Axial strain

Nous avons défini les propriétés géométriques et matérielles aux noeuds et nous avons fait l'hypothèse qu'elles restaient uniformes sur l'intervalle $]s_{i-1/2}, s_{i+1/2}[$. Par ailleurs, nous avons supposé l'effort normal $(\boldsymbol{N})$ uniforme sur l'interval $]s_i, s_{i+1}[$. De fait, la déformation axiale $(\epsilon)$ est une fonction constante par morceaux sur les intervalles $]s_i, s_{i+1/2}[$.

Connaissant l'élongation totale du segment $\boldsymbol{e}_i$, et puisque nous avons supposé l'effort normal uniforme sur le segment, il est possible de calculer les déformations axiales $\epsilon_i^+$ et $\epsilon_{i+1}^-$ respectivement pour les intervalles $]s_i, s_{i+1/2}[$ et $]s_{i+1/2}, s_{i+1}[$ :

$$N_i = [ES]_i \epsilon_i^+ = [ES]_{i+1} \epsilon_{i+1}^- = \alpha_i \epsilon_i \tag{6.5}$$

Avec $\alpha_i$ la raideur axiale équivalente sur le segment $\boldsymbol{e}_i$ qui permet de calculer l'effort normal sur le segment en fonction de l'élongation totale du segment $\boldsymbol{e}_i$ bien que, comme énoncé précédemment, la déformation axiale puisse être différente entre $]s_i, s_{i+1/2}[$ et $]s_{i+1/2}, s_{i+1}[$ si l'on a un changement de raideur axiale $ES$ entre les noeuds $\boldsymbol{x}_i$ et $\boldsymbol{x}_{i+1}$.

Les élongations des demis segments et du segment entier sont données par les équations suivantes, où l'on a considéré $l_i^+$ et $l_{i+1}^-$ les longueurs respectives des demi segments $]s_i, s_{i+1/2}[$ et $]s_{i+1/2}, s_{i+1}[$ :

$$\epsilon_i^+ = \frac{l_i^+ - \overline{l}_i/2}{\overline{l}_i/2} \quad , \quad \epsilon_{i+1}^- = \frac{l_i^- - \overline{l}_i/2}{\overline{l}_i/2} \quad , \quad \epsilon_i = \frac{l_i}{\overline{l}_i} = \frac{\epsilon_i^+}{2} + \frac{\epsilon_{i+1}^-}{2} \tag{6.6}$$

Ces équations de continuité permettent de déduire la raideur axiale équivalente $\alpha_i$ à considérer sur le segement $\boldsymbol{e}_i$ pour obtenir l'effort normal à partir de la déformation globale

du segment sur $s \in ]s_i, s_{i+1}[$ :

$$N(s) = N_i = \alpha_i \epsilon_i \quad , \quad \alpha_i = \frac{2[ES]_i[ES]_{i+1}}{[ES]_i + [ES]_{i+1}} \quad , \quad \epsilon_i = \frac{|l_i| - |\bar{l}_i|}{|\bar{l}_i|} \tag{6.7}$$

On obtient également les déformations axiales sur chacun des intervalles :

$$\epsilon(s) = \epsilon_i^+ = \frac{\alpha_i}{[ES]_i}\epsilon_i \quad , \quad s \in ]s_i, s_{i+1/2}[ \tag{6.8a}$$

$$\epsilon(s) = \epsilon_{i+1}^- = \frac{\alpha_i}{[ES]_{i+1}}\epsilon_i \quad , \quad s \in ]s_{i+1/2}, s_{i+1}[ \tag{6.8b}$$

On remarque que pour une poutre aux propriétés uniformes, les déformations sont continues (il n'y a plus de saut) et $\alpha_i = [ES]_i = [ES]_{i+1}$.

### 6.4.3 Moment of torsion and rate of twist

#### Moment of torsion

$\boldsymbol{Q}$ is supposed to be piecewise constant between verticies on $[0, L]$ :

$$\boldsymbol{Q}(s) = Q_i \boldsymbol{t}_i, \quad s \in ]s_i, s_{i+1}[ \tag{6.9}$$

Note that this function may be discontinous at edges midspan ($s_{i+1/2}$).

#### Rate of twist

Nous avons défini les propriétés géométriques et matérielles aux noeuds et nous avons fait l'hypothèse qu'elles restaient uniformes sur l'intervalle $]s_{i-1/2}, s_{i+1/2}[$. Par ailleurs, nous avons supposé le moment de torsion ($\boldsymbol{Q}$) uniforme sur l'interval $]s_i, s_{i+1}[$. De fait, the rate of twist ($\tau = \theta'$) est une fonction constante par morceaux sur les intervalles $]s_i, s_{i+1/2}[$.

Considérons une poutre droite sans twist au repos. Connaissant le twist dans l'état déformé, c'est à dire la variation de $\theta$, sur le segment $\boldsymbol{e}_i$, et puisque nous avons supposé le moment de torsion uniforme sur le segment, il est possible de calculer les rate of twist $\tau_i^+$ et $\tau_{i+1}^-$ respectivement pour les intervalles $]s_i, s_{i+1/2}[$ et $]s_{i+1/2}, s_{i+1}[$ :

$$Q_i = [GJ]_i \tau_i^+ = [GJ]_{i+1} \tau_{i+1}^- = \beta_i \tau_i \tag{6.10}$$

Avec $\beta_i$ la raideur en torsion équivalente sur le segment $\boldsymbol{e}_i$ qui permet de calculer le moment de torsion sur le segment en fonction de l'élongation totale du segment $\boldsymbol{e}_i$ bien que, comme énoncé précédemment, le rate of twist puisse être différente entre $]s_i, s_{i+1/2}[$ et $]s_{i+1/2}, s_{i+1}[$ si l'on a un changement de raideur en torsion $GJ$ entre les noeuds $\boldsymbol{x}_i$ et $\boldsymbol{x}_{i+1}$.

Les twists des demis segments et du segment entier sont données par les équations suivantes,

où l'on a considéré $\theta_i^{mid}$ l'angle de rotation de la section en $s_{i+1/2}$ :

$$\tau_i^+ = \frac{\theta_i^{mid} - \theta_i}{l_i/2} \quad , \quad \tau_{i+1}^- = \frac{\theta_{i+1} - \theta_i^{mid}}{l_i/2} \quad , \quad \tau_i = \frac{\theta_{i+1} - \theta_i}{l_i} = \frac{\tau_i^+}{2} + \frac{\tau_{i+1}^-}{2} \tag{6.11}$$

Ces équations de continuité permettent de déduire la raideur en torsion équivalente $\beta_i$ à considérer sur le segment $\boldsymbol{e}_i$ pour obtenir le moment de torsion à partir du twist global le long du segment sur $s \in ]s_i, s_{i+1}[$ :

$$Q(s) = Q_i = \beta_i(\tau_i - \overline{\tau_i}) \quad , \quad \beta_i = \frac{2[GJ]_i[GJ]_{i+1}}{[GJ]_i + [GJ]_{i+1}} \quad , \quad \tau_i = \frac{\theta_{i+1} - \theta_i}{l_i} \tag{6.12}$$

On obtient également les rate of twist sur chacun des intervalles dans la configuration au repos ($\overline{\tau}$) comme déformée ($\tau$) :

$$\tau(s) = \tau_i^+ = \frac{\beta_i}{[GJ]_i}\tau_i \quad , \quad s \in ]s_i, s_{i+1/2}[ \tag{6.13a}$$

$$\tau(s) = \tau_{i+1}^- = \frac{\beta_i}{[GJ]_{i+1}}\tau_i \quad , \quad s \in ]s_{i+1/2}, s_{i+1}[ \tag{6.13b}$$

On remarque que pour une poutre aux propriétés uniformes, les déformations sont continues (il n'y a plus de saut) et $\beta_i = [GJ]_i = [GJ]_{i+1}$.

### 6.4.4 Bending moment and curvature

#### Bending moment

$\boldsymbol{M}$ is supposed to be continuous and piecewise linear on $[0, L]$. This assumption is quite reasonable because the bending moment is effectively continous for a beam subject to punctual forces and moments. Thus, $\boldsymbol{M}$ is interpolated from the moment computed at vertices :

$$\boldsymbol{M}(s) = \boldsymbol{M}_{i+1/2} + (s - \tfrac{l_i}{2})\boldsymbol{M}'_{i+1/2} \quad , \quad s \in [s_i, s_{i+1}] \tag{6.14}$$

With

$$\boldsymbol{M}_{i+1/2} = \frac{\boldsymbol{M}_i + \boldsymbol{M}_{i+1}}{2} \tag{6.15a}$$

$$\boldsymbol{M}'_{i+1/2} = \frac{\boldsymbol{M}_{i+1} - \boldsymbol{M}_i}{l_i} \tag{6.15b}$$

#### Curvature

Il y a une sorte de dualité entre le moment et la courbure. Parfois c'est la mesure de la courbure qui donne accès au moment de flexion. Parfois la courbure c'est la connaissance du moment de flexion qui donne la courbure. Si le moment est continu et linéaire par morceaux, la courbure elle est seulement linéaire par morceau. En effet, il peut y a voir un saut de courbure entre deux éléments de $EI$ distinct.

On interpole la courbure à partir des courbures discrètes aux noeuds et des $EI$ (également définis aux noeuds) de part et d'autre des noeuds. On revient à la continuité du moment. Puis on déduit la courbure du moment.

Donc au repos, on considère que $\boldsymbol{B}\kappa\boldsymbol{b}$ est continu et linéaire par morceaux, qui donne l'interpolation de la courbure suivante :

$$\boldsymbol{B}\kappa\boldsymbol{b}(s) = \frac{\boldsymbol{B}_i\kappa\boldsymbol{b}_i + \boldsymbol{B}_{i+1}\kappa\boldsymbol{b}_{i+1}}{2} + (s - \tfrac{l_i}{2})\frac{\boldsymbol{B}_{i+1}\kappa\boldsymbol{b}_{i+1} - \boldsymbol{B}_i\kappa\boldsymbol{b}_i}{l_i} \quad , \quad s \in [s_i, s_{i+1}] \tag{6.16}$$

On défnit alors les courbures binormales à gauche ($\kappa\boldsymbol{b}^-_{i+1/2}$) et à droite ($\kappa\boldsymbol{b}^+_{i+1/2}$) du point $\boldsymbol{x}_{i+1/2}$ tel que :

$$\kappa\boldsymbol{b}^-_{i+1/2} = \frac{\kappa\boldsymbol{b}_i + \boldsymbol{A}_i\kappa\boldsymbol{b}_{i+1}}{2} \tag{6.17a}$$

$$\kappa\boldsymbol{b}^+_{i+1/2} = \frac{\boldsymbol{A}_i{}^{-1}\kappa\boldsymbol{b}_i + \kappa\boldsymbol{b}_{i+1}}{2} \tag{6.17b}$$

Où l'on a posé $\boldsymbol{A}_i = \boldsymbol{B}_i{}^{-1}\boldsymbol{B}_{i+1}$, la matrice qui représente le saut des propriétés matérielles de flexion entre les noeuds $i$ et $i+1$. Comme attendu, $\boldsymbol{A}_i$ vaut l'identité lorsque $\boldsymbol{B}_i = \boldsymbol{B}_{i+1}$.

De même, on défnit la dérivée de la courbure binormale à gauche ($\kappa\boldsymbol{b}'^-_{i+1/2}$) et à droite ($\kappa\boldsymbol{b}'^+_{i+1/2}$) du point $\boldsymbol{x}_{i+1/2}$ tel que :

$$\kappa\boldsymbol{b}'^-_{i+1/2} = \frac{\boldsymbol{A}_i\kappa\boldsymbol{b}_{i+1} - \kappa\boldsymbol{b}_i}{l_i} \tag{6.18a}$$

$$\kappa\boldsymbol{b}'^+_{i+1/2} = \frac{\kappa\boldsymbol{b}_{i+1} - \boldsymbol{A}_i{}^{-1}\kappa\boldsymbol{b}_i}{l_i} \tag{6.18b}$$

Ainsi, on peut donner les lois d'interpolation des courbures en tout point de la centerline, dans n'importe quelle configuration (repos ou déformée) :

$$\kappa\boldsymbol{b}(s) = \kappa\boldsymbol{b}^-_{i+1/2} + (s - \tfrac{l_i}{2})\kappa\boldsymbol{b}'^-_{i+1/2} \quad s \in [s_i, s_{i+1/2}[ \tag{6.19a}$$

$$\kappa\boldsymbol{b}(s) = \kappa\boldsymbol{b}^+_{i+1/2} + (s - \tfrac{l_i}{2})\kappa\boldsymbol{b}'^+_{i+1/2} \quad s \in ]s_{i+1/2}, s_{i+1}] \tag{6.19b}$$

Dans le cas où les propriétés de la poutre sont conservées ($\boldsymbol{A}_i = \boldsymbol{I}$), on écrira :

$$\kappa\boldsymbol{b}(s) = \kappa\boldsymbol{b}_{i+1/2} + (s - \tfrac{l_i}{2})\kappa\boldsymbol{b}'_{i+1/2} \quad , \quad s \in [s_i, s_{i+1}] \tag{6.20}$$

With

$$\kappa\boldsymbol{b}_{i+1/2} = \kappa\boldsymbol{b}^-_{i+1/2} = \kappa\boldsymbol{b}^+_{i+1/2} = \frac{\kappa\boldsymbol{b}_i + \kappa\boldsymbol{b}_{i+1}}{2} \tag{6.21a}$$

$$\kappa\boldsymbol{b}'_{i+1/2} = \kappa\boldsymbol{b}'^-_{i+1/2} = \kappa\boldsymbol{b}'^+_{i+1/2} = \frac{\kappa\boldsymbol{b}_{i+1} - \kappa\boldsymbol{b}_i}{l_i} \tag{6.21b}$$

En pratique, si la correction apportée n'est pas pertinente, on négligera le saut de courbure dans les calculs discrets.

### 6.4.5 Discretization

#### Constitutive Equations

$$\tau = \theta' \tag{6.22a}$$
$$Q = ES\epsilon \tag{6.22b}$$
$$Q = GJ(\tau - \overline{\tau}) \tag{6.22c}$$
$$M1 = EI_1(\kappa_1 - \overline{\kappa_1}) \tag{6.22d}$$
$$M1 = EI_2(\kappa_2 - \overline{\kappa_2}) \tag{6.22e}$$
$$\boldsymbol{M} = M_1\boldsymbol{d}_1 + M_2\boldsymbol{d}_2 \tag{6.22f}$$
$$\boldsymbol{Q} = Q\boldsymbol{d}_3 \tag{6.22g}$$

Notes :

$$\boldsymbol{d}_3 \cdot (\boldsymbol{M} \times \boldsymbol{d}_3) = \kappa_1 M_1 + \kappa_2 M_1 \tag{6.23a}$$
$$\boldsymbol{d}_3 \cdot (\kappa\boldsymbol{b} \times \boldsymbol{M}) = \kappa_1 M_2 - \kappa_2 M_1 \tag{6.23b}$$
$$(\boldsymbol{\omega} - \overline{\boldsymbol{\omega}})^T \boldsymbol{B}\boldsymbol{J}\boldsymbol{\omega} = -\kappa\boldsymbol{b} \cdot (\boldsymbol{d}_3 \times \boldsymbol{M}) = \kappa_1 \boldsymbol{M}_2 - \kappa_2 \boldsymbol{M}_1 \tag{6.23c}$$

#### Axial Force

$$\boldsymbol{N} = (ES\epsilon)\boldsymbol{d}_3 \tag{6.24}$$

#### Shear Force

$$\boldsymbol{T} = \boldsymbol{d}_3 \times \boldsymbol{M}' + Q\kappa\boldsymbol{b} - \tau\boldsymbol{M} \tag{6.25}$$

#### Rotational Moment

$$\boldsymbol{\Gamma}(s) = (Q' + \kappa_1 M_2 - \kappa_2 M_1)\boldsymbol{d}_3 = Q'\boldsymbol{d}_3 + \kappa\boldsymbol{b} \times \boldsymbol{M} \tag{6.26}$$

#### Quasistatic hypothesis

$$Q' + \kappa_1 M_2 - \kappa_2 M_1 \simeq 0 \tag{6.27}$$

#### Inextensibility hypothesis

$$\|\boldsymbol{x}'\| = \|(\boldsymbol{x} + \boldsymbol{\epsilon})'\| = 1 \tag{6.28a}$$
$$\|\boldsymbol{e}_i\| = \|\overline{\boldsymbol{e}_i}\| \tag{6.28b}$$

En fait il faut faire quelques hypothèses sur la nature des efforts pour pourvoir les interpoler convenablement le long de la courbe. On va faire qqch qui ressemble à la super-clothoide de Bertails, et qui semble une hypothèse naturelle pour une poutre continue sur plusieurs appuis soumise à des forces et moments ponctuels :

- le moment est continu et linéaire par morceaux. Il est évalué ponctuellement aux noeuds et interpolé linéairement entre les noeuds.
- la courbure est donc continue par morceaux et linéaire par morceaux. Elle est obtenue à partir du moment et de $\boldsymbol{B}$
- N et Q sont constants par morceaux

$$\boldsymbol{N}(s) = \boldsymbol{N}_i \quad , \quad s \in ]0, |\boldsymbol{e}_i|[ \tag{6.29a}$$

$$\boldsymbol{M}(s) = \boldsymbol{M}_i + s\boldsymbol{M}'_i \quad s \in [0, |\boldsymbol{e}_i|] \quad , \quad \boldsymbol{M}'_i = \frac{\boldsymbol{M}_{i+1} - \boldsymbol{M}_i}{|\boldsymbol{e}_i|} \tag{6.29b}$$

$$\boldsymbol{Q}(s) = \boldsymbol{Q}_i \quad , \quad s \in ]0, |\boldsymbol{e}_i|[ \tag{6.29c}$$

Faire un tableau vertex / edge quantities :

- les propriétés mécaniques sont définies aux noeuds
- les repères matériels sont définis aux noeuds
- les courbures sont définies aux noeuds
- les moments sont définis aux noeuds et sont interpolés linéairement entre les noeuds
- l'effort normal et le moment de torsion sont supposés uniformes sur les segments (ils sont donc définis aux segments)
- $\alpha$ et $\beta$ sont des propriétés équivalentess définies sur les segments (égales à celles de noeuds s'il n'y a pas de saut de propriété).

### 6.4.6 Force

#### Axial Force

Axial Force exercée par la poutre sur le point courant $\boldsymbol{x}_i$ :

$$\boldsymbol{F}_i^{\parallel} = [\boldsymbol{N}]_{i-1/2}^{i+1/2} = \boldsymbol{N}_i - \boldsymbol{N}_{i-1} \tag{6.30}$$

Axial Force exercée par la poutre sur le premier point $\boldsymbol{x}_0$ :

$$\boldsymbol{F}_i^{\parallel} = [\boldsymbol{N}]_0 = \boldsymbol{N}_0 \tag{6.31}$$

Axial Force exercée par la poutre sur le dernier point $\boldsymbol{x}_n$ :

$$\boldsymbol{F}_i^{\parallel} = -\left[\boldsymbol{N}\right]_0 = -\boldsymbol{N}_n \tag{6.32}$$

### Shear Force

Shear Force exercée par la poutre sur le point courant $\boldsymbol{x}_i$ :

$$\begin{aligned}\boldsymbol{F}_i^{\perp} &= \left[\boldsymbol{d}_3 \times \boldsymbol{M}' + Q\kappa\boldsymbol{b}\right]_{i-1/2}^{i+1/2} \\ &= \frac{\boldsymbol{e}_i}{|\boldsymbol{e}_i|} \times \frac{\boldsymbol{M}_{i+1} - \boldsymbol{M}_i}{|\boldsymbol{e}_i|} - \frac{\boldsymbol{e}_{i-1}}{|\boldsymbol{e}_{i-1}|} \times \frac{\boldsymbol{M}_i - \boldsymbol{M}_{i-1}}{|\boldsymbol{e}_{i-1}|} + Q_i\kappa\boldsymbol{b}_{i+1/2}^- - Q_{i-1}\kappa\boldsymbol{b}_{i-1/2}^+ \\ &= (\boldsymbol{F}_i^1 + \boldsymbol{F}_i^2 + \boldsymbol{H}_i^-) - (\boldsymbol{F}_{i-1}^1 + \boldsymbol{F}_{i-1}^2 + \boldsymbol{H}_{i-1}^+)\end{aligned} \tag{6.33}$$

Ici, on a un problème de définition de $\kappa\boldsymbol{b}$ en milieu de segment. En effet, bien que le moment soit continu, la courbure ne l'est pas nécessairement. Lorsqu'il y a un saut de $EI$ il y a nécessairement un saut de $\kappa\boldsymbol{b}$. On pourrait plutôt interpoler le moment à mi-travée et remonter à la courbure - soit à gauche, soit à droite - en fonction des propriétés géométriques locales :

$$\boldsymbol{M}_{i+1/2} = \frac{\boldsymbol{M}_i + \boldsymbol{M}_{i+1}}{2} \tag{6.34a}$$

$$\kappa\boldsymbol{b}_{i+1/2}^- = \boldsymbol{B}_i^{-1}\boldsymbol{M}_{i+1/2} + \overline{\kappa\boldsymbol{b}}_{i+1/2}^- \tag{6.34b}$$

$$\kappa\boldsymbol{b}_{i+1/2}^+ = \boldsymbol{B}_{i+1}^{-1}\boldsymbol{M}_{i+1/2} + \overline{\kappa\boldsymbol{b}}_{i+1/2}^+ \tag{6.34c}$$

$$\boldsymbol{H}_i^- = Q_i\kappa\boldsymbol{b}_{i+1/2}^- = Q_i(\boldsymbol{B}_i^{-1}\boldsymbol{M}_{i+1/2} + \overline{\kappa\boldsymbol{b}}_{i+1/2}^-) \tag{6.34d}$$

$$\boldsymbol{H}_i^+ = Q_i\kappa\boldsymbol{b}_{i+1/2}^+ = Q_i(\boldsymbol{B}_{i+1}^{-1}\boldsymbol{M}_{i+1/2} + \overline{\kappa\boldsymbol{b}}_{i+1/2}^-) \tag{6.34e}$$

L'autre approche consiste à ignorer la discontinuité et à simplement prendre la moyenne :

$$\kappa\boldsymbol{b}_{i+1/2} = \kappa\boldsymbol{b}_{i+1/2}^- = \kappa\boldsymbol{b}_{i+1/2}^+ = \frac{\kappa\boldsymbol{b}_i + \kappa\boldsymbol{b}_{i+1}}{2} \tag{6.35a}$$

$$\boldsymbol{H}_i^- = Q_i\kappa\boldsymbol{b}_{i+1/2}^- \tag{6.35b}$$

$$\boldsymbol{H}_i^+ = Q_i\kappa\boldsymbol{b}_{i+1/2}^+ \tag{6.35c}$$

$$\boldsymbol{H}_i^- = \boldsymbol{H}_i^+ = \frac{\kappa\boldsymbol{b}_i + \kappa\boldsymbol{b}_{i+1}}{2} \tag{6.35d}$$

Cette idée reste intéressante et élégante. Elle n'a de sens que pour une poutre à propriétés variables (sinon on a la continuité de la courbure également).

Shear Force exercée par la poutre sur le premier point $\boldsymbol{x}_0$ :

$$\begin{aligned}\boldsymbol{F}_0^{\perp} &= \left[\boldsymbol{d}_3 \times \boldsymbol{M}' + Q\kappa\boldsymbol{b}\right]_0 \\ &= \frac{\boldsymbol{e}_0}{|\boldsymbol{e}_0|} \times \frac{\boldsymbol{M}_1 - \boldsymbol{M}_0}{|\boldsymbol{e}_0|} + Q_0\frac{\kappa\boldsymbol{b}_0}{2} \\ &= \boldsymbol{F}_0^1 + \boldsymbol{F}_0^2 + \boldsymbol{H}_0^-\end{aligned} \tag{6.36}$$

Shear Force exercée par la poutre sur le dernier point $\boldsymbol{x}_n$ :

$$\begin{aligned}\boldsymbol{F}_n^{\perp} &= -\left[\boldsymbol{d}_3 \times \boldsymbol{M}' + Q\kappa\boldsymbol{b}\right]_n \\ &= -\frac{\boldsymbol{e}_{n-1}}{|\boldsymbol{e}_{n-1}|} \times \frac{\boldsymbol{M}_n - \boldsymbol{M}_{n-1}}{|\boldsymbol{e}_{n-1}|} - Q_n \frac{\kappa\boldsymbol{b}_n}{2} \\ &= -(\boldsymbol{F}_n^1 + \boldsymbol{F}_n^2 + \boldsymbol{H}_n^+)\end{aligned} \tag{6.37}$$

**Moment of Torsion**

$$\Gamma_i = \int_{i-1/2}^{i-1/2} m(s) = Q_i - Q_{i-1} + \int_{i-1/2}^{i+1/2} \kappa_1 M_2 - \kappa_2 M_1 \tag{6.38}$$

Note que le terme dans l'intégrale est nul pour une section isotrope. On retrouve les résultats bien connus sur les poutres axisymétriques à courbure au repos nulle. Ici, 2 possibilitées :

- soit on considère que le moment varie lentement sur l'intervalle $]i-1/2, i+1/2[$ et on considère donc le terme $\kappa\boldsymbol{b}_i \times \boldsymbol{M}_i$ constant dans l'intégrale, ce qui donne en découpant l'intervalle en $[i-1/2, i]$ et $[i, i+1/2]$ :

$$\begin{aligned}\Gamma_i &= Q_i - Q_{i-1} + \frac{\boldsymbol{e}_{i-1}}{|\boldsymbol{e}_{i-1}|} \cdot (\kappa\boldsymbol{b}_i \times \boldsymbol{M}_i)\frac{|\boldsymbol{e}_{i-1}|}{2} + \frac{\boldsymbol{e}_i}{|\boldsymbol{e}_i|} \cdot (\kappa\boldsymbol{b}_i \times \boldsymbol{M}_i)\frac{|\boldsymbol{e}_i|}{2} \\ &= Q_i - Q_{i-1} + \frac{\boldsymbol{e}_{i-1} + \boldsymbol{e}_i}{2} \cdot (\kappa\boldsymbol{b}_i \times \boldsymbol{M}_i)\end{aligned} \tag{6.39}$$

- soit on revient à l'hypothèse de continuité et de linéarité par morceaux sur le moment:

$$\boldsymbol{M}(s) = \boldsymbol{M}_i + s\boldsymbol{M}_i' \quad \forall s \in [0, |\boldsymbol{e}_i|] \quad , \quad \boldsymbol{M}_i' = \frac{\boldsymbol{M}_{i+1} - \boldsymbol{M}_i}{|\boldsymbol{e}_i|} \tag{6.40a}$$

$$\kappa\boldsymbol{b}(s) = \boldsymbol{B}_i^{-1}\boldsymbol{M}(s) + \overline{\kappa\boldsymbol{b}}(s) \tag{6.40b}$$

$$\tag{6.40c}$$

d'où :

$$\begin{aligned}&= \int_{i-1/2}^{i} \kappa_1 M_2 - \kappa_2 M_1 \\ &= \int_{i-1/2}^{i} (\tfrac{1}{[EI]_{1,i}} - \tfrac{1}{[EI]_{2,i}}) M_1 M_2\end{aligned} \tag{6.41}$$

With

$$[EI]_i \tag{6.42a}$$

$$[GJ]_i \tag{6.42b}$$

$$\kappa \boldsymbol{b}_i = \frac{2\boldsymbol{e}_{i-1} \times \boldsymbol{e}_i}{|\boldsymbol{e}_{i-1}||\boldsymbol{e}_i||\boldsymbol{e}_{i-1} + \boldsymbol{e}_i|} \tag{6.42c}$$

$$\tau_i = \frac{\theta_{i+1} - \theta_i}{|\boldsymbol{e}_i|} \tag{6.42d}$$

$$\boldsymbol{N}_i = N_i \boldsymbol{d}_3 \quad where \quad N_i = \alpha_i \epsilon_i \quad \alpha_i = \frac{2[ES]_i[ES]_{i+1}}{[ES]_i + [ES]_{i+1}} \tag{6.42e}$$

$$\boldsymbol{M}_i = [EI]_{1,i}(\kappa_{1,i} - \bar{\kappa}_{1,i})\boldsymbol{d}_{1,i} + [EI]_{2,i}(\kappa_{2,i} - \bar{\kappa}_{2,i})\boldsymbol{d}_{2,i} \tag{6.42f}$$

$$\boldsymbol{Q}_i = Q_i \boldsymbol{d}_3 \quad where \quad Q_i = \beta_i(\tau_i - \bar{\tau}_i) \quad \beta_i = \frac{2[GJ]_i[GJ]_{i+1}}{[GJ]_i + [GJ]_{i+1}} \tag{6.42g}$$

$$\boldsymbol{F}_i^1 = -\frac{\boldsymbol{e}_i \times \boldsymbol{M}_i}{|\boldsymbol{e}_i|^2} \tag{6.42h}$$

$$\boldsymbol{F}_i^2 = +\frac{\boldsymbol{e}_i \times \boldsymbol{M}_{i+1}}{|\boldsymbol{e}_i|^2} \tag{6.42i}$$

$$\boldsymbol{H}_i^- = Q_i \kappa \boldsymbol{b}_{i+1/2}^- \tag{6.42j}$$

$$\boldsymbol{H}_i^+ = Q_i \kappa \boldsymbol{b}_{i+1/2}^+ \tag{6.42k}$$

$$\tag{6.42l}$$

Ici il y a une ambiguité sur $M_i$ en fonction d'un éventuel changement de propriété méca $EI_1$ ou $EI_2$. En fait il faudrait préciser un moment à droite et un moment à gauche (ce qui correspond à la réalité). Le moment étant la courbure au noeud i pondérée par $2EI$ à droite ou à gauche

Toutes les discrétisations ne se valent pas ....

En fait, ça n'a pas vraiment de sens de définir $EI$ sur le segment. Le moment est continu. Donc il est uniquement défini par la donnée de la courbure en un noeud et du $EI$ associé à ce noeuds. Introduire un moment à gauche et un moment à droite est problématique. Ce qui ce passe, pour une poutre isostatique simple qui change de $EI$ à mi-travée, c'est une discontinuité de courbure $y''$ alors que $y$ et $y'$ restent continues. Donc il semble plus pertinent de définir $EI$ aux noeuds car notre modèle ne peut pas représenter des discontinuitées de courbure (ou alors il faut connecter des poutres entre-elles.

Pour la torsion, on peut s'en sortir également en définissant $\beta$ aux noeuds et en supposant $GJ$ constant entre $[i - 1/2, i + 1/2]$. Il y a donc (éventuellement) un saut de $\beta$ au milieu de chaque $\boldsymbol{e}_i$.

On ne peut pas faire autrement que supposer la torsion uniforme entre 2 noeuds, c'est à dire une variation linéaire (par morceaux) de $\theta$. Et il y a donc une discontinuité potentielle aux noeuds.

On écrit la continuité du champs de torsion entre les noeuds 1 et 2 malgré le saut de $\beta$ :

A mi travée

$$Q_{12} = Q_{mid} = Q_1^+ = Q_2^- = [GJ]_1 \frac{\theta_{mid} - \theta_1}{|\boldsymbol{e}|/2} = [GJ]_2 \frac{\theta_2 - \theta_{mid}}{|\boldsymbol{e}|/2} \tag{6.43}$$

D'où :

$$\theta_{mid} = \frac{[GJ]_1}{[GJ]_1 + [GJ]_2}\theta_1 + \frac{[GJ]_2}{[GJ]_1 + [GJ]_2}\theta_2 \tag{6.44}$$

On en déduit :

$$Q_{12} = Q_{mid} = Q_1^+ = Q_2^- = \frac{2[GJ]_1[GJ]_2}{[GJ]_1 + [GJ]_2}\left(\frac{\theta_2 - \theta_1}{|\boldsymbol{e}|}\right) \tag{6.45}$$

Donc il faut plutôt définit $Q_i$ la torsion uniforme sur le segment $\boldsymbol{e}_i$ comme :

$$Q_i = \beta_i(\tau_i - \overline{\tau_i}) \quad where \quad \beta_i = \frac{2[GJ]_i[GJ]_{i+1}}{[GJ]_i + [GJ]_{i+1}} \tag{6.46}$$

On retrouve bien le cas d'une poutre de propriété constante lorsque $[GJ]_i = [GJ]_{i+1} = GJ$ alors $\beta_i = GJ$.

De manière identique, on résonne pour l'effort axial entre deux noeuds 1 et 2 auxquels sont associés des raideurs axiales $[ES]_1$ et $[ES_2]$. On cherche la raideur équivalente connaissant uniquement l'allongement de l'ensemble du segment :

$$N_1 = [ES]_1 \cdot \epsilon_1 \tag{6.47a}$$
$$N_2 = [ES]_2 \cdot \epsilon_2 \tag{6.47b}$$
$$N = [ES]_2 \cdot \frac{\epsilon_1 + \epsilon_2}{2} \tag{6.47c}$$

Avec :

$$\epsilon_1 = \frac{l_1 - l_0/2}{l_0/2} \tag{6.48a}$$
$$\epsilon_2 = \frac{l_2 - l_0/2}{l_0/2} \tag{6.48b}$$
$$\epsilon = \frac{l}{l_0} = \frac{\epsilon_1}{2} + \frac{\epsilon_2}{2} \tag{6.48c}$$
$$\tag{6.48d}$$

Thus,

$$N_i = N_1 = N_2 \quad \Rightarrow \quad \alpha_i = \frac{2[ES]_i[ES]_{i+1}}{[ES]_i + [ES]_{i+1}} \tag{6.49}$$

# Bibliography

[Ala12] Javad Alamatian. A new formulation for fictitious mass of the Dynamic Relaxation method with kinetic damping. *Computers and Structures*, 90-91:42–54, 2012.

[Day65] Alister Day. An Introduction to dynamic relaxation. *The Engineer*, 1965.

[MAIK14] Masaaki Miki, Sigrid Adriaenssens, Takeo Igarashi, and Ken'ichi Kawaguchi. The geodesic dynamic relaxation method for problems of equilibrium with equality constraint conditions. *International Journal for Numerical Methods in Engineering*, 99(9):682–710, 2014.

[Ott65] J.R.H. Otter. Computations for prestressed concrete reactor pressure vessels using dynamic relaxation. *Nuclear Structural Engineering*, 1(1):61–75, jan 1965.

[Pap81] M Papadrakakis. A method for the automatic evaluation of the dynamic relaxation parameters. 1981.

[RPKAZ11] M Rezaiee-Pajand, M Kadkhodayan, Javad Alamatian, and L C Zhang. A new method of fictitious viscous damping determination for the dynamic relaxation method. *Computers and Structures*, 89(9-10):783–794, 2011.

# Appendix Part III

# A Calculus of variations

## A.1 Introduction

In this appendix we drawback essential mathematical concepts for the calculus of variations. Recall how the notion of energy, gradients are extended to function spaces.

[AMR02]

## A.2 Spaces

### A.2.1 Normed space

A *normed space* $V(\mathbb{K})$ is a vector space $V$ over the scalar field $\mathbb{K}$ with a norm $\|.\|$.

A *norm* is a map $\|.\| : V \times V \longmapsto \mathbb{K}$ which satisfies :

$$\forall x \in V, \qquad \|x\| = 0_{\mathbb{K}} \Rightarrow x = 0_V \tag{A.1a}$$

$$\forall x \in V, \forall \lambda \in \mathbb{K}, \qquad \|\lambda x\| = |\lambda| \, \|x\| \tag{A.1b}$$

$$\forall (x, y) \in V^2, \qquad \|x + y\| \leqslant \|x\| + \|y\| \tag{A.1c}$$

### A.2.2 Inner product space

A *inner product space* or *pre-hilbert space* $E(\mathbb{K})$ is a vector space $E$ over the scalar field $\mathbb{K}$ with an inner product.

An *inner product* is a map $\langle \, ; \, \rangle : E \times E \longmapsto \mathbb{K}$ which is bilinear, symmetric, positive-definite

:

$$\forall (x,y,z) \in E^3, \forall (\lambda,\mu) \in \mathbb{K}^2, \quad \begin{aligned} &\langle \lambda x + \mu y \,;\, z\rangle = \lambda\langle x \,;\, z\rangle + \mu\langle y \,;\, z\rangle \\ &\langle x \,;\, \lambda y + \mu z\rangle = \lambda\langle x \,;\, y\rangle + \mu\langle x \,;\, z\rangle \end{aligned} \tag{A.2a}$$

$$\forall (x,y) \in E^2, \quad \langle x \,;\, y\rangle = \langle y \,;\, x\rangle \tag{A.2b}$$

$$\forall x \in E, \quad \langle x \,;\, x\rangle \geqslant 0_{\mathbb{K}} \tag{A.2c}$$

$$\forall x \in E, \quad \langle x \,;\, x\rangle = 0_{\mathbb{K}} \Rightarrow x = 0_E \tag{A.2d}$$

Moreover, an inner product naturally induces a norm on $E$ defined by :

$$\forall x \in E, \quad \|x\| = \sqrt{\langle x \,;\, x\rangle} \tag{A.3}$$

Thus, an inner product vector space is also naturally a normed vector space.

### A.2.3 Euclidean space

An *Euclidean space* $\mathcal{E}(\mathbb{R})$ is a finite-dimensional real vector space with an inner product. Thus, distances and angles between vectors could be defined and measured regarding to the norm associated with the chosen inner product.

An Euclidean space is nothing but a finite-dimensional real pre-hilbert space.

### A.2.4 Banach space

A *Banach space* $\mathcal{B}(\mathbb{K})$ is a complete normed vector space, which means that it is a normed vector space in which every Cauchy sequence of $\mathcal{B}$ converges in $\mathcal{B}$ for the given norm.

Thus, a Banach space is a vector space with a metric that allows the computation of vector length and distance between vectors and is complete in the sense that a Cauchy sequence of vectors always converges to a well defined limit in that space.

### A.2.5 Hilbert space

A *Hilbert space* is an inner product vector space $\mathcal{H}(\mathbb{K})$ such that the natural norm induced by the inner product turns $\mathcal{H}$ into a complete metric space (i.e. every Cauchy sequence of $\mathcal{H}$ converges in $\mathcal{H}$).

The Hilbert space concept is a generalization of the Euclidean space concept. In physics it's common to encounter Hilbert spaces as infinite-dimensional function spaces.

Hilbert spaces are Banach spaces, but the converse does not hold generally.

For example, $\mathcal{L}^2([a,b])$ is an infinite-dimensional Hilbert space with the canonical inner product $\langle f \,;\, g\rangle = \int_a^b fg$.

Note that $\mathcal{L}^2$ is the only Hilbert space among the $\mathcal{L}^p$ spaces.

## A.3 Derivative

The well known notion of function derivative in $\mathbb{R}^{\mathbb{R}}$ can be extended to maps between Banach spaces. This is useful in physics when formulating problems as variational problems, usually in terms of energy minimization. Indeed, energy is generally defined over a functional vector space and not simply over the real line.

In this case, the research of minimal values of a potential energy rests on the calculus of variations of the energy function compared to variations to other functions defining the problem (geometry, materials, boundary conditions, ...).

Mathematical concepts extended well-known notions of derivative, jacobian and hessian in Euclidean spaces (typically $\mathbb{R}^2$ or $\mathbb{R}^3$) for Banach functional spaces.

### A.3.1 Fréchet derivative

#### Differentiability

Let $\mathcal{B}_V$ and $\mathcal{B}_W$ be two Banach spaces and $U \subset \mathcal{B}_V$ an open subset of $\mathcal{B}_V$. Let $f : u \longmapsto f(u)$ be a function of $U^{\mathcal{B}_W}$. $f$ is said to be *Fréchet differentiable* at $u_0 \in U$ if there exists a continious linear operator $\boldsymbol{D}f(u_0) \in \mathcal{L}(\mathcal{B}_V, \mathcal{B}_W)$ such that :

$$\lim_{h \to 0} \frac{f(u_0 + h) - f(u_0) - \boldsymbol{D}f(u_0) \cdot h}{\|h\|} = 0 \tag{A.4a}$$

Or, equivalently :

$$f(u_0 + h) = f(u_0) + \boldsymbol{D}f(u_0) \cdot h + o(h) \quad , \quad \lim_{h \to 0} \frac{o(h)}{\|h\|} = 0 \tag{A.4b}$$

In the literature, it is common to found the following notations : $df = \boldsymbol{D}f(u_0) \cdot h = \boldsymbol{D}f_{u_0}(h) = \boldsymbol{D}f(u_0, h)$ for the differential of $f$, which means nothing but $\boldsymbol{D}f(u_0)$ is linear regarding $h$. The dot denotes the evaluation of $\boldsymbol{D}f(u_0)$ at $h$. This notation can be ambiguous as far as the linearity of $\boldsymbol{D}f(u_0)$ in $h$ is denoted as a product which is not explicitly defined.

#### Derivative

If $f$ is Fréchet differentiable at $u_0 \in U$, the continous linear operator $\boldsymbol{D}f(u_0) \in \mathcal{L}(\mathcal{B}_V, \mathcal{B}_W)$ is called the *Fréchet derivative* of $f$ at $u_0$ and is also denoted :

$$f'(u_0) = \boldsymbol{D}f(u_0) \tag{A.5}$$

$f$ is said to be $\mathcal{C}^1$ in the sens of Fréchet if $f$ is Fréchet differentiable for all $u \in U$ and the function $\boldsymbol{D}f : u \longmapsto f'(u)$ of $U^{\mathcal{L}(\mathcal{B}_V, \mathcal{B}_W)}$ is continuous.

#### Differential or total derivative

$df = \boldsymbol{D}f(u_0) \cdot h$ is sometimes called the *differential* or *total derivative* of $f$ and represents the change in the function $f$ for a perturbation $h$ from $u_0$.

#### Higer derivatives

Because the differential of $f$ is a linear map from $\mathcal{B}_V$ to $\mathcal{L}(\mathcal{B}_V, \mathcal{B}_W)$ it is possible to look for the differentiability of $\boldsymbol{D}f$. If it exists, it is denoted $\boldsymbol{D}^2 f$ and maps $\mathcal{B}_V$ to $\mathcal{L}(\mathcal{B}_V, \mathcal{L}(\mathcal{B}_V, \mathcal{B}_W))$.

### A.3.2 Gâteaux derivative

#### Directional derivative

Let $\mathcal{B}_V$ and $\mathcal{B}_W$ be two Banach spaces and $U \subset \mathcal{B}_V$ an open subset of $\mathcal{B}_V$. Let $f : u \longmapsto f(u)$ be a function of $U^{\mathcal{B}_W}$. $f$ is said to have a *derivative in the direction* $h \in \mathcal{B}_V$ at $u_0 \in U$ if :

$$\frac{d}{d\lambda} f(u_0 + \lambda h)\Big|_{\lambda=0} = \lim_{\lambda \to 0} \frac{f(u_0 + \lambda h) - f(u_0)}{\lambda} \tag{A.6}$$

exists. This element of $\mathcal{B}_W$ is called the *directional derivative* of $f$ in the direction $h$ at $u_0$.

#### Differentiability

Let $\mathcal{B}_V$ and $\mathcal{B}_W$ be two Banach spaces and $U \subset \mathcal{B}_V$ an open subset of $\mathcal{B}_V$. Let $f : u \longmapsto f(u)$ be a function of $U^{\mathcal{B}_W}$. $f$ is said to be *Gâteaux differentiable* at $u_0 \in U$ if there exists a continious linear operator $\boldsymbol{D}f(u_0) \in \mathcal{L}(\mathcal{B}_V, \mathcal{B}_W)$ such that :

$$\forall h \in \mathcal{U}, \quad \lim_{\lambda \to 0} \frac{f(u_0 + \lambda h) - f(u_0)}{\lambda} = \frac{d}{d\lambda} f(u_0 + \lambda h)\Big|_{\lambda=0} = \boldsymbol{D}f(u_0) \cdot h \tag{A.7a}$$

Or, equivalently :

$$\forall h \in \mathcal{U}, \quad f(u + \lambda h) = f(u) + \lambda \boldsymbol{D}f(u_0) \cdot h + o(\lambda) \quad , \quad \lim_{\lambda \to 0} \frac{o(\lambda)}{\lambda} = 0 \tag{A.7b}$$

In other words, it means that all the directional derivatives of $f$ exist at $u_0$.

### Derivative

If $f$ is Gâteaux differentiable at $u_0 \in U$, the continous linear operator $\boldsymbol{D}f(u_0) \in \mathcal{L}(\mathcal{B}_V, \mathcal{B}_W)$ is called the *Gâteaux derivative* of $f$ at $u_0$ and is also denoted :

$$f'(u_0) = \boldsymbol{D}f(u_0) \tag{A.8}$$

$f$ is said to be $\mathcal{C}^1$ in the sens of Gâteaux if $f$ is Gâteaux differentiable for all $u \in U$ and the function $\boldsymbol{D}f : u \longmapsto f'(u)$ of $U^{\mathcal{L}(\mathcal{B}_V, \mathcal{B}_W)}$ is continuous.

The Gâteaux derivative is a weaker form of derivative than the Fréchet derivative. If $f$ is Fréchet differentiable, then it is also Gâteaux differentiable and its Fréchet and Gâteaux derivatives agree, but the converse does not hold generally.

## A.3.3 Useful properties

Let $\mathcal{B}_V$, $\mathcal{B}_W$ and $\mathcal{B}_Z$ be three Banach spaces. Let $f, g : \mathcal{B}_V \longmapsto \mathcal{B}_W$ and $h : \mathcal{B}_W \longmapsto \mathcal{B}_Z$ be three Gâteaux differentiable functions. Then, the following useful properties holds :

$$\boldsymbol{D}(f+g)(u) = \boldsymbol{D}f(u) + \boldsymbol{D}g(u) \tag{A.9}$$

$$\boldsymbol{D}(f \circ h)(u) = \boldsymbol{D}h(f(u)) \circ \boldsymbol{D}f(u) = \boldsymbol{D}h(f(u)) \cdot \boldsymbol{D}f(u) \tag{A.10}$$

Recall that the composition of $\boldsymbol{D}h(f(u))$ with $\boldsymbol{D}f(u)$ means "$\boldsymbol{D}h(f(u))$ applied to $\boldsymbol{D}f(u)$" and is also denoted by $\cdot$ as explained previously.

## A.3.4 Partial derivative

Following [AMR02] the main results on partial derivatives of two-variables functions are presented here. They are generalizable to n-variables functions.

### Definition

Let $\mathcal{B}_{V_1}$, $\mathcal{B}_{V_2}$ and $\mathcal{B}_W$ be three Banach spaces and $U \subset \mathcal{B}_{V_1} \oplus \mathcal{B}_{V_2}$ an open subset of $\mathcal{B}_{V_1} \oplus \mathcal{B}_{V_2}$. Let $f : u \longmapsto f(u)$ be a function of $U^{\mathcal{B}_W}$. Let $u_0 = (u_{01}, u_{02}) \in U$. If the derivatives of the following functions exist :

$$\begin{array}{rccc} f_1 : & \mathcal{B}_{V_1} & \longrightarrow & \mathcal{B}_W \\ & u_1 & \longmapsto & f(u_1, u_{02}) \end{array} \quad , \quad \begin{array}{rccc} f_2 : & \mathcal{B}_{V_2} & \longrightarrow & \mathcal{B}_W \\ & u_2 & \longmapsto & f(u_{01}, u_2) \end{array} \tag{A.11}$$

they are called *partial derivatives* of $f$ at $u_0$ and are denoted $\boldsymbol{D}_1 f(u_0) \in \mathcal{L}(\mathcal{B}_{V_1}, \mathcal{B}_W)$ and $\boldsymbol{D}_2 f(u_0) \in \mathcal{L}(\mathcal{B}_{V_2}, \mathcal{B}_W)$.

### Differentiability

Let $\mathcal{B}_{V_1}$, $\mathcal{B}_{V_2}$ and $\mathcal{B}_W$ be three Banach spaces and $U \subset \mathcal{B}_{V_1} \oplus \mathcal{B}_{V_2}$ an open subset of $\mathcal{B}_{V_1} \oplus \mathcal{B}_{V_2}$. Let $f : u \longmapsto f(u)$ be a function of $U^{\mathcal{B}_W}$. If $f$ is differentiable, then the partial derivatives exist and satisfy for all $h = (h_1, h_2) \in \mathcal{B}_{V_1} \oplus \mathcal{B}_{V_2}$ :

$$\boldsymbol{D}_1 f(u) \cdot h_1 = \boldsymbol{D} f(u) \cdot (h_1, 0) \tag{A.12}$$

$$\boldsymbol{D}_2 f(u) \cdot h_2 = \boldsymbol{D} f(u) \cdot (0, h_2) \tag{A.13}$$

$$\boldsymbol{D} f(u) \cdot (h_1, h_2) = \boldsymbol{D}_1 f(u) \cdot h_1 + \boldsymbol{D}_2 f(u) \cdot h_2 \tag{A.14}$$

## A.4 Gradient vector

Let $\mathcal{H}$ be a Hilbert space with the inner product denoted $\langle \, ; \, \rangle$. Let $U \subset \mathcal{H}$ an open subset of $\mathcal{H}$. Let $F : u \longmapsto F(u)$ be a scalar function of $U^{\mathbb{R}}$. The *gradient* of $F$ is the map $grad\, F : x \longmapsto (grad\, F)(x)$ of $U^{\mathcal{H}}$ such that :

$$\forall h \in \mathcal{H}, \quad \langle (grad\, F)(x) \, ; h \rangle = \boldsymbol{D} F(x) \cdot h \tag{A.15}$$

Note that the gradient vector depends on the chosen inner product. For $\mathcal{H} = \mathbb{R}^n$ with the canonical inner product, one can recall the usual definition of the gradient vector and the corresponding linear approximation of $F$ :

$$\boldsymbol{F}_{x+h} = \boldsymbol{F}_x + (grad\, F)_x^T H + \boldsymbol{o}(H) \quad , \quad grad\, F_x = \begin{bmatrix} \frac{\partial F}{\partial x_1} \\ \vdots \\ \frac{\partial F}{\partial x_n} \end{bmatrix} \in \mathbb{R}^n \tag{A.16}$$

Recall that the canonical inner product on $\mathbb{R}^n$ is such that $\langle x \, ; y \rangle = X^T Y$ in a column vector representation. In this case it is common to denote $grad\, F = \nabla F$.

For function spaces the usual definition of the gradient can be extended. For instance if $F$ is a scalar function on $\mathcal{L}^2$, the gradient of $F$ is the unique function (if it exists) from $\mathcal{L}^2$ which satisfies :

$$\forall h \in \mathcal{L}^2, \quad \boldsymbol{D} F(x) \cdot h = \langle (grad\, F)(x) \, ; h \rangle = \int (grad\, F) h \tag{A.17}$$

In this case it is common to denote $grad\, F = \frac{\delta F}{\delta x}$. The gradient is also known as the *functional derivative*. The existence and unicity of $grad\, F$ is ensured by the *Riesz representation theorem*.

## A.5 Jacobian matrix

Let $f$ be a differentiable function from $\mathbb{R}^n$ to $\mathbb{R}^m$. The *differential* or *total derivative* of such a fonction is a linear application from $\mathbb{R}^n$ to $\mathbb{R}^m$ which could be represented with the

following matrix called the *jacobian matrix* :

$$\boldsymbol{D}f(x) = \boldsymbol{J}_x = \frac{df}{dx} = \begin{bmatrix} \frac{\partial f}{\partial x_1} & \cdots & \frac{\partial f}{\partial x_n} \end{bmatrix} = \begin{bmatrix} \frac{\partial f_1}{\partial x_1} & \cdots & \frac{\partial f_1}{\partial x_n} \\ \vdots & \ddots & \vdots \\ \frac{\partial f_m}{\partial x_1} & \cdots & \frac{\partial f_m}{\partial x_n} \end{bmatrix} \in \mathcal{M}_{m,n}(\mathbb{R}) \tag{A.18}$$

Thus, with the matrix notation, the Taylor expansion takes the following form :

$$\boldsymbol{F}_{x+h} = \boldsymbol{F}_x + \boldsymbol{J}_x H + \boldsymbol{o}(H) \tag{A.19}$$

In the cas $m = 1$, the jacobian matrix of the functional $F$ is nothing but the gradient vector transpose itself :

$$\boldsymbol{D}F(x) = \boldsymbol{J}_x = \frac{dF}{dx} = \begin{bmatrix} \frac{\partial F}{\partial x_1} & \cdots & \frac{\partial F}{\partial x_n} \end{bmatrix} = \nabla F^T \tag{A.20}$$

## A.6 Hessian

Let $F$ be a differentiable scalar function from $\mathbb{R}^n$ to $\mathbb{R}$. The second order differential of such a fonction is a linear application from $\mathbb{R}^n$ to $\mathbb{R}^n$ which could be represented with the following matrix called the *hessian matrix* :

$$\boldsymbol{D}^2F(x) = \boldsymbol{H}_x = \frac{d^2F}{dx}(x) = \begin{bmatrix} \frac{\partial F_1^2}{\partial x_1^2} & \frac{\partial F_1^2}{\partial x_1 \partial x_2} & \cdots & \frac{\partial F_1^2}{\partial x_1 \partial x_n} \\ \frac{\partial F_1^2}{\partial x_2 \partial x_1} & \frac{\partial F_1^2}{\partial x_2^2} & \cdots & \frac{\partial F_1^2}{\partial x_2 \partial x_n} \\ \vdots & & \ddots & \vdots \\ \frac{\partial F_p^2}{\partial x_n \partial x_1} & \frac{\partial F_p^2}{\partial x_n \partial x_2} & \cdots & \frac{\partial F_p^2}{\partial x_n^2} \end{bmatrix} \in \mathcal{M}_{n,n}(\mathbb{R}) \tag{A.21}$$

Thus, with the matrix notation, the Taylor expansion takes the following form :

$$\boldsymbol{F}_{x+h} = \boldsymbol{F}_x + \boldsymbol{J}_x H + \tfrac{1}{2} H^T \boldsymbol{H}_x H + \boldsymbol{o}(H) \tag{A.22}$$

## A.7 Functional

A *functional* is a map from a vector space $E(\mathbb{K})$ into its underlying scalar field $\mathbb{K}$. Here $\mathcal{E}_p[\boldsymbol{x}, \theta]$ is a functional depending over $\boldsymbol{x}$ and $\theta$.

## Bibliography

[AMR02] Ralph Abraham, Jerrold E. Marsde, and Tudor Ratiu. *Manifolds, Tensor Analysis, and Applications (Ralph Abraham, Jerrold E. Marsden and Tudor Ratiu)*. 2002.